Regulation of Zn^{2+} and aggregation affects $A\beta_{1-42}$-induced changes in cell culture viability.

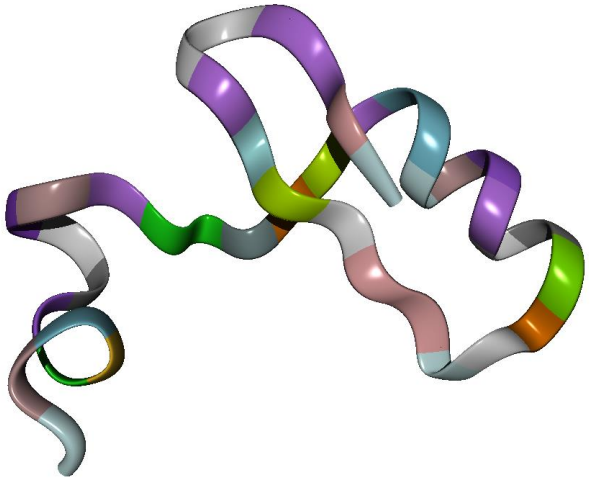

Nikita Potemkin

Submitted in fulfilment of the

degree of Master of Science at the

University of Otago

Dunedin, New Zealand

February 2017

Abstract

In the story of the pathogenesis of Alzheimer's Disease, Amyloid-Beta (Aβ) is believed to play a key role. However, evidence suggests that metal ions, in particular Zn^{2+}, may have strong modulatory, or even causative effects on the development of the disease. This study aimed to shed more light on the relationship between Aβ and Zn^{2+}, especially with regards to their effects on cell viability.

First, a protocol for the production of recombinant $A\beta_{1-42}$ was followed to produce and purify the peptide. The next step was to establish a consistent cellular insult paradigm using $A\beta_{1-42}$ in SH-SY5Y neuroblastoma cells, paying particular attention to aggregating the peptide – an important factor in Aβ toxicity. Subsequently this study aimed to investigate the effect of addition of exogenous Zn^{2+} on cell viability and its interaction with $A\beta_{1-42}$.

The production and purification protocol was successful in yielding quantities of pure Aβ. However, this protocol may require further optimisation. It was noted that while many research groups continue to use the MTT assay to measure cell viability, the large variability of the assay and the reported biochemical interaction with the Aβ peptide make it inappropriate. As such, this study used the resazurin assay. This research was unable to establish a consistent cellular insult paradigm in either SH-SY5Y neuroblastoma cells or cultured rat hippocampal or cortical cells ($p>0.05$; $n=3$). This was despite an ageing protocol able to produce oligomers and protofibrils of Aβ, species previously shown to have toxic effects on cell cultures. In fact, protofibril-containing samples of the peptide at 20 and 40 µM increased cell viability of neuroblastoma cultures above the control (by 0.22±0.039 and 0.36±0.041 respectively; $p<0.01$; $n=2$). No effect of $A\beta_{1-42}$ was observed in the primary cells ($p>0.1$; $n=4$). Finally, addition of exogenous Zn^{2+} in some cases complimented Aβ-induced increases in cell viability, although this effect was inconsistent.

This research highlighted some of the difficulties in examining Aβ in cell culture. In particular, it seemed important to not only identify the aggregation state of Aβ peptides, but also isolate and test specific species. This research suggests, however, that Zn^{2+} does modulate the effects of Aβ on cell viability and this relationship requires further investigation.

Acknowledgements

Those who have been with me throughout this journey know the difficulties I have faced and the obstacles I have had to overcome to get to where I am now, despite it being far later than I originally planned. Nevertheless, here I am now, and I will continue moving forward if Science allows me.

The greatest thanks have to go to my supervisors, Dr. Joanna Williams and Prof. Warren Tate, firstly for allowing me into your labs in the first place; second, for encouraging my slightly hair-brained experiments; third, for your continuing support when things went wrong (as they are wont to do). Finally, Warren, thank you for reminding me that it's "Second", and not "Secondly".

To all members of the Williams and Tate labs, past and present, through whose tireless efforts over was this project made possible – I say thank you. All your input at various lab meetings, and your probing questions, certainly helped me in interpreting some difficult data.

Thank you to Katie Peppercorn and Tina Edgar for being my first port of call with technical questions, be they cell culture-, protein purification- or gel-related. Your experience and advice have been invaluable

A big thank you to Megan Elder for providing me with primary rat neuronal cultures. You are one of the most talented young scientists I know, and I hope to work with you more in the future.

To all my long-suffering friends who have had to listen to me complain (almost) endlessly about failed experiments and confusing data, thank you for your patience – the end is nigh.

Annabel – although life has taken us down very different paths, I am still grateful for your support and the time we had together.

To you, I dedicate this research.

"If I have seen further it is by standing on the shoulders of Giants" – Isaac Newton

Table of Contents

Abstract i

Acknowledgements ii

Table of Contents iii

List of Tables vi

List of Figures vii

Abbreviations viii

1. Introduction 1

1.1 Prevalence and Incidence 2

1.2 Economic and Social Impact 2

1.3 Biology of Alzheimer's Disease 3

1.3.1 Disease Progression 3

1.3.2 Pathology of Alzheimer's Disease 5

1.3.3 Diagnosis 6

1.4 Theories of AD 8

1.4.1 The Amyloid Hypothesis 8

1.4.2 Protein Aggregation and Toxicity 12

1.4.3 The Tau Hypothesis 16

1.4.4 The Vascular Hypothesis 17

1.4.5 Neuroinflammation in AD 17

1.4.6 Metal Ion Homeostasis 18

1.5 Past, Present and Developing Treatments 22

1.5.1 Pharmacological Intervention 22

1.5.2 Targeting Amyloid-Beta 23

1.5.3 Immunotherapy 25

1.5.4 Metal Protein Targeting Compounds 26

1.6 A Physiological Role for Amyloid-Beta 27

1.6.1 Anti-bacterial Role 27

1.6.2 Anti-oxidant Properties 28

1.6.3 Amyloid-Beta in Learning and Memory 29

1.6.4 Amyloid-Beta as a Neurotrophic Factor 29

1.7 Aims 31

2 Materials and Methods 32
2.1 Amyloid-Beta Preparation 32
2.1.1 Induction of $A\beta_{1-42}$ expression in bacteria 32
2.1.2 Bacterial lysis and protein extraction 33
2.1.3 Affinity chromatography 33
2.1.4 Ammonium sulphate fractionation 33
2.1.5 Desalting chromatography 34
2.1.6 Fusion protein cleavage 34
2.1.7 Reverse Phase chromatography 34
2.1.8 Size-exclusion chromatography 35
2.1.9 Bicinchoninic acid (BCA) protein concentration assay 35
2.1.10 Sodium dodecyl sulphate polyacrylamide gel electrophoresis (SDS-PAGE) 36
2.1.11 Coomassie staining 37
2.1.12 Commercial Aβ peptides 37
2.2 Cell culture techniques 38
2.2.1 Cell lines 38
2.2.2 Growth of cells 38
2.2.3 Storage of cells 39
2.2.4 Seeding cells from frozen stock 39
2.2.5 Passaging of cells 39
2.2.6 Seeding cells into 24- or 96-well plates 40
2.2.7 Treating SH-SY5Y cells with Aβ and Zn^{2+} 40
2.2.8 Glucose deprivation (GD) insult 40
2.2.9 Primary cells 41
2.3 Cell viability assays 41
2.3.1 MTT cell viability assay 41
2.3.2 Resazurin cell viability assay 42
2.4 Amyloid-Beta Aggregation 42
2.5 Data Analysis 43
3 Results 44
3.1 Amyloid-Beta production 44
3.1.1 Aβ induction in bacterial culture 44
3.1.2 Purification of MBP-$A\beta_{1-42}$ from bacterial lysate 45

3.1.3 Cleavage of Aβ from MBP 45
3.1.4 Reverse-Phase chromatography 47
3.1.5 Quantification of Aβ concentration 48
3.2 Amyloid-Beta toxicity in SH-SY5Y neuroblastoma cell cultures 50
3.2.1 Initial probe of effective $A\beta_{1-42}$ concentration 50
3.2.2 Comparing the MTT cell viability assay to the resazurin assay 51
3.3 Amyloid-Beta aggregation and toxicity 53
3.3.1 Effects of different buffers on Aβ aggregation 55
3.3.2 Structural analysis and aggregation prediction of Aβ peptides 57
3.3.3 Effect of ageing Aβ on cell viability 58
3.4 Comparing toxicity in primary cells and neuroblastoma cells 60
3.4.1 Aβ effects on SH-SY5Y neuroblastoma cell cultures 61
3.4.2 Aβ effects on primary cortical and hippocampal cell cultures 62
3.5 Zinc and Amyloid-Beta toxicity 64
3.5.1 Concentration-dependent effect of Zinc on neuroblastoma cell culture viability 64
3.5.2 Effect of combined zinc and Aβ on neuroblastoma cell culture viability ... 65
4 Discussion 68
4.1 Amyloid-Beta production 68
4.2 Cellular insult paradigm 70
4.2.1 The MTT assay is inappropriate for examining Amyloid-Beta toxicity 70
4.2.2 Amyloid-Beta effects on cell viability are dependent on its aggregation 71
4.2.3 Amyloid-Beta is inconsistent as a cellular insult 72
4.3 Zinc and Amyloid-Beta interactions 74
4.3.1 Zinc has a dose-dependent effect on SH-SY5Y cell viability 74
4.3.2 Zinc modulates Amyloid-Beta induced changes in cell viability 75
4.4 Conclusions 75
4.5 Future Directions 76
References 79
Appendices 106
Appendix A. R statistical analysis scripts 106
Appendix B. Size-exclusion chromatography to separate $A\beta_{1-42}$ from MBP 108
Appendix C. Standard curve of BSA amount used to determine Aβ concentration 109
Appendix D. Individual primary cell culture data 110

List of Tables

Table 1. Constituents of SDS-PAGE gel solutions 36

Table 2. Constituents of staining and destain solutions 37

List of Figures

Figure 1. Progression of Amyloid-Beta aggregation 13

Figure 2. $A\beta_{1-28}$ conformation around the Zn^{2+} ion 19

Figure 3. Representative SDS-PAGE gel of protein synthesis induction samples 44

Figure 4. Representative FPLC plot of desalting chromatography 46

Figure 5. Representative SDS-PAGE KOLBE gel showing Factor Xa cleavage of MBP-Aβ 47

Figure 6. FPLC plot of reverse-phase chromatography to separate Aβ and MBP 49

Figure 7. 24 h treatment with 1µM Aβ has no effect on cell viability 51

Figure 8. Comparison of Resazurin and MTT assays using GD 52

Figure 9. 24 (10a) or 48 h (10b) treatment with 1, 5 and 10µM Aβ has no effect on SH-SY5Y cell viability 54

Figure 10(a-f). Coomassie-stained KOLBE SDS-PAGE gels of Aβ peptides after ageing 56

Figure 11. Predicted secondary structure and aggregation propensity of Aβ peptides 58

Figure 12. Effect of ageing Aβ peptides in water (13a) or aCSF (13b) on SH-SY5Y cell viability 59

Figure 13. 20 and 40µM Aβ aged with aCSF increases SH-SY5Y cell viability 61

Figure 14. aCSF-aged Aβ peptides have no effect on rat cortical cell cultures 62

Figure 15. aCSF-aged Aβ peptides have no effect on rat hippocampal cell cultures 63

Figure 16. Zn^{2+} has a concentration-dependent effect on SH-SY5Y cell viability 65

Figure 17. Zn^{2+} modulates the effect of Aβ on SH-SY5Y cell viability 66

Figure 18. aCSF-aged Aβ with Zn^{2+} has no effect on SH-SY5Y cell viability 67

Abbreviations

Aβ: Amyloid-Beta

$A\beta_{1-42}$: full-length amyloid-beta

ACHEI: Acetylcholinesterase inhibitor

aCSF: artificial cerebrospinal fluid

AD: Alzheimer's disease

- fAD: familial Alzheimer's disease
- sAD: sporadic Alzheimer's disease

ADAM: A Disintegrin and Metalloproteinase domain-containing protein

AMP: antimicrobial peptide

APP: Amyloid Precursor Protein

BACE: beta-site amyloid precursor protein cleaving enzyme

BCA: bicinchoninic acid

BSA: bovine serum albumin

CA: cornus ammonis

CSF: cerebrospinal fluid

DMEM: Dulbecco's modified Eagle medium

DMSO: dimethyl sulfoxide

FBS: fetal bovine serum

FPLC: fast protein liquid chromatography

GD: Glucose deprivation

LB: Lysogeny broth

MBP: maltose-binding protein

MCI: Mild cognitive Impairment

MOPS: 3-(*N*-morpholino)propanesulfonic acid

MRI: Magnetic resonance imaging

MTT: 3-(4,5-dimethylthiazol-2-yl)-2,5-diphenyltetrazolium bromide

NMDA: N-methyl-D-aspartate

NFT: neurofibrillary tangles

PBS: Phosphate buffered saline

PET: Positron emission tomography

RPC: Reverse phase chromatography

sAPPα: Secreted amyloid precursor protein alpha

sAPPβ: Secreted amyloid precursor protein beta

SDS-PAGE: Sodium dodecyl sulphate polyacrylamide gel electrophoresis

Chapter 1

Introduction

The world's population is ageing. With greatly improved sanitation, healthcare and medicine, many of the formerly significant causes of mortality are being better controlled and treated, meaning more people are living longer. This is especially noticeable in developing countries, where average life expectancy has risen by 2-6 years in the last two decades (World Health Organisation, 2008). With an ageing population comes an increase in the prevalence of ageing-related diseases, of which one of the most impactful, both socially and economically, is dementia. Dementia describes those neurodegenerative diseases that lead to impairment of cognitive abilities – in particular memory and reasoning – as well as changes in personality and emotions, and that markedly disrupt a person's ability to function normally. Dementia itself is a heterogeneous umbrella term for a number of different conditions, including vascular dementia, fronto-temporal dementia and Lewy-body dementia. However, by far the most common form is Alzheimer's disease (AD), making up approximately 50-70% of global dementia cases (ADI, 2009). AD is characterised by severe and progressive memory loss, personality change and behavioural issues, mood disturbances, loss of motivation and self-care, with eventual loss of essential bodily functions that lead to death.

Unfortunately, the aetiology of AD is currently still poorly-defined. Age appears to be the largest risk factor, although there is a subset of patients whose symptoms manifest relatively early in life, often by the age of 40. These patients generally have a family history of what has been termed early-onset AD, commonly also called familial AD (fAD), and it often has a clear genetic and hereditary component.

Since the genetic component of many cases of fAD has been well-defined, fAD has long shaped and guided research into late-onset Alzheimer's disease, often referred to as sporadic AD (sAD).

1.1 Prevalence and Incidence

In 2015, 46.8 million people worldwide were estimated to be living with dementia (Prince et al., 2015). While recent trends have indicated a slight decline in rates of AD in the USA, believed to be due to improved nutrition, fitness and health trends (Langa et al., 2017), the number of dementia sufferers is projected to double every 20 years. This increase will be especially marked in low- and middle-income countries, many of whom are predicted to see a greater than 200% increase in the incidence of dementia by 2050. In New Zealand, as of 2012, dementia affected nearly 50 000 people (Alzheimers New Zealand, 2012) with 13 000 new cases currently diagnosed annually – of those, 40% were male and 60% female. Alzheimer's New Zealand suggests that by 2050, nearly 150 000 New Zealanders will have been diagnosed with dementia, this number rising by an additional 40 000 a year due to ever-increasing life expectancy and an ageing population.

1.2 Economic and Social Impact

Since dementia is not immediately lethal, the economic impact of protracted treatment and care is considerable. Covering all health system costs, including hospital, pharmaceutical, diagnostic, care costs, as well as research funding and allied care costs for services such as physiotherapy or counselling, dementia costs New Zealand nearly $600 million a year (Alzheimers New Zealand, 2012). Productivity losses (in the form of lower employment rates, absenteeism and premature mortality), welfare payments, carer support and other costs add another $360 million to that total. Across the globe, this figure is as high as US$818 billion, and expected to breach the US$2 trillion mark by 2030 as incidence rates increase (Prince et al., 2015).

In addition to the economic burden, dementia also carries a significant social cost. A diagnosis of dementia is extremely traumatic, not only for the patient, but also for their family and friends. Often spouses or family members need to give up their jobs to provide care for the patient, which is not only financially challenging, but can also lead to huge pressure on the relationship between patient and caregiver, and to social isolation, depression and poor physical health of both (Brodaty and Hadzi-Pavlovic, 1990; Springate and Tremont, 2014).

1.3 Biology of Alzheimer's Disease

1.3.1 Disease Progression

The progressive memory loss characterizing AD is often divided into four stages – pre-dementia, mild, moderate, and severe dementia (Förstl and Kurz, 1999). Thorough neuropsychological investigation can sometimes highlight symptoms predictive of the pre-clinical form of the disease up to 5 years earlier than more obvious symptoms appear. Pre-dementia often manifests as an impairment in acquiring new information, as well as difficulties in performing other cognitively demanding tasks such as planning, or recalling semantic memory. In addition, patients may exhibit non-cognitive behavioural changes such as social withdrawal (Jost and Grossberg, 1995). At this stage, the symptoms typically do not greatly interfere with a patient's daily life, and given their vague nature, they are not only difficult to identify, but are also hard to distinguish from cognitive deficits experienced due to normal ageing, or with conditions such as depression or senility.

Mild or early-stage AD essentially marks when cognitive and memory deficits begin to affect the patient's activities of daily living. Declarative recent memory tends to be preferentially affected, while short-term, long-term declarative and implicit memory remain largely intact. Activities such as planning, judgement and organization are impaired, and vocabulary deficits begin to interfere with basic communication. Spatial awareness and judgement are impaired and non-cognitive disturbances

such as depression and apathy become more prevalent (Benoit et al., 2012). At this stage, patients may still be able to live independently, but, especially in organizational matters, some kind of support network is needed.

By the moderate stage of AD, memory deficits become very pronounced. Reasoning, planning and organization are heavily impaired. Reading, writing and comprehension are strongly affected by the loss of semantic memory. Episodic memory for most recent events is lost, often including anosognosia (loss of awareness of one's condition). Patients lose the ability to organize motor activity sequences until everyday actions such as dressing, preparing food or eating become impossible. Hallucinations and delusions occur in a significant minority of patients, as well as visual agnosias such as prosopagnosia (Reisberg et al., 1996). Difficulties with ostensibly easy tasks, coupled with anosognosia often lead to outbreaks of temper with verbal or physical aggression. At this point, institutionalization can be avoided only rarely where there is a strong socio-familial support network.

In the late stage of AD, specific cognitive and behavioural deficits become all but impossible to differentiate. Patients begin to lose even very early biographical memories and language is impaired to the point of incoherence. Aggression and restlessness occur in response to unfamiliar situations and environments and as a result of misunderstanding interventions. The development of extreme apraxia makes chewing and swallowing difficult, leaving the patient heavily dependent on institutionalized care. Median life expectancy following a diagnosis of AD ranges from 8.3 years for those diagnosed in their 60s to 3.4 years if diagnosed in their 90s (Brookmeyer et al., 2002), with the most common causes of death being pneumonia and ischaemic heart disease (Brunnstrom and Englund, 2009).

1.3.2 Pathology of Alzheimer's Disease

The post-mortem investigation of AD patients shows considerable global loss of cortical volume, which is especially evident in the hippocampus and surrounding temporal cortical regions, leading to greatly enlarged ventricles (Hyman et al., 1984). Now visible with brain imaging techniques such as MRI and PET, before post-mortem histopathology, this atrophy is generally most prominent in the hippocampus and parahippocampal gyrus, particularly in area CA1 and the subiculum, as well as layer II of the entorhinal cortex. Cell death in the entorhinal cortex results in a severance of the perforant path, which makes up the main cortical afferent to the hippocampus – a structure important in learning and memory – effectively disconnecting it from the cortex. In addition, cell loss in the subiculum and CA1 regions of the hippocampus greatly reduces hippocampal output pathways to the thalamus, hypothalamus, amygdala and cortex. The effective isolation of what few hippocampal cells remain from the rest of the brain, both in terms of afferent and efferent pathways, helps to explain not only the memory deficits, but also many of the other cognitive and non-cognitive impairments seen in the disease. It is important to note that this pattern of cell degeneration is specific to AD, and is not observed in normal ageing – even in very old age – or in any other age-related neurodegenerative condition (Hyman et al., 1984; West et al., 1994).

The pathological hallmarks of AD, the amyloid plaques and neurofibrillary tangles (NFTs), were first described by Alois Alzheimer in 1907 (Stelzmann et al., 1995) in the study of his patient, Auguste D. Post-mortem analysis of brain tissue from AD patients revealed intracellular plaques of tangled insoluble protein, now isolated and identified as aggregates of the peptide Amyloid-Beta (Aβ; Glenner and Wong, 1984), and long filaments and fibrils of aggregated protein, isolated and identified as tau protein (Grundke-Iqbal et al., 1986). The deposition of these protein aggregates has been well characterised, and tends to follow a pattern. Amyloid plaques begin forming in the medial temporal cortex, from there spreading to the hippocampus, amygdala and thalamus, before reaching the

neocortex in the later stages of the disease. By contrast, the deposition of NFTs begins in the locus coeruleus and spreads outwards into the amygdala and neocortex (Braak and Braak, 1991).

1.3.3 Diagnosis

The diagnosis of AD remains imprecise. Although a number of methods exist that are able to determine cases of dementia, it is more difficult to differentially diagnose AD specifically. Currently, even with modern neuroimaging techniques, the only way to truly identify whether a patient had AD is with post-mortem analysis, looking for the amyloid plaques and NFTs. However, it is more possible today to give a probable diagnosis of AD within a patient's lifespan, with a combination of neuropsychiatric, brain imaging and biochemical diagnostic methods.

Psychiatric methods are usually the first line of diagnosis, often occurring soon after the onset of noticeable symptoms. Psychiatric diagnosis of probable AD tended to be by exclusion, and often required a lengthy process of ruling out other dementias, depression and delirium, although it is possible now to determine with more certainty whether a patient has the disease using the DSM-IV (Diagnostic and Statistical Manual of Mental Disorders) diagnostic criteria. These methods are usually combined with thorough physical and neurological examination, as well as blood screens and radiography, to rule out other possible causes of dementia (Grossberg and Lake, 1998).

A more robust diagnosis, especially during the middle stages of the disease, can come from diagnostic imaging – either MRI or PET scanning. An MRI scan, often recommended for all patients with some kind of cognitive impairment, can not only rule out other causes such as meningioma or subdural hematoma, but can also provide positive diagnostic information about potential AD (Scheltens et al., 1995). The most commonly used method is a visual scale rating of medial temporal lobe atrophy, though volumetric analysis of the hippocampus can give a more quantitative result (Scheltens et al., 2016). Confirmation of AD pathology can be obtained using PET scans. Measuring glucose uptake by

neurons and glial cells using ^{18}F-fluorodeoxyglucose PET can be used to either rule out neurodegenerative diseases altogether, or, if the pattern of hypometabolism is temporoparietal, positively diagnose AD with impressive sensitivity and specificity (Bloudek et al., 2011). An alternative method is PET using ligands of Aβ – one of the key pathological hallmarks of the disease – which allow visualisation of areas of cortical amyloidosis. However, given that Aβ aggregation is not specific to AD (though it is necessary for a positive diagnosis) and is present in up to 35% of cognitively healthy individuals over 60 (Bennett et al., 2006; Rowe et al., 2007), Aβ-PET is more useful for exclusionary than inclusionary diagnosis.

Biochemical – blood and CSF (cerebrospinal fluid) – biomarkers have taken centre-stage recently as the most sought-after diagnostic tool for AD. In CSF, the traditional method is to look at levels of Aβ and tau protein, both key identifying features of AD. Levels of a common allomer of Aβ, $A\beta_{1-42}$, in CSF act as an approximate measure of its deposition in the brain, with lower CSF $A\beta_{1-42}$ correlating with greater plaque deposition in the brain as confirmed by autopsy (Tapiola et al., 2009). A meta-analysis of CSF $A\beta_{1-42}$ biomarker studies showed an average ratio of 0.56 between AD and controls (Olsson et al., 2016). Other allomers of the Aβ peptide such as $A\beta_{1-40}$ or $A\beta_{1-38}$ did not show significant differences between AD patients and controls. CSF tau, both total- and phosphorylated-, is arguably a better biomarker for AD, as meta-analyses suggest ratios of 2.54 and 1.88 respectively (Olsson et al., 2016), and a significant relationship between CSF tau and stages of NFT pathology (Tapiola et al., 2009). Other CSF molecules have been suggested as biomarkers and examined, including neurofilament light protein (NFL), neuron-specific enolase (NSE) and glial fibrillary acidic protein (GFAP), but none have yet stood up to rigorous analysis.

Suitable blood or serum biomarkers are even more difficult to identify, given the effect of the blood-brain barrier (BBB) and the ambiguity of the relationship between biomarkers in the blood and CSF. The naturally low levels of plasma $A\beta_{1-42}$ shows no discernible difference between AD and control, nor do $A\beta_{1-40}$, NSE, HFABP or NCP1 (Rosen et al., 2011; Zhang et al., 2013; Chiu et al., 2014; Olsson et al.,

2016). More recent research has looked into micro-RNA biomarkers, which can circulate the body without being degraded (Kosaka et al., 2010; Vickers et al., 2011), and have been implicated in AD pathogenesis (Hebert et al., 2008; Geekiyanage and Chan, 2011). A number of possible micro-RNA biomarkers have been identified, which are differentially regulated in AD and MCI (Mild Cognitive Impairment) patients (Geekiyanage et al., 2012; Femminella et al., 2015), however these are far from being reproducible, and sample handling and processing techniques need to be standardized to ensure accurate diagnosis. It seems likely that rather than one single micro-RNA, a comprehensive battery of micro-RNAs will need to be examined for optimum diagnostic sensitivity and specificity. Overall, blood-based (serum or plasma) biomarkers are preferable, given the highly invasive nature of CSF sampling, though the field remains incomplete.

1.4 Theories of AD

1.4.1 The Amyloid Hypothesis

The most enduring hypothesis of AD aetiology is the Amyloid Hypothesis, arising from the association between Aβ and AD pathology. This hypothesis proposes that AD is caused by aberrant metabolism of Amyloid Precursor Protein (APP), located on chromosome 21, to preferentially overexpress Aβ, leading to cellular and synaptic changes and eventually cell death. Amyloid-β is derived from proteolytic cleavage of APP sequentially by β- and γ-secretase. APP itself is a large, transmembrane protein thought to be involved in synapse formation and cell adhesion (Priller et al., 2006) and metal ion homeostasis (Barnham et al., 2003; Wong et al., 2014), ranging in size from 365 to 770 amino acids, although the 695 amino acid isoform is the most common in the brain (Chen et al., 2013). APP undergoes cleavage by a number of proteolytic enzymes called secretases, each of which gives rise to a different set of peptide and protein fragments with differing roles and effects.

Currently, there are eight confirmed and proposed cleavage sites on APP, each targeted by various secretases – the well-characterised alpha, beta, gamma, delta, epsilon and zeta, and the recently-identified but yet to be characterised eta and theta. Alpha-, beta- and gamma-secretases are believed to be the most relevant to AD. The most important alpha-secretase cleavage is by proteins in the ADAM family (A Disintegrin and Metalloproteinase domain-containing protein), especially ADAM10 (Lammich et al., 1999), while beta-secretase cleavage most often occurs by activity of BACE1 (beta-site APP cleaving protein 1) (Vassar et al., 1999). Gamma-, zeta- and epsilon- cleavage is performed by the presenilin-1 complex with nicastrin, APH-1 (anterior pharynx-defective 1), and PEN-2 (presenilin enhancer 2) (Kaether et al., 2006).

Alpha-secretase cleavage of APP occurs at residue 612 of the 695 amino acid isoform, releasing the extracellular N-terminal processed secreted APP-alpha protein (sAPPα) (Esch et al., 1990). The remaining C-terminal transmembrane part of APP (CTF) is further cleaved by γ-secretase to give rise to the amyloid intracellular domain fragment (AICD) and the transmembrane region fragment (p3). Beta-secretase (BACE1), on the other hand, cleaves APP at residue 596 of the 695 amino acid isoform to form secreted APP-beta (sAPPβ), with the remaining C99 CTF undergoing proteolysis by γ-secretase to form a range of Aβ peptides (36-43 amino acids) and the AICD. $A\beta_{1-40}$ and $A\beta_{1-42}$ are the most common alloforms, with the 42 amino acid species being the predominant constituent of amyloid plaques (Mann et al., 1996). There has been some suggestion that the cleavage site of γ-secretase, and therefore the alloform of Aβ produced, may be dependent on the location of metabolism - $A\beta_{1-40}$ may be produced from proteolysis in the trans-Golgi network, while $A\beta_{1-42}$ may be produced in the endoplasmic reticulum (Hartmann et al., 1997). It has also been suggested that intracellular APP metabolism is unique to neurons and this processing only occurs at the cell membrane in other cell types expressing APP (Tomita et al., 1998).

Far less is known about the other secretases and their cleavage sites. Delta-secretase, identified as asparagine endopeptidase (AEP), cleaves APP at two sites, N585 and N373, the former of which has

been demonstrated to enhance β-secretase activity and therefore production of Aβ species by up to 50% in primary cell cultures (Zhang et al., 2015). Epsilon (ε) secretase is even less understood and has yet to be fully identified, although its cleavage site is known to be at residues 49/50 of the C99 fragment (Weidemann et al., 2002). Eta (η) secretase is postulated to be Matrix Metalloproteinase 5 (MMP-5), which cleaves APP at M505, resulting in sAPPη and CTF-η, the latter is then metabolised by α- or β- and γ-secretase (Willem et al., 2015). One of its metabolic products, Aη-β, impairs hippocampal LTP *ex vivo*, but its physiological validity is yet to be determined, given that its activity is largely masked by BACE1. Zeta (ζ) secretase cleavage results in a 46 amino acid amyloid peptide and its secretase is believed to be a part of the presenilin/γ-secretase complex, but its biological relevance is unclear (Zhao et al., 2004). Theta (θ) secretase has been identified as BACE2 and cleaves APP downstream of the α-site, reducing Aβ production (Sun et al., 2006). However, similarly to η-cleavage, this is difficult to see without upregulating the enzyme, and whether it has any clinical or therapeutic significance is unknown.

The N-terminal protein sAPPα has been extensively investigated since the discovery of its neuroprotective properties (Goodman and Mattson, 1994), showing 100-fold greater ability to protect hippocampal neurons from excitotoxicity than sAPPβ (Furukawa et al., 1996). Furthermore, it has been demonstrated that sAPPα facilitates changes in gene expression, with downstream effects that include upregulation of trophic genes such as insulin-like growth factor 2 (IGF2), transthyretin (TTR) and NF-κB and regulation of pro-apoptotic and pro-inflammatory genes such as Bcl-2-associated death promoter (BAD) that, when phosphorylated, releases anti-apoptotic factors, ETS homologous factor (Ehf) and Granzyme B (GZMB) (Stein et al., 2004; Ryan et al., 2013).

It is inferred that AD develops as a result of an imbalance between α- and β-secretase cleavage of APP, the former having its neuroprotective and trophic downstream effects mitigated, while the latter's neurotoxic effects are amplified. Evidence for the Amyloid Hypothesis stems from a number of sources. Firstly, mutations in APP and presenilin 1 have been discovered in cases of familial early-onset

AD (Chartier-Harlin et al., 1991; Goate et al., 1991), and people with Down's syndrome, who carry three copies of chromosome 21, not only show amyloid pathology (Glenner and Wong, 1984b), but also often go on to develop early-onset AD-type dementia (Tyrrell et al., 2001). Furthermore, analysis of genetic risk factors for late-onset AD revealed that the ε4 allele of the Apolipoprotein E gene (ApoE4) and an allele of the microglial receptor TREM2 were significantly more prevalent in AD patients than in the general population (Farrer et al., 1997; Hickman and El Khoury, 2014). It was then discovered that ApoE and TREM2 are involved in clearing Aβ from the brain, and that the ε4 allele and the TREM2 variant produce species of the proteins that are less effective at this clearance (Jiang et al., 2008; Wang et al., 2015).

Aβ itself has been thoroughly researched and found to have profound effects on cellular function, not least in terms of neurotoxicity and interference with synaptic function. Aβ is highly prone to aggregation, progressing very quickly from a solution of monomers to form dimers and trimers, swiftly followed by higher-order oligomers and finally the fibrillary plaques characteristic of AD. Much debate has been had with regards to the relative toxicity and other effects of these aggregate species and the consistency of these aspects in a laboratory setting (see 1.4.2 below), although a majority consensus is that the smaller soluble oligomers are the most toxic species and these may be responsible for much of the pathology (Walsh et al., 2002b). In AD patients, *in vivo*, and in slice cultures, administration of exogenous Aβ impairs synaptic function – decreasing synaptic density (Davies et al., 1987; Shankar et al., 2007), impairing long-term potentiation (LTP; Walsh et al., 2002a; Wang et al., 2004) and facilitating long-term depression (LTD; Shankar et al., 2008). These effects are thought to manifest before the deposition of amyloid plaques. Further accumulation of Aβ of the fibrillary form leads to an inflammatory response, activating astrocytes and microglia and initiating processes that lead to neuronal atrophy – loss of dendritic spines, reduction in dendrite number and formation of axonal varicosities that interfere with normal neuronal function and eventually lead to extensive cell death (Tsai et al., 2004).

The amyloid hypothesis has undergone intensive scrutiny, with opponents citing the lack of correlation between amyloid plaques and disease progression, the presence of plaques in healthy adults and the failure of numerous clinical studies of drugs targeting Aβ (explored further in section 1.5). However, the hypothesis endures, and continues to be dominant in shaping research into the disease, both in terms of experimental models of AD and developing treatments and interventions (Reviewed in Selkoe and Hardy, 2016).

1.4.2 Protein Aggregation and Toxicity

One of the key aspects of the Amyloid hypothesis is the understanding that Aβ is highly prone to aggregation and that its toxicity, both *in vivo* and *in vitro*, is to some extent dependent on its aggregation state. Initial focus was on the fibrillary aggregates characteristic of the later stages of the disease, but more recent research has highlighted the importance of lower-order Aβ assemblies, in particular the soluble oligomers, comprising of 3-50 monomers. The amounts of these species correlate better with measures of disease progression than do the plaques (Dahlgren et al., 2002; Walsh et al., 2002b), and their levels are elevated in the brains of AD patients (Kuo et al., 1996). However, much of the literature on aggregation and toxicity is fraught with inconsistencies, as the Aβ peptide is notoriously difficult to work with.

Research has identified at least nine different stages of Aβ aggregation (Illustrated in Figure 1). Monomers represent the starting molecular species released by proteolytic degradation of APP, and are soluble amphipathic molecules with a molecular weight of around 4-5kDa. The conformation of Aβ monomers appears to be determined by the pH of its solvent. A pH of 1-4 and 7-10 is conducive to the α-helical conformation, while a pH of 5-6 tends to form β-sheet monomers (Fraser et al., 1992). Furthermore, the nature of the solvent has an impact, with organic solvents leaning towards α-helical conformations and aqueous solvents giving rise to the β-sheet conformation (Barrow and Zagorski, 1991; Fraser et al., 1992). However, it appears as though a combination of the two factors eventually

determines the final conformation (Reviewed in Serpell, 2000; Finder and Glockshuber, 2007). Common structural elements exist in all forms of Aβ monomer, however. Residues 6-8 and 23-27 of the sequence form β-"kinks" that dictate the remaining structure (Xu et al., 2005; Ahmed et al., 2010). The rest of the sequence folds in around these residues, leaving the N-terminal tail free. The central and C-terminal residues are mostly hydrophobic, and this character helps explain the capacity for aggregation of the peptide. $A\beta_{1-42}$ is significantly more prone to aggregation than $A\beta_{1-40}$, and its aggregates show greater neurotoxicity (Eisenhauer et al., 2000; Dahlgren et al., 2002; Zhang et al., 2002). This section will mostly focus on the $A\beta_{1-42}$ alloform.

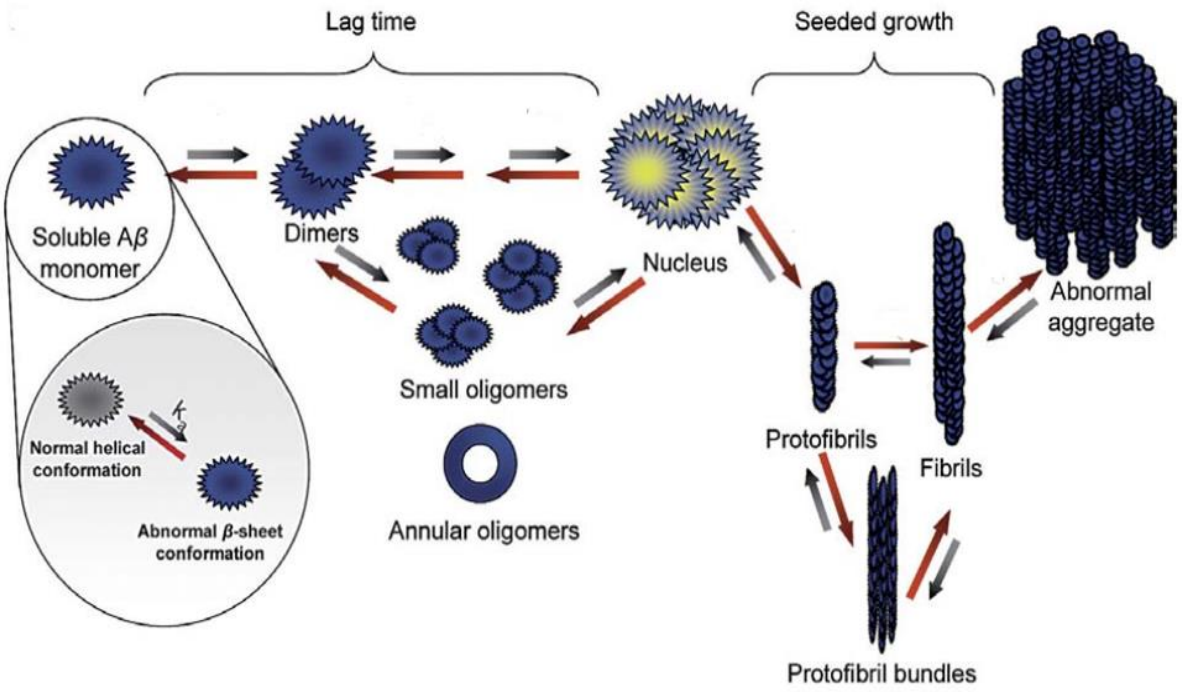

Figure 1: Diagram describing the progression of amyloid-beta aggregates. Soluble monomers form dimers, trimers and other small oligomers, which in turn aggregate to form protofibrils, fibrils and the large aggregates referred to as plaques. Image reproduced with permission from Finder and Glockshuber (2007). Copyright 2007 S. Karger AG, Basel.

Aβ dimers and trimers have been isolated from human (Roher et al., 1996) and mouse (Lesne et al., 2006) brain extracts, as well as *in vitro* preparations (Podlisny et al., 1995), and mark the first stage of aggregation. Dimers show some toxicity, but only in certain conditions, for example only in the

presence of microglia (Roher et al., 1996), while trimers have been shown to act as potent inhibitors of LTP (Townsend et al., 2006).

The next stage of aggregation is into small oligomers of approximately 3-50 subunits, which have been found *in vitro* and *in vivo* (Kuo et al., 1996; Walsh et al., 2002a). Depending on the conditions of their preparation, the form these oligomers take is variable, although they are almost exclusively more soluble than larger aggregates. Some groups have reported seeing disc-shaped pentamers and decamers forming in low-temperature and low-salt conditions (Ahmed et al., 2010), while others have demonstrated a wider range of oligomers, up to dodecamers (Bitan et al., 2003). These small soluble oligomers have been extensively investigated, both in terms of neurotoxicity and behavioural effects in animal models. Firstly, several groups have independently found that levels of soluble oligomers of Aβ better correlate with disease progression in AD than do insoluble fibrils and plaques (McLean et al., 1999; Wang et al., 1999). Second, application *in vivo* of soluble oligomers impairs memory and cognitive function in animal models (Cleary et al., 2005; Lesne et al., 2006). Third, several groups report that these aggregates induce much more significant cell death in primary cells and immortal cell lines than larger aggregates (Dahlgren et al., 2002; Ahmed et al., 2010) although others dispute these findings (Wogulis et al., 2005). This combined evidence suggests that these soluble $A\beta_{1-42}$ oligomers are responsible for much of the cellular damage and systemic impairment seen in AD.

Protofibrils and fibrils make up the ante- and penultimate stages of $A\beta_{1-42}$ aggregation. Protofibrils are flexible, rod-like structures that are considered to be direct precursors of mature fibrils (Walsh et al., 1997). Protofibrils are thought to form a regular parallel β-sheet hairpin conformation (Ahmed et al., 2010), and have been demonstrated to fall out of this structure in equilibrium with smaller oligomers in a concentration, pH and temperature-dependent manner (Walsh et al., 1999; Arimon et al., 2005). The neurotoxicity of protofibrils has been reported in several studies (Hartley et al., 1999; Ahmed et al., 2010), but others have failed to replicate these findings (Wogulis et al., 2005). Multiple protofibrils aggregated together make up fibrillary Aβ, although their overall three-dimensional structure varies

according to the aggregation conditions (Petkova et al., 2005). It has been observed that fibrils formed by *in vitro* aggregation are similar to those extracted from human AD plaques (Kirschner et al., 1987). With regards to the neurotoxicity of fibrils, while some studies have reported that application of Aβ fibrils causes cell loss, astrocytosis and microgliosis (Stephan et al., 2001), others suggest that only soluble oligomers have these toxic effects (Nimmrich et al., 2008; He et al., 2012). Other groups have suggested that neither soluble nor fibrillary Aβ alone are sufficient to induce marked cell loss, but rather both forms are necessary (Wogulis et al., 2005).

Overall, the literature on Aβ aggregation, while extensive, is conflicted. While there seems to be some agreement that the soluble oligomers of the peptide are the most neurotoxic species, the methods used to either isolate or prepare them for laboratory use vary wildly (e.g. Fraser et al., 1991; Wogulis et al., 2005; Ahmed et al., 2010). Many groups tend to use simple "ageing" protocols in order to produce toxic aggregates – lyophilized powder reconstituted in water or NaOH and phosphate-buffered saline (PBS) and aged for 3 days at 37°C (Howlett et al., 1995; Hartley et al., 1999; Wogulis et al., 2005). While this is believed to be a consistent protocol for fibril formation, it seems that it is not the only one. Some groups report consistent fibril formation by dimethyl sulfoxide (DMSO) disaggregation followed by addition of HCl and ageing at 37°C for 24 h, while ageing at 4°C for 24 h seems to result in smaller oligomeric peptides (Hartley et al., 1999; He et al., 2012). Other protocols include dissolution in physiological salt buffer and incubation at 37°C for up to 12 days (Ahmed et al., 2010). Similarly, some groups report protofibril and low molecular-weight oligomer formation by 2-3 days of ageing at room temperature followed by separation by size-exclusion chromatography (Hartley et al., 1999). Globular oligomeric species have been observed following 24-h ageing in PBS/SDS at 37°C (Nimmrich et al., 2008) and mid-size oligomers have been prepared by dissolution in low-salt buffer and kept at 4°C for 6 h (Ahmed et al., 2010). The literature is further complicated by the use of different allomers of Aβ, with $A\beta_{1-40}$ aggregating differently compared to $A\beta_{1-42}$ (Garai et al., 2006, 2007; Solomonov et al., 2012). Whether findings with one allomer can be related to others is

unclear. This leads to difficulties in interpreting data, as well as for planning experiments using amyloid peptides.

Furthermore, a technical caveat exists with regards to experimental techniques evaluating the effects of Aβ. It has been noted that the 3-(4,5-dimethylthiazol-2-yl)-2,5-diphenyltetrazolium bromide (MTT) assay has an interesting interaction with Aβ specifically, such that the use of the MTT assay with Aβ as the insult may give inaccurate estimates of cell viability (Shearman et al., 1995; Hertel et al., 1996; Wogulis et al., 2005), in turn suggesting that the interpretation of results obtained from such experiments may be brought into question. This is an important factor to consider when reading literature, since the interaction has been reported as early as 1995, and yet even in 2015, groups continue to use this combination of assay and insult.

1.4.3 The Tau Hypothesis

Alongside extracellular amyloid beta plaques, intracellular aggregates of hyperphosphorylated tau are one of the main hallmarks of AD. The tau hypothesis of AD suggests that the pathogenesis of the disease is more due to hyperphosphorylation and aggregation of the tau protein than of Aβ. The intracellular tangles observed by Alois Alzheimer in his post-mortem studies were finally identified in 1986 as aggregates of axonal microtubule-associated protein tau, an important cytoskeletal protein involved in stabilizing microtubules (Wood et al., 1986). The stabilizing effect of tau is modulated by its phosphorylation, with greater phosphorylation leading to a reduction in tau binding to microtubules and greater microtubule instability (Rodriguez-Martin et al., 2013). It has been suggested that pathological changes in tau phosphorylation are the early-stage triggers for the development of further AD pathology, and the amyloid pathology is a downstream effect (Maccioni et al., 2010). Not only does tau pathology appear at very early stages of AD, but it also appears to correlate with cognitive impairment (Maeda et al., 2006) and is a more effective CSF biomarker (Olsson et al., 2016). It has also been demonstrated that the tau protein constituting the NFTs in AD

brains is phosphorylated to the point of insolubility (Johnson and Stoothoff, 2004). Furthermore, reducing or knocking-out tau in animal models increases resistance to Aβ-induced toxicity (Rapoport et al., 2002; Roberson et al., 2007). It is therefore possible that pathological tau phosphorylation and aggregation may, in fact, cause Aβ toxicity by its absence. However, the main inconsistency with the tau hypothesis is the knowledge that no known forms of early-onset AD have genetic components involving tau directly – the vast majority carry mutations directly or indirectly relating to amyloid pathology.

1.4.4 The Vascular Hypothesis

This hypothesis suggests that AD is a vascular disorder, caused by impaired cerebral perfusion and circulation (de la Torre and Mussivand, 1993). Most of the risk factors associated with AD – ageing, atherosclerosis, stroke, diabetes mellitus, smoking, high cholesterol, cardiac disease, hyper- and hypo-tension and high fat intake – are vascular in nature (Breteler, 2000), and also common risk factors for vascular dementia, which is difficult to differentially diagnose (Bowler et al., 1997; Ransmayr, 1998). Furthermore, one of the clinical hallmarks of early MCI is hypoperfusion, and this strongly correlates with later conversion to an AD diagnosis (Johnson et al., 1998). Similarly, it has been suggested that altered and lowered metabolism of specific pathways occurs prior to either amyloid or tau pathology, leading to impaired synaptic function (Hatanpaa et al., 1996). Considering the evidence that hippocampal regions are highly susceptible to oxygen deprivation (Burmester et al., 2000), this may help explain why more overt neuropathlogy manifests in these areas.

1.4.5 Neuroinflammation in AD

A number of studies have suggested that neuroinflammation may play an important role in AD. First, immune cell activation has been reported around plaques in the AD brain, in particular microglia (Rogers, 1998), and cultured microglia accumulate around and internalize Aβ (Bard et al., 2000; Lue et

al., 2001b). Furthermore, Aβ induces expression of many pro-inflammatory mediators such as reactive oxygen species (ROS), macrophage inflammatory proteins (MIP) and other cytokines and chemokynes (Lue et al., 2001a; Walker et al., 2001), whose elevation in AD brains correlates with areas of pathology (Reviewed in Rogers et al., 2007). It is therefore proposed that dysregulation of the brain's immune system may lead to microglial hyperactivity and subsequent damage to neurons, a phenomenon observed in animal models (e.g. Cunningham et al., 2005).

1.4.6 Metal Ion Homeostasis

Recently, a novel hypothesis of AD aetiology and pathogenesis has been developed, that hopes to combine several aspects of the Amyloid Hypothesis with new evidence implicating metal ions – in particular the transition metals zinc, iron and copper – in the disease. It has been reported that the AD brain undergoes significant changes to metal ion homeostasis (Reviewed in Barnham and Bush, 2014; Ayton et al., 2015). To summarise, levels of cortical zinc are significantly elevated in AD patients, and this elevation is strongly correlated with disease progression, and in particular amyloid plaque burden (Religa et al., 2006). In fact, amyloid plaques in AD brains and those of APP transgenic mice contain tremendously high concentrations of zinc (>1mM), iron (~1mM) and copper (~400μM) (Lovell et al., 1998; Falangola et al., 2005; Jack et al., 2005) and furthermore, the highest density of amyloid plaques in APP/PS1 transgenic mice are found in regions of the cortex with the highest levels of exchangeable zinc (Stoltenberg et al., 2007). Zinc is also significantly increased in the soluble fraction and synaptic vesicles of AD patients, but notably not in those individuals showing AD neuropathology (amyloid plaques), without the accompanying memory and behavioural deficits (Bjorklund et al., 2012). In addition, levels of zinc transporters – ZnT1, 3, 4, 6 – have been demonstrated to be altered in AD brains, showing a pattern of region- and disease-severity-dependent dysregulation (Lovell et al., 2005; Adlard et al., 2010; Lyubartseva et al., 2010), and ZnT3 knock-out mice show very similar behavioural deficits to other murine AD models (Adlard et al., 2010).

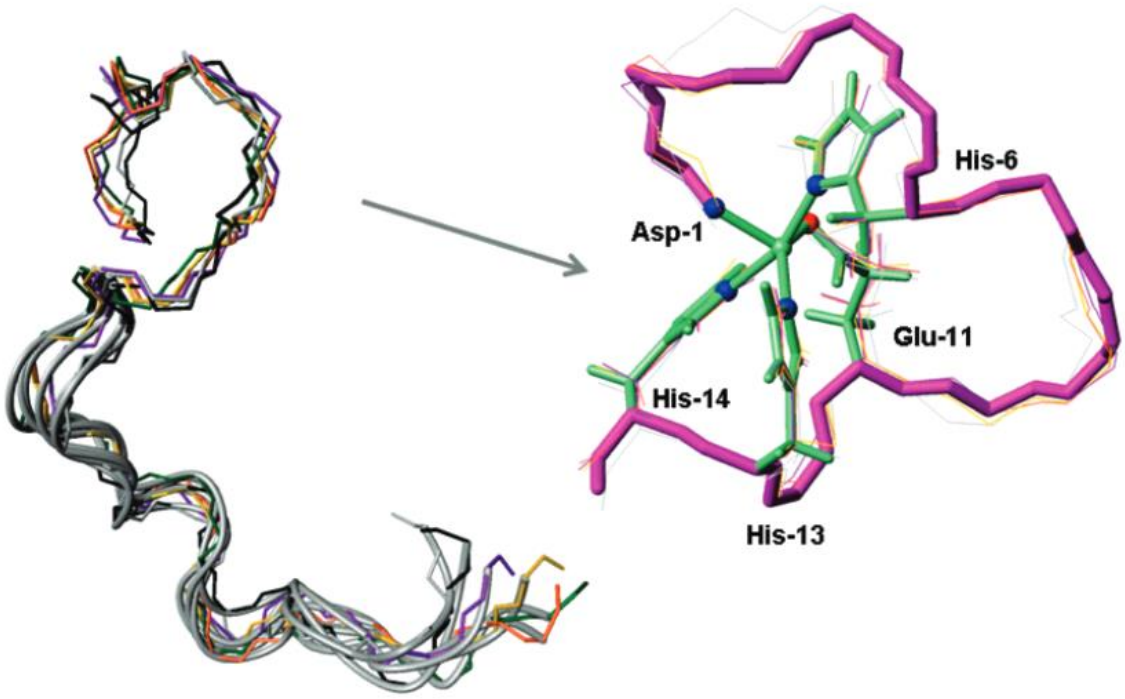

Figure 2: Graphical representation of $A\beta_{1-28}$ conforming around a Zn^{2+} ion (right; in green) from data obtained by NMR and molecular dynamics simulations. The amino acid residues Asp-1, His-6, Glu-11, His-13 and His-14 coordinate pentamerically around the metal ion. Image reproduced with permission from (Gaggelli et al., 2008). Copyright (2008), American Chemical Society.

Further evidence comes from the Aβ peptide itself. The difference between α- and β-secretase cleavage, and in turn the production of amyloidogenic Aβ and neuroprotective sAPPα, is a 16 amino acid peptide sequence that makes up the N-terminal of sAPPα and the C-terminal of Aβ. This so-called 16mer has been itself studied for its potential neuroprotective properties, but the interesting aspect of the sequence is the identification by NMR of five residues involved in the binding of Zn^{2+} ions (in the human sequence) – Asp-1, His-6, Glu-11, His-13 and His-14 (Gaggelli et al., 2008) – amino acids common to both the toxic Aβ and the neuroprotective sAPPα (Figure 2). Though not much is understood about the conformation of sAPPα with metal ions, it has been shown that in certain peptides, this sequence conforms around the zinc ion in a pentameric structure, with each amino acid contributing to its binding. Initial exploration of this had focused on the His-13/14 zinc-binding motif. Substitution of these two amino acids yielded no effect on the neuroprotective ability of sAPPα (Singh,

2010). However, since the zinc binding in the sequence is pentameric, rather than relying solely on this motif, it seems likely the other zinc-binding residues can compensate for the loss of two amino acids. Aβ also binds copper and the 16mer contains 4 Cu^{2+} binding sites – Asp-1, His-6, His-13 and His-14 (Drew and Barnham, 2011; Faller et al., 2014) – which, similar to zinc, help explain the co-precipitation of copper in amyloid plaques (Lovell et al., 1998).

In vitro, Zn^{2+} has been shown to interact with and alter the behaviour of Aβ. When aged in salt buffer at pH 7.4, addition of $ZnCl_2$ eliminated the production of $Aβ_{1-42}$ soluble oligomers, as well as decreasing the solubility of the peptides (Garai et al., 2006), leading to accelerated aggregation kinetics and the preferential precipitation of higher-weight aggregates (Garai et al., 2007). Further, Aβ-induced cell death is significantly decreased by addition of 8μM $ZnCl_2$, showing a 50% reduction in the toxicity of 10μM $Aβ_{1-42}$ at 9 h, and a 30-40% reduction of 50μM $Aβ_{1-42}$ toxicity at 4 h (Garai et al., 2007). On the other hand, ageing of $Aβ_{1-40}$ with $ZnCl_2$ is supposed to form quasi-spherical oligomers which actually significantly increase Aβ-induced cell death, reducing cell viability by over 80%, compared with only 10-15% by Zn-free $Aβ_{1-40}$ (Solomonov et al., 2012). While this research highlights some inconsistencies in the behaviour of amyloid peptides, generally the evidence suggests a strong involvement of metal ions, Zn^{2+}, in particular, in the pathogenesis of AD.

With regards to biological copper, it has been noted that a reduction of intracellular copper can markedly increase secretion of Aβ, with the proposed mechanisms of either influencing APP cleavage by β-secretase or by inhibiting the intracellular degradation of Aβ (Cater et al., 2008), while application of exogenous copper to cells inhibits Aβ production and promotes α-secretase cleavage of APP (Borchardt et al., 1999). This relationship is notable, as mentioned above, since brain copper levels decrease with old age (Religa et al., 2006) and are especially low in patients with AD (Deibel et al., 1996; James et al., 2012). Counterintuitively, low cortical copper causes enrichment of copper in the cell membrane, where it complexes with Aβ (Hung et al., 2009) and may contribute to the creation of reactive oxygen species (ROS), especially H_2O_2 (Opazo et al., 2002; Nelson and Alkon, 2005; Puglielli et

al., 2005). Copper at different concentrations alters the aggregation of Aβ. At stoichiometric or greater concentrations, Cu^{2+} prevents fibril formation of both $A\beta_{1-42}$ (Mold et al., 2013) and $A\beta_{1-40}$ (Jun et al., 2009; Pedersen et al., 2011), preferentially inducing formation of dimers (Bush et al., 1994). At lower concentrations, on the other hand, Cu^{2+} promotes fibril formation (Huang et al., 2004; Sarell et al., 2010; Pedersen et al., 2011). Furthermore, Cu^{2+} increases Aβ-induced neurotoxicity, believed to be as a result of H_2O_2 production (Huang et al., 1999; Cuajungco et al., 2000).

Iron also plays a role in AD directly, by affecting the metabolism of APP, through promotion of amyloidogenic processing (Becerril-Ortega et al., 2014), and potentially by promoting aggregation and cytotoxicity of Aβ (Huang et al., 2004; Liu et al., 2011). Furthermore, iron has an interaction with tau, promoting its aggregation (Ledesma et al., 1995), and since tau is involved with APP in iron trafficking (Lei et al., 2012), this relationship may underlie the intracellular retention of iron seen in AD brains (Goodman, 1953). High levels of intracellular iron also promote oxidative stress leading to synaptic dysfunction and cell death (Mattson, 2004), even inducing apoptotic processes (Salvador et al., 2010).

The metal ion homeostasis hypothesis of AD, developed by Ashley Bush and Kevin Barnham, proposes that AD is as much a metallopathy as a proteopathy. They suggest that since metal ion homeostasis becomes perturbed in normal ageing, it seems logical that this may be a contributing factor to the development of AD. The change in levels and compartmentalisation of metal ions in the brain – zinc, copper and iron – is thought to occur prior to any of the protein pathology, evidenced by the finding that altered levels of these metals, either by addition of exogenous compounds or chelation by pharmacological agents, has a profound impact on the aggregation and toxicity of Aβ. Once amyloidogenic processing has begun, the co-localization of Zn and Cu with Aβ is believed to induce oxidative stress on cells, ostensibly by the production of H_2O_2. Furthermore, co-precipitation of these metal ions with Aβ may deprive other metalloproteins of their co-factors, and such a relationship is supported by the finding that the activity of Cu- and Zn-dependent enzymes cytochrome c oxidase (COX), peptidylglycine α-amidating monooxygenase (PAM) and Cu/Zn-superoxide dismutase (Cu/Zn-

SOD) are significantly changed in the AD brain and those of APP transgenic mice (Famulari et al., 1996; Maurer et al., 2000; Bayer et al., 2003). While this hypothesis currently has no explanation for the aetiology of AD, it does have a reasonable explanation for contributing to its pathogenesis, though the progress of clinical interventions based on it (*vide infra*) will be its biggest challenge.

1.5 Past, Present and Developing Treatments

1.5.1 Pharmacological Intervention

Among the first approved treatments for AD were simple pharmacological manipulations of neurotransmitters. One of the earlier neuropharmacological findings with relation to AD was the discovery of profound changes to the levels of acetylcholine (ACh) and the activity of NMDA glutamate receptors. ACh synthesis is significantly reduced in the AD brain (Sims et al., 1980) and it was originally thought that targeting ACh metabolism might help alleviate some symptoms of AD. As such, a number of ACh-targeting compounds were developed. The first was Tacrine (Cognex), an acetylcholinesterase inhibitor (AChEI) that increases ACh tone. While clinical trials showed some improvements in cognition and memory, reduced likelihood of institutionalization and improved quality of life, these effects were short-lived and the medication induced significant peripheral side effects such as nausea and vomiting, diarrhoea, headaches, dizziness and some hepatotoxicity (Knopman et al., 1996). Donepezil, another AChEI, showed better and longer-lasting clinical outcomes and slightly reduced peripheral side-effects, but also in some patients cause bradycardia and vivid dreams (Rogers, 1998; Rogers et al., 1998). Even later versions of AChEIs, Rivastigmine and Galantamine, were better tolerated compared with Tacrine and Donepezil (Gottwald and Rozanski, 1999; Tariot et al., 2000), though it has been suggested that the positive effects of Galantamine may be more likely due to its role as a nicotinic ACh receptor agonist, rather than as an AChEI (Samochocki et al., 2003). Donepezil, Rivastigmine and Galantamine

remain FDA-approved drug treatments for AD, although they tend to only be effective in mild-to-moderate cases and only for a short period.

The other neuropharmacological aspect of AD is glutamate excitotoxicity, thought to result from an interaction of N-methyl-D-aspartate (NMDA) receptors with Aβ (Tominaga-Yoshino et al., 2001). To combat this neurotoxicity, a number of NMDA receptor antagonists have been clinically examined, of which the most successful was Memantine, which was even able to moderately slow and slightly improve cognitive and memory decline in moderate-to-severe AD, though its side effects include confusion, dizziness, drowsiness, insomnia and even, in few cases, hallucinations (Reisberg et al., 2003). Memantine remains a recommended treatment strategy for moderate-to-severe AD and those with intolerance of or contraindication for AChEIs. Regardless, all these drugs are only effective at treating symptoms - temporarily slowing the cognitive decline in AD, and none are as yet able to halt or reverse disease progression.

1.5.2 Targeting Amyloid-Beta

A different approach was taken with other pharmacological agents. Since the Amyloid Hypothesis suggests that AD is characterised by aberrant processing of APP to preferentially form Aβ, several drugs were developed aiming to inhibit the action of β-secretase, simultaneously reducing the formation of Aβ and potentially consequentially promoting formation of neuroprotective sAPPα. The first developed of these types of agents were Rosiglitazone and Pioglitazone, which suppressed β-secretase expression and promoted phagocytosis of Aβ in animal models (Mandrekar-Colucci et al., 2012). While initial clinical trials showed some promising results in improving cognition and memory, there soon emerged several important caveats. Rosiglitazone only saw some effectiveness in individuals not carrying the APOEε4 allele (Risner et al., 2006; Gold et al., 2010), while Pioglitazone only worked in individuals with type II Diabetes Mellitus (Hanyu et al., 2009; Sato et al., 2011). However, both these drugs showed significant side effects of bone weakness, hypoglycaemia, fluid

retention, peripheral oedema, heart failure and ischaemic cardiac events, stroke, macular oedema, hepatotoxicity and bladder cancer. Given these adverse effects and the insufficient evidence for positive effects, it was recommended these drugs not be approved for clinical use, and approval was removed from all countries by 2011 (Miller et al., 2011).

The next family of Aβ-targeting compounds to be tested were two direct β-secretase inhibitors – CTS-21166 and LY2811376 (Reviewed in Mikulca et al., 2014). CTS-21166 acts as a transition-state analogue inhibitor and showed promising results in animal studies in APP transgenic mouse models, significantly lowering Aβ levels and plaque load. A proof-of-concept study in humans showed a reduction in plasma Aβ levels. LY2811376 is a highly selective competitive inhibitor of BACE1 and similarly showed positive results from animal studies, significantly reducing cortical β-secretase cleavage of APP (May et al., 2011). Again, this compound initially showed a good reduction in plasma Aβ in human patients. However, continuing animal studies noted severe side effects of retinal degeneration. Neither of these drugs have undergone further clinical trials, and safety results from either Phase I trial have not been released.

Alternatively, pharmacological manipulation of α-secretase seemed a promising strategy, potentially both inhibiting production of Aβ and promoting neuroprotective sAPPα. As such, an α-secretase activator EHT0202 (Etazolate) was tested in a Phase IIA randomized, placebo-controlled, double-blind study. Despite showing good safety and tolerability, there were no reported cognitive improvements and no further trials have been published (Vellas et al., 2011). Similarly, attempts to combat Aβ aggregation into higher molecular-weight species, for example by the anti-aggregant homotaurine (Tramiprosate), have shown mixed results. Tramiprosate was shown in preclinical trials to bind soluble Aβ, prevent the formation of fibrils, decrease $A\beta_{1-42}$-induced cell death in cell cultures and inhibit amyloid deposition (Gervais et al., 2007). However, while tramiprosate showed promising safety and tolerability results (Aisen et al., 2007), the most recent Phase III trials revealed clinically meaningful benefits only in patients with the APOEε4 genotype (Alzheon, 2016). All-in-all, success of treatments

targeting Aβ have been limited at best and dangerous and life-threatening at worst. None are currently FDA-approved for treating AD. To some, this may be considered a damning indictment of the Amyloid Hypothesis of AD, but otherwise suggests alternative methods are required.

1.5.3 Immunotherapy

Another approach to treat AD has been immunotherapy – attempting to augment or supplement the innate immune system to clear Aβ from the brain or arrest its aggregation. These treatments generally take two forms – either via passive immunity with "vaccines" against Aβ peptides to promote endogenous antibody production or direct treatment with exogenous monoclonal Aβ antibodies to promote the clearance or halt aggregation of the endogenous peptide. The Aβ vaccines were highly effective in animal models of AD, successfully attenuating AD-like pathology and behavioural deficits in APP transgenic mice (Schenk et al., 1999; Janus et al., 2000; Morgan et al., 2000). However, human clinical trials proved less fruitful. While mostly the developed vaccines, using aggregated $A\beta_{1-42}$ peptide, were found to be relatively safe and tolerable in Phase I clinical trials, their progression to Phase IIa trials were fraught with difficulty. Not only were the vaccines shown to be significantly less effective than in animal models, but a number of patients who received the AN1792 vaccine developed meningoencephalitis, caused by an immune response and further trials were abandoned due to understandable safety concerns (Orgogozo et al., 2003).

The monoclonal antibody treatments encompass bapineuzumab, solanezumab and most recently aducanumab. These antibodies penetrate the brain and react with Aβ aggregates, encouraging their clearance. Bapineuzumab and solanezumab showed acceptable safety and tolerability in Phase II trials, but no clinically significant changes in primary cognitive outcomes, though the latter showed some small treatment differences in biomarkers in APOEε4 allele carriers (Doody et al., 2014; Salloway et al., 2014). Aducanumab, though having only just completed a Phase II clinical trial, showed far better responses to treatment. Amyloid plaque load was significantly reduced after one year of

monthly intravenous injections and this was accompanied by a significant slowing of cognitive decline as measures by the Clinical Dementia Rating – Sum of Boxes (CDR-SB) and Mini Mental State Examination (MMSE) scores (Sevigny et al., 2016). Notably, this antibody differs from the others in that it shows a more effective binding to both insoluble fibrils and plaques and soluble oligomers. Some adverse effects were noted, especially in the highest dosage group (10mg kg^{-1}), with the most common were ARIA (amyloid-related imaging abnormalities) and headaches. The authors are optimistic that the slowing of cognitive decline will be confirmed in the ongoing Phase III trials.

1.5.4 Metal Protein Targeting Compounds

The development of the metal ion homeostasis hypothesis of AD over the last 15-20 years has also led to the development of novel pharmacological treatments targeting biological metals. Their goal is to restore normal compartmentalization of biological metals, especially Zn and Cu. These compounds, termed metal protein attenuating compounds (MPACs), are not chelators in the strictest sense of the word – rather they ligate metal ions and redistribute them to other cellular compartments. Clioquinol was one of the first examined for its effectiveness in AD. It is a small organic molecule capable of penetrating the brain and showing moderate affinity for both Cu^{2+} and Zn^{2+} (Ferrada et al., 2007). It has been shown to inhibit aggregation of Aβ and reduce production of ROS by its interaction with metal ions, as well as decreasing amyloid plaque burden in Tg2576 mutant mice expressing the Swedish mutant of APP (Cherny et al., 2001). In human phase II clinical trials clioquinol was able to significantly reduce cognitive decline (Ritchie et al., 2003). Further trials were discontinued due to unrelated manufacturing problems.

The “next generation” of MPACs came in the form of PBT2, which showed improved solubility and bioavailability compared with clioquinol. Preclinical *in vivo* trials reported greater efficacy at improving cognitive performance in APP/PS1 and Tg2576 mice models, along with reduction in amyloid plaque burden and tau phosphorylation (Adlard et al., 2008). Phase II human clinical trials were successfully

completed, showing good tolerability and safety, reduction in CSF $A\beta_{1-42}$, as well as slight improvement in certain cognitive test scores (Lannfelt et al., 2008; Faux et al., 2010). Most recently, a 12-month phase II PET study found that the PBT2 group showed a significant decline in cortical Aβ signal, though this stabilised in the 12-month extension study (Villemagne et al., 2016). Further examination of these compounds revealed evidence as to their mechanism of action, and it is now suggested that they act not as chelators, but by transporting Zn and Cu into cells, where the metals set off a neuroprotective signalling cascade, leading to degradation of Aβ (White et al., 2006; Caragounis et al., 2007), inhibition of tau phosphorylation by activating GSKβ (Crouch et al., 2011) and promoting neurite growth and dendritic spine density (Adlard et al., 2011). While phase III clinical trials are still some way off for PBT2, these data prove encouraging, and may help integrate metal ion homeostasis into more mainstream theories and therapies for AD.

1.6 A Physiological role for Amyloid-Beta

For a long time, the Aβ peptide was, by many, considered a redundant metabolic by-product of APP catabolism, lacking a normal physiological function. However, recent research has found that not only does it have numerous interactions with receptors and other molecules, but it may also be modulated in response to certain physiological events and may play an important role in several areas of normal brain function. As outlined below, Aβ has been implicated in the innate immune system, in the brain's response to oxidative stress, in learning and memory, and in brain growth and development.

1.6.1 Anti-bacterial Role

In investigating a potential role for Aβ in health, it was noted that the peptide shares remarkable similarities in its physiochemical and biological properties with a group of compounds called antimicrobial peptides (AMPs). AMPs are a part of the innate immune system, and show effective, broad-spectrum antibiotic activity targeting both Gram-negative and Gram-positive bacteria, as well

as viruses, fungi, protozoans and even malignant host cells (Nguyen et al., 2011). Mammalian AMPs are divided into three broad groups – defensins, histatins and cathelicidins. The human cathelicidin LL-37 has been demonstrated to show similar biochemical behaviour to Aβ, notably a tendency to form neurotoxic oligomers (Oren et al., 1999) and insoluble fibrils (Sood et al., 2008). In a comparison of antimicrobial efficacy between LL-37 and Aβ, it was found that the latter not only compared favourably with LL-37 against seven clinically relevant organisms, including *Candida albicans*, *Escherichia coli* and *Staphylococcus aureus*, but was actually more effective at inhibiting bacterial growth of three of the pathogens (Soscia et al., 2010). The same effect was seen using human AD brain homogenate containing Aβ. This has been further confirmed – increasing survival of mice with meningitis caused by *Salmonella typhimurium*, increasing survival of *Caenorhabditis elegans* infected with *C. albicans*, and protecting cultured H4 (human brain neuroglioma) and CHO (Chinese Hamster ovary) cells from the same (Kumar et al., 2016). Furthermore, this latest work suggests that the protective effect of Aβ is dependent on its ability to aggregate into oligomers and fibrils, which promote pathogen binding and entrapment.

1.6.2 Anti-oxidant Properties

Closely tied to metal ion homeostasis is the theory that Aβ plays a role in mitigating oxidative damage due to oxidative stress. It is believed by some that the physiological role of Aβ is linked to its ability to sequester metal ions, in particular Cu and Zn, via the metal binding sites located at its N-terminal part. This sequestration is thought to activate the redox properties of the peptide, including reduction of the metal ions and catalysing the dismutation of superoxide (O_2^-) to H_2O_2 (Zou et al., 2002). Increased Aβ production leads to a decrease in ROS production in cell culture (Gibson et al., 2000) and increases resistance to metal-induced oxidation in transgenic mice (Leutner et al., 2000). On the other hand, reducing Aβ production in mutant mice and cell cultures leads to increased ROS production and activation of apoptotic pathways (Guo et al., 1999a, 1999b). This evidence suggests the importance of

monomeric Aβ, bearing in mind its affinity for transition metal binding, in controlling metal ion homeostasis and alleviating oxidative stress in the brain by either direct or indirect reduction of ROS.

1.6.3 Amyloid-Beta in Learning and Memory

It has been suggested that far from its pathogenic effects when aggregated, endogenous Aβ may play an important role in the modulation of learning and memory. Despite nanomolar to micromolar concentrations of Aβ having severe deleterious consequences on LTP (Cleary et al., 2005; Shankar et al., 2008), it has been found that much lower concentrations – in the picomolar range or at physiological concentrations – may in fact facilitate synaptic plasticity, or at least play an important role in the acquisition of memory. Firstly, depletion of endogenous Aβ by antibodies disrupts memory retention in an inhibitory avoidance task in rats, while treatment with exogenous $A\beta_{1-42}$ was sufficient to restore memory retention to near control levels. Second, application of exogenous $A\beta_{1-42}$ peptide significantly improved memory retention (Garcia-Osta and Alberini, 2009). Third, APP knockout mice not only show severe cognitive deficits, but also significantly impaired LTP (Dawson et al., 1999; Morley et al., 2010). It believed that these memory-enhancing (or facilitating) effects may be through an interaction of Aβ with the nicotinic ACh receptor (nAChRs), to which it binds (Wang et al., 2000), since nAChR antagonists mimic the memory inhibition seen with anti-Aβ antibodies (Garcia-Osta and Alberini, 2009). This may also help explain why Aβ is localised to synapses (Fein et al., 2008), from where it can act on receptors.

1.6.4 Amyloid-Beta as a Neurotrophic Factor

Research has identified that in certain situations and under certain conditions, Aβ has considerable neurotrophic effects. This was highlighted by the finding that in cases of acute brain injury, levels of brain interstitial fluid (ISF) Aβ were strongly correlated with neurological status and recovery (Brody et al., 2008). When neurological status improved, the ISF concentration of Aβ was increased and *vice*

versa. *In vitro*, Aβ addition to cell cultures induces an enhancement of glucose metabolism, activating hypoxia inducible factor 1 (HIF-1), part of a significant network of neuroprotective and neurotrophic molecules that also includes VEGF and erythropoietin (Soucek et al., 2003). Furthermore, adding exogenous $A\beta_{1-42}$ to cultured rat cortical cells protects them from NMDA excitotoxicity and insulin deprivation, well-established paradigms of neuronal stress (Giuffrida et al., 2009). This is believed to be via the interaction of the peptide with either the PI-3-K pathway, involved in cell growth and survival (Giuffrida et al., 2009), or by interacting with cellular prion protein (PrP(C)), a known receptor for Aβ and mediator of NMDAR activity (Black et al., 2014). In addition, Aβ has been demonstrated to interact with other known neurotrophic pathways. The peptide upregulates brain-derived neurotrophic factor (BDNF) release from astrocytes (Kimura et al., 2006), potentially by its action as a p75(NTR) antagonist, a growth factor receptor whose activation activates apoptotic pathways (Arevalo et al., 2009) or by activating TrkB receptors, whose primary role is one of cell survival, differentiation and synaptic plasticity (Lopez-Toledo et al., 2016).

All the above evidence implicates a role for Aβ in normal brain function and even in modes of protection. However, the levels of Aβ required for these positive effects always appears to be in the low-nanomolar to picomolar range, and even this literature agrees that higher concentrations of Aβ tend to be more toxic than trophic. Nevertheless, there is clear evidence that in the non-diseased brain, Aβ has important roles to play in protection, neurotrophy and synaptic plasticity, as well as potentially being an important part of the brain's innate immune system.

1.7 Aims

With the evidence that metal ions, in particular Zn^{2+}, are linked so closely to theories of AD aetiology and pathogenesis, this research aimed to better understand the relationship between zinc and Aβ. In fact, metal ion dyshomeostasis seems to play a role in a number of different theories of AD pathology. As described above, Zn^{2+}, Fe^{3+} and Cu^{2+} homeostases are disturbed in AD, leading to aberrant compartmentalization of metal ions, allowing them to interact with Aβ and tau proteins in a pathological manner. Dysregulation of copper promotes amyloidogenic processing of APP; zinc modulates Aβ aggregation and its overall effect on neurons; iron interacts with the tau protein to alter its aggregation. Focussing on zinc, its binding to Aβ and co-precipitation in amyloid plaques, as well as its strong correlation with AD pathology strongly suggest a pivotal role in the development of the disease. It is even possible that dyshomeostasis of metal ions, common in old age, may be a trigger of AD, initiating the cascade of downstream metabolic and cellular changes characteristic of the disease.

This project aimed to investigate specifically the interaction between zinc and Aβ in the context of Aβ-induced cytotoxicity. While several functional interactions have been described between these two compounds, the literature remains conflicted. The goals of this research were to:

i) produce and purify recombinant $Aβ_{1-42}$.

ii) establish and optimize a cellular insult paradigm using Aβ, paying special attention to the aggregation and ageing of the peptide, and,

iii) to examine what effect, if any, exogenous Zn^{2+} has on the toxicity of the Aβ peptide.

Chapter 2

Materials and Methods

2.1 Amyloid-Beta Preparation

The DNA encoding $A\beta_{1-42}$ (DAEFRHDSGYEVHHQKLVFFAEDVGSNKGAIIGLMVGGVVIA) had been previously cloned into the pMal-c2 vector. It was expressed as a fusion protein with maltose binding protein (MBP) at the N-terminus to increase solubility and prevent aggregation. Overexpression in *Escherichia coli* bacteria was driven by activation of the upstream lac-promoter. MBP-$A\beta_{1-42}$ was separated from other proteins on an affinity column and Factor Xa protease was used to cleave the $A\beta_{1-42}$ from the MBP. The two were then separated by reverse-phase chromatography and the eluted pure $A\beta_{1-42}$ was quantified by the BCA protein concentration assay.

2.1.1 Induction of $A\beta_{1-42}$ expression in bacteria

Expression of MBP-$A\beta_{1-42}$ was induced from *Escherichia coli* bacteria, transfected with human $A\beta_{1-42}$ cloned into the pMal-c2 vector, which had been stored as a glycerol stock at -80°C. Cultures were inoculated with a few µl into 5 ml Lysogeny Broth (LB) (10% bacto-tryptone [peptone], 5% bacto-yeast extract and 10% NaCl, autoclaved for 20 min at 121°C) containing 100 µg/ml ampicillin. Following overnight incubation (Innova®40 incubator shaker; New Brunswick Scientific Co Inc, USA) at 37°C, cultures were transferred to a large bevelled flask containing 500 ml LB, 10 mM glucose and 100 µg/ml ampicillin and further incubated at 37°C with shaking. Samples were taken regularly and the optical density (OD) at 600 nm measured until it reached 0.4-0.6. Synthesis of MBP-$A\beta_{1-42}$ was induced by addition of 1 mM isopropyl β-D-1-thiogalactopyranoside (IPTG) (4 h, 37°C, shaking).

2.1.2 Bacterial lysis and protein extraction

After induction, the bacterial cells were collected by centrifuging (4000g, 4°C, 15 min) using a JSP250 rotor in an Avanti® J-26S XP centrifuge (Beckman Coulter Inc, USA). The supernatant was decanted and the pellet re-suspended in Affinity Chromatography buffer (2 mM Tris Cl [pH 7.5], 0.2 M NaCl). To lyse the bacterial cells, the suspension was sonicated using a Vibra-Cell™ Ultrasonic Liquid Processor (Sonics and Materials Inc, USA) for 4x30 sec bursts (20 KHz, 20% amplitude). Cellular debris was removed from the suspension by centrifuging using a JA20 rotor (Beckman Coulter Inc, USA; ~11000 x g, 4°C, 20 min). The protein-rich supernatant was retained for affinity chromatography.

2.1.3 Affinity chromatography

The MBP-$A\beta_{1-42}$ was separated from the other bacterial proteins via affinity chromatography on an amylose column that binds MBP. The protein-rich supernatant was run through a column of the amylose resin (New England BioLabs, USA, #E8021L). The supernatant fraction was applied to the column, allowed to enter the resin, the flow stopped, and the column left to incubate at 4°C for 30 min for interaction to occur. Non-bound proteins were eluted with 10 column volumes of affinity chromatography buffer, before bound proteins were eluted with 10 column volumes of elution buffer (20 mM Tris Cl [pH 7.5], 0.2 M NaCl, 10 mM Maltose). Eluate fractions were frozen at -20°C until ammonium sulphate fractionation.

2.1.4 Ammonium sulphate fractionation

Ammonium sulphate was used to precipitate the MBP-$A\beta_{1-42}$ from the affinity chromatography eluate. Ammonium sulphate was added to 60% saturation with constant stirring for 30 min at 4°C. The precipitated protein was pelleted by centrifuging at 10000 x g for 30 min in a JSP250 rotor (Beckman Coulter Inc, USA), resulting in a white precipitate. The supernatant was removed and discarded and

the pellet re-suspended in a low salt buffer (1 mM Tris HCl, pH 7.5), aliquoted into 1.5 ml Eppendorf tubes, and frozen at -80°C.

2.1.5 Desalting chromatography

Desalting to remove residual ammonium sulphate was achieved using fast protein liquid chromatography (FPLC). Samples (1 ml) of the re-suspended precipitate were individually desalted through a HiTrap® (GE Healthcare Life Sciences, USA) desalting column attached to an ÄKTA™ Purifier FPLC system (GE Healthcare Life Sciences, USA) into low salt buffer (20 mM Tris HCl, pH 7.5). Protein elution was monitored by absorbance at 280nm using UNICORN control software (GE Healthcare Life Sciences, USA), while salt elution was monitored with a conductivity meter. Eluate fractions containing protein were collected with the Fraction Collector Frac-950 (Amersham Biosciences, Sweden) and stored at -20°C.

2.1.6 Fusion protein cleavage

Factor Xa protease (New England BioLabs, USA) was used to cleave the MBP from the Aβ. Desalted protein-containing fractions were freeze-dried and the resulting precipitate re-suspended in Factor Xa cleavage buffer (20 mM Tris HCL pH 7.5, 100 mM NaCl, 2 mM $CaCl_2$) and pooled. Protein concentration was determined using a NanoDrop ND-1000 Spectrophotometer (NanoDrop Technologies, USA). Factor Xa protease was added at a concentration of 10 µl/mg protein, and the solution incubated at 23°C for 16 h in a PTC-200 Thermal Cycler (MJ Research, Canada).

2.1.7 Reverse Phase Chromatography

The samples were then applied to a HiTrap® Resource RPC column (GE Healthcare Life Sciences, USA) to separate the Aβ from the MBP and Factor Xa enzyme. A cleaved sample (100 µl) was brought to 5%

(v/v) acetonitrile and 0.1% (v/v) trifluoroacetic acid and applied to the column until UV absorbance at 215 nm had stabilized. A gradient (0-100%) of a 50% acetonitrile and 0.1% trifluoroacetic acid solution was applied until all bound protein had been eluted. All fractions were collected using a Fraction Collector Frac-950 and stored at -80°C.

2.1.8 Size-exclusion chromatography

Size Exclusion chromatography was used to complete separation of MBP from Aβ in those fractions containing both. Fractions were diluted 1:1 with 1xPBS (Phosphate Buffered Saline; Oxoid Ltd., UK; 1 tablet dissolved in 100ml MilliQ H_2O) and loaded onto a Superdex 75 agarose-dextrose column (GE Healthcare Life Sciences, USA) with 1xPBS. Fractions were collected until all material had passed though the column and the UV215 nm signal had stabilized.

2.1.9 Bicinchoninic acid (BCA) protein concentration assay

Purified protein-containing fractions were pooled and their concentration determined using a BCA assay (Smith et al., 1985). This is a colorimetric assay reliant on the reduction of Cu^{2+} to Cu^{+} by peptide bonds in the protein, resulting in a green to purple colour change proportional to the amount of protein present. In a 96-well microplate, a 25 µl aliquot was added to 200 µl of the BCA reagent (50:1 Bicinchoninic acid: $CuSO_4$) in triplicate, along with a standard curve of known concentrations of bovine serum albumin (BSA). The plate was incubated (60°C, 20 min), then the absorbance at 562 nm was measured using an Elx808™ Ultra Microplate Reader (Bio-Tek Instruments Inc, USA). The absorbance values of the samples were compared to the standard curve to calculate protein concentration

2.1.10 Sodium dodecyl sulphate polyacrylamide gel electrophoresis (SDS-PAGE)

At each stage of the production and purification process samples of all products, eluates and supernatants were taken for analysis by sodium dodecyl sulphate polyacrylamide gel electrophoresis (SDS-PAGE). Constitution of the gel and buffer solutions is detailed in Table 1. Samples were diluted 1:1 with cracking buffer, heated to 96°C for 10 min to denature the protein, and separated by 16% Kolbe SDS-PAGE (Schägger & von Jagow, 1987). A 15 µl aliquot of the mixture was loaded with 5 µl Polypeptide SDS-PAGE Molecular Weight Standards marker (Bio-Rad Laboratories Inc, USA), diluted 1:20 in cracking buffer. Gels were initially run at 96 V using a Model 200/2.0 Power Supply (Bio-Rad Laboratories Inc, USA) until the dye front passed the stacking gel, and then at 110 V for 90 min. Proteins were detected using either Coomassie Blue R or colloidal Coomassie (Section 2.1.11).

Solution	**Ingredient**	**Amount**	**To make:**
4x separating gel buffer	3 M Tris 0.4% (w/v) SDS Adjusted to pH 8.8 with HCl	90.86 g 10 ml (w/v) 10%	250 ml
4x stacking gel buffer	500 mM Tris 0.4% (w/v) SDS Adjusted to pH 6.8 with HCl	6.057 g 4 ml (w/v) 10%	100 ml
3x Cracking buffer	4x stacking buffer 1% (w/v) SDS 8 M Urea 0.3% (w/v) Bromophenol Blue (BPB) 1% B-Mercaptoethanol	50 ml 10 ml (w/v) 10% 36.3 g 10 µl	100 ml 1 ml
Inner running buffer	0.1 M Tris Cl 0.1 M Tricine 0.1% (w/v) SDS Adjusted to pH 8.25 with HCl	9.688 g 14.336 g 8 ml (w/v) 10%	800 ml
Outer running buffer	0.2 M Tris Cl Adjusted to pH 8.9 with HCl	19.376 g	800 ml
Kolbe separating gel 16%	4x Separating buffer 30% (w/v) Acrylamide MilliQ H_2O 10% (w/v) Ammonium Persulphate (APS) TEMED (Tetramethylethylenediamine)	2.5 ml 5.364 ml 2.136 ml 50 µl 7.5 µl	2x gels
Kolbe stacking gel 16%	4x Stacking buffer 30% (w/v) Acrylamide MilliQ H_2O 10% (w/v) APS TEMED	1.25 ml 0.84 ml 2.88 ml 25 µl 5 µl	2x gels

Table 1: Constituents of SDS-PAGE gel solutions

2.1.11 Coomassie Staining

Coomassie blue R and colloidal Coomassie G staining were used to visualise protein bands on SDS-PAGE (solutions detailed in Table 2). Polyacrylamide gels were removed from the cassettes and washed 3 x 10 min in MilliQ H_2O. Gels were either incubated in Coomassie blue R Stain (1 h, RT) and then destained (Super Destain, 30-45 min, destain overnight) or colloidal Coomassie G stain (overnight, RT), washed (1 h, MilliQ H_2O) and destained (2 h), then finally washed with MilliQ H_2O until the background cleared. Stained gels were scanned with an ImageScanner III (GE Healthcare Life Sciences, USA) using Epson Scan Software (Epson, Japan) and the images processed for optimising brightness and contrast using Image Studio Lite (LI-COR Biosciences, USA).

Solution	**Ingredient**	**Amount**	**To make:**
Coomassie Stain	Brilliant Blue R MilliQ H_2O Methanol Glacial acetic acid	0.5 g 90 ml 90 ml 20 ml	200 ml
Colloidal Coomassie Stain	Coomassie Blue G250 Ammonium sulphate Orthophosphoric acid (50% v/v) Ethanol	600 mg 50 g 100 ml 100 ml	500 ml in MilliQ H_2O
Colloidal Coomassie Destain	Ethanol Orthophosphoric acid MilliQ H_2O	50 ml 25 ml 425 ml	500 ml
Coomassie Destain	Methanol Glacial Acetic acid H_2O	25 ml 37.5 ml 437.5 ml	500 ml
Coomassie Super Destain	Methanol Glacial Acetic acid H_2O	180 ml 40 ml 180 ml	400 ml

Table 2: Constituents of staining and destain solutions

2.1.12 Commercial Aβ peptides

Additional Aβ peptides – $Aβ_{1-42}$ and scrambled $Aβ_{42}$ as HCl salts – were purchased from Chempeptide (PRC; Catalog #A-1021-1 and A-1022-1 respectively). The sequence of the scrambled peptide was as follows – AIAEGDSHVLKEGAYMEIFDVQGHVFGGKIFRVVDLGSHNVA.

2.2 Cell culture techniques

2.2.1 Cell lines

Two lines of cells in culture were used in this study. The SH-SY5Y human-derived neuroblastoma cell line (ATCC® reference number CRL-2266) was generated from a bone marrow biopsy of a metastatic neuroblastoma site. These cells show neuronal characteristics and exhibit multiple neurite-like outgrowths. This cell line was used as the initial experimental model due to their growth characteristics. Later, primary rat neuronal cell cultures were also used, as these are more physiologically relevant, especially since they also contain supporting glial cells. Further information can be found in section 2.2.9.

2.2.2 Growth of cells

SH-SY5Y cells were grown in Dulbecco's Modified Eagle Medium (DMEM, Gibco® Invitrogen Corporation, USA) with added 1% (v/v) Antibiotic-Antimycotic (Thermo Fisher Scientific, USA) and 10% (v/v) fetal bovine serum (FBS, Gibco® Invitrogen Corporation, USA). This is henceforth referred to as DMEM+. Experiments were performed with FBS-free medium (referred to as DMEM-), to control for unknown components of the FBS.

Cells were grown at 37°C in a 5% (v/v) CO_2 atmosphere in an incubator (Forma® Steri-Cycle CO_2 incubator, Thermo Fisher Scientific, USA) in 250 ml T75 flasks with filter caps, with the media volume maintained at 12 ml. The medium was aspirated and replaced every 2-3 days to maintain a nutrient-rich and pH-stable environment.

2.2.3 Storage of cells

Long-term preservation of cells was achieved by freezing low-passage cells. Initially grown to 80-90% confluence, the cultures were trypsinized (see section 2.2.5) and pelleted by centrifuging at 168 x g for 4 min (CL10 Centrifuge, Thermo Fisher Scientific, USA). The supernatant was aspirated and the pellet re-suspended in 5 ml freezing medium consisting of 90% (v/v) FBS and 10% (v/v) DMSO, before being transferred in 1ml aliquots to cryo-tubes and stored at either -80°C for short-term or in liquid nitrogen for long-term storage.

2.2.4 Seeding cells from frozen stock

Frozen cell stocks were rapidly thawed in a 37°C water bath (SUB Aqua 12, Grant, UK), taken up in 9 ml of pre-warmed DMEM+ and pelleted by centrifuging at 1000 rpm for 4 min. The supernatant containing the freezing medium was aspirated and the pellet re-suspended in 10ml DMEM+, before being seeded in T75 flasks and made up to 12 ml.

2.2.5 Passaging of cells

When cell cultures reached 80-90% confluence, they were passaged to ensure a sufficient supply of cells and to prevent overcrowding. The medium was aspirated and the cells washed with 1x PBS to remove cell debris. To detach the cells from the flask, 1ml of 0.05% (w/v) Trypsin (Gibco™ Invitrogen Corporation, USA) was pipetted onto the cells and incubated for 4 min. DMEM+ (9 ml) was added to stop the digestion and re-suspend the cells, and the suspension was centrifuged at 1000 rpm for 4 min. The supernatant was aspirated and the cell pellet re-suspended in 10 ml DMEM+. Cells were split either 1:5 or 1:10 into separate new T75 flasks and the volume made up to 12 ml. Cells were maintained for a maximum of 15 passages before being discarded, as they tend to lose their neuronal characteristics at higher passage numbers.

2.2.6 Seeding cells into 24- or 96-well plates

Cultured cells were seeded into 24- or 96-well plates for treatment. Cells were passaged by trypsinization, the cell pellet re-suspended in 10 ml DMEM+. A 10 µl sample of the suspension was taken and 10 µl Trypan Blue solution (Thermo Fisher Scientific, USA) added to stain dead cells. Cells were counted using a hemocytometer (Weber Scientific International Ltd, UK) under a Nikon Eclipse TS100 microscope (Japan) and the concentration of the cell suspension adjusted to $4x10^5$ cells/ml. Appropriate volumes of the cell suspension were added to the wells of the plates – 500 µl for 24-well plates and 100 µl for 96 well plates – and placed in the incubator for at least 24 h for the cells to adhere.

2.2.7 Treating SH-SY5Y cells with Aβ and Zn^{2+}

Once plated cells had been given time to adhere, they were treated with Aβ peptides, $ZnCl_2$ or both. DMEM+ was carefully aspirated, then a volume of DMEM- added such that the total volume in each well, including the Aβ and/or $ZnCl_2$, equalled 500 µl for 24-well plates or 100 µl for 96-well plates. Then the insult or treatment was added to each well, and the plate returned to the incubator for a further 24-48 h. Cell viability was measured using the 3-(4,5-dimethylthiazol-2-yl)-2,5-diphenyltetrazolium bromide (MTT) assay or the Resazurin cell viability assay (Section 2.3).

2.2.8 Glucose Deprivation (GD) insult

The glucose deprivation (GD) insult was used as a well-established paradigm that results in consistent cell death (Furukawa et al., 1996). Cells were seeded in 96-well plates and allowed to adhere. DMEM+ was carefully aspirated and replaced with no-glucose DMEM (Gibco™ Invitrogen Corporation, USA), and a volume of either MTT or resazurin to make up to 500 µl for 24-well plates or 100 µl for 96-well

plates. Cells were incubated at 37°C for 4 h and either absorbance of MTT or fluorescence of resazurin measured at the end of the 4 h period as described in section 2.3.

2.2.9 Primary cells

Primary rat hippocampal and cortical cultures were prepared by PhD student Megan Elder (Department of Anatomy). Briefly, postnatal day 0-1 Sprague-Dawley pups were sacrificed by pentobarbital and decapitation, the brain removed and dissected. Cells were dissociated by trituration, pelleted by centrifuging and the pellet resuspended in normal growth medium (NGM; 97% (v/v) Neurobasal-A medium (Gibco 10888022), 2% (v/v) B-27 Supplement (50x, Gibco, 17504001), 1% (v/v) GlutaMAX Supplement (Gibco, 35050061)). Cells were plated in poly-D-lysine-coated 96-well plates at a density of 40,000 cells/well (160,000 cells/ml) and incubated at 37°C, 2% (v/v) CO_2 for between 7-25 days. Primary cell cultures were treated very similarly to SH-SY5Y cells – media were made up to 100 µl with NGM and either Aβ, $ZnCl_2$ or both. Plates were then returned to the incubator for 24 h, at which time cell viability was measured using the Resazurin assay.

2.3 Cell viability assays

2.3.1 MTT cell viability assay

The MTT assay is a method of indirectly measuring cell viability (Mosmann T, 1983). It relies on cellular NAD(P)H-dependent oxidoreductases to convert MTT (a yellow salt) to its formazan, which are insoluble purple crystals. A reduction in cell viability would be reflected by a decrease in cellular metabolic activity and therefore a decrease in the production of formazan crystals, a change that can be measured by colorimetry. Four hours prior to the end of the treatment period, MTT was added at 0.32 mg/ml and the treatment incubation period completed for an additional 4 h. Media was then carefully aspirated and DMSO:EtOH (4:1) added to each well, and the plate agitated at room

temperature for 10 min to solubilise the formazan crystals. Absorbance was measured at 562nm using an Elx808™ Ultra Microplate Reader (Bio-Tek Instruments Inc, USA).

2.3.2 Resazurin cell viability assay

The resazurin cell viability assay was used as an alternative to MTT (Anoopkumar-Dukie et al., 2005), particularly given the finding that there is a proposed interaction between MTT and Aβ (discussed in section 1.4.5). This assay is based on the metabolic reduction of resazurin, a weakly fluorescent blue dye, to resorufin, a highly red fluorescent dye, both of which are minimally toxic to living cells. Similar to how the MTT was applied, 4 h prior to the end of the treatment period, 25 µl of 0.15 mg/ml resazurin sodium salt (Sigma-Aldrich Corporation, USA) was added to each well, and incubated at 37°C for an additional 4 h. At the end of this incubation period, fluorescence in the 96-well plates was measured at wavelengths of 530nm excitation and 590nm emission.

2.4 Amyloid-Beta Aggregation

Aggregation of Aβ peptides was undertaken to determine optimum conditions for formation of toxic species (discussed in section 1.4.5). Aliquots of $A\beta_{1-42}$ and scrambled $A\beta_{42}$ were diluted to 110 µM with the following vehicles: MilliQ H_2O, 1x PBS, DMSO, DMEM, 10 mM 3-(N-morpholino)propanesulfonic acid (MOPS) and artificial cerebrospinal fluid (aCSF; 124 mM NaCl, 26 mM $NaHCO_3$, 10 mM glucose, 3.2 mM KCl, 1.25 mM NaH_2PO_4, 2.5 mM $CaCl_2$, 1.3 mM $MgCl_2$). The aliquots were incubated at 37°C and samples taken at time-points of day 0, 2, 3, 4 and 7. Samples were immediately frozen at -80°C to halt aggregation and stored until analysis. Samples were analysed by running on 16% (w/v) Kolbe SDS-PAGE gels and stained by Coomassie staining as described in section 2.1.11.

Furthermore, structural analysis of $A\beta_{1-42}$ and scrambled $A\beta_{1-42}$ peptides was performed using the Aggrescan3D server (Zambrano et al., 2015), which can predict aggregation propensity in protein structures, as well as predicting tertiary protein structure.

2.5 Data Analysis

Cell viability data were analysed using scripts written in R (R Project for Statistical Computing; http://www.r-project.org/; scripts available in Appendix I). Data were calculated as a fold-change from the mean of the controls. Statistical significance was determined using Kruskal-Wallis one-way analysis of variance with Dunn's post-hoc test and Holm-Šidák correction. A p-value of <0.05 was considered significant.

Chapter 3

Results

3.1 Amyloid-Beta production

3.1.1 Aβ induction in bacterial culture

In order to test Aβ-induced toxicity, production of the peptide was necessary and this was achieved using a bacterial protein over-expression system. Gene expression was induced in the *E. coli* bacterial stocks transfected with a plasmid encoding an MBP- human $A\beta_{1-42}$ fusion protein. In order to determine the efficiency of expression on the MBP-$A\beta_{1-42}$ complex, samples of cultures were taken following induction and analysed by SDS-PAGE. Figure 3 shows a representative SDS-PAGE of three preparations demonstrating successful induction of protein synthesis driven by the lac-promoter. The

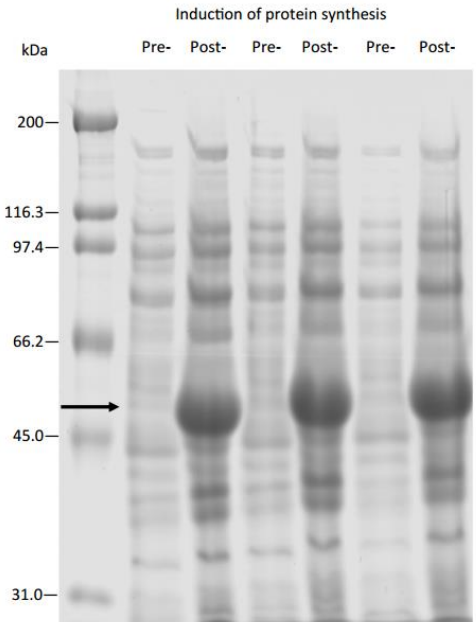

Figure 3: Representative Coomassie stained SDS-PAGE of samples before and 3 h after protein synthesis induction of *E. coli* cultures by IPTG. The band of interest is marked with an arrow. Molecular weight estimated using broad-range marker (left-most column).

presence of a strong protein band at approximately 47 kDa post-induction (marked with the arrow) reproduced in three replicate cultures is consistent with the expected molecular weight of the MBP-$A\beta_{1-42}$ fusion protein. The absence of any other differences in protein banding suggests that this is the product of activation of the lac promoter immediately upstream of the encoded fusion protein.

3.1.2 Purification of MBP-$A\beta_{1-42}$ from bacterial lysate

In order to purify the MBP-$A\beta_{1-42}$ from other protein and cellular residue, samples underwent firstly affinity chromatography and then desalting chromatography. Following induction of MBP-Aβ synthesis in the bacterial cultures, the protein complex was isolated by binding to an amylose resin column that interacts with MBP. This column binds the associated Aβ in the fusion protein indirectly, while allowing other proteins to elute. Bound proteins were eluted with free maltose and the resulting fractions were concentrated by ammonium sulphate precipitation and the resulting precipitate desalted using FPLC. A representative FPLC plot showing both 280 nm absorbance – denoting protein – and salt concentration is shown in Figure 4. The large peaks in blue denote successful separation of protein from the salt – in this case the protein was the MBP-Aβ complex, endogenous bacterial MBP and other amylose-interacting proteins. All protein-containing fractions were collected for further purification.

3.1.3 Cleavage of Aβ from MBP

In order to separate $A\beta_{1-42}$ from the MBP in the fusion protein, the samples were cleaved by Factor Xa protease, which specifically cleaves at Ile-(Glu or Asp)-Gly-Arg, the sequence at the border of MBP and its fused protein moiety, in this case $A\beta_{1-42}$. Figure 5 shows a representative gel of pre- and post-cleavage samples. The highest molecular weight band represents the complete MBP-$A\beta_{1-42}$ complex, while the slightly lower band represents cleaved MBP, and the protein band just below the 6.5 kDa marker is $A\beta_{1-42}$. There were two higher molecular weight bands and the lower molecular weight band

($A\beta_{1-42}$-MBP, MBP and $A\beta_{1-42}$ respectively) also surprisingly in the pre-cleavage samples. Cleavage in the absence of incubation with Factor Xa suggests either non-specific cleavage at the linkage site has occurred or there has been some contamination of the sample with Factor Xa cleavage enzyme. Some endogenous MBP would be expected in the pre-cleavage sample but Aβ is not found in *E. coli*. Nevertheless, it is clear that post-cleavage, the band corresponding to $A\beta_{1-42}$-MBP has completely disappeared, and the staining shows only the fully-cleaved separate bands. This indicates successful cleavage of $A\beta_{1-42}$ from the MBP fusion protein, despite the lack of enrichment of the protein band at ~6.5 kDa corresponding to $A\beta_{1-42}$.

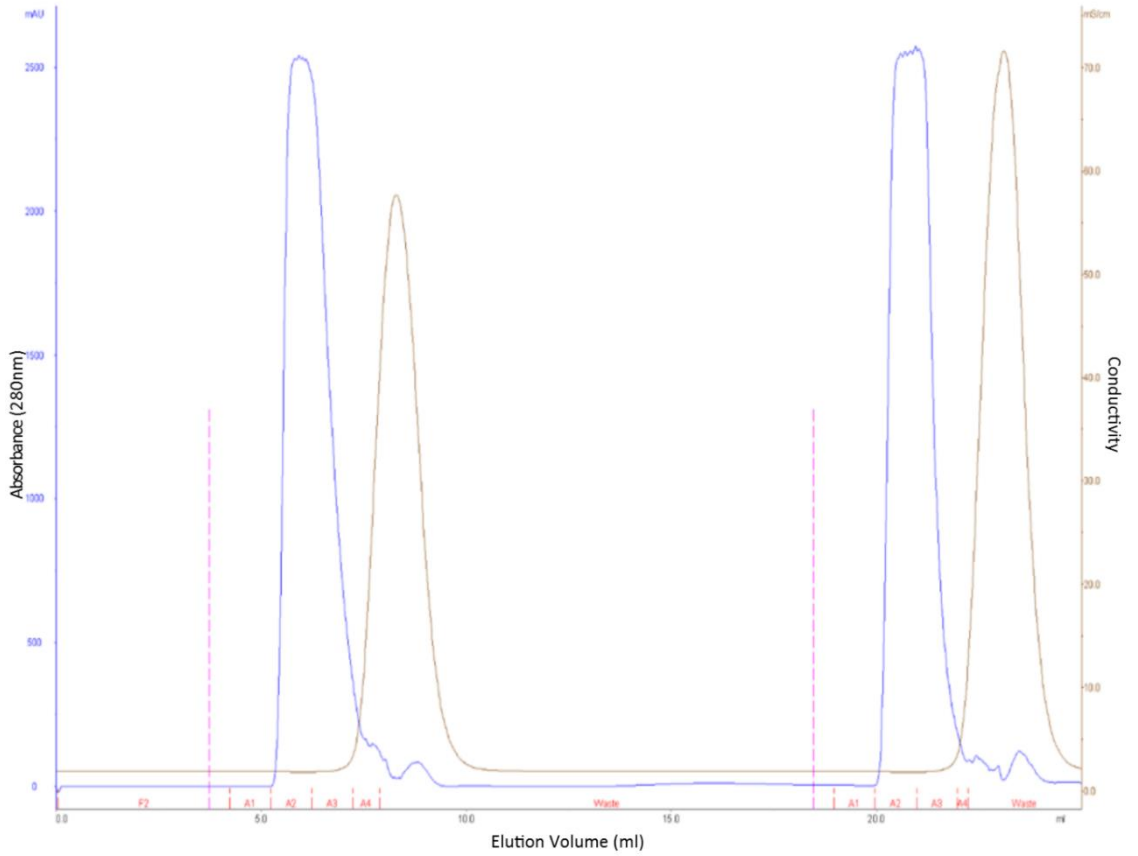

Figure 4: Representative FPLC plot from desalting chromatography on a HiTrap® desalting column showing two 1 ml aliquots of re-suspended ammonium sulphate precipitated Aβ-MBP in low-salt buffer (20 mM Tris, pH 7.5). The blue trace represents absorbance at 280 nm (denoting protein), while the brown trace represents salt concentration. Collected fractions are noted on the x-axis in red. Fractions 2 and 3 from each run, containing the highest protein signal, were retained and pooled for further purification.

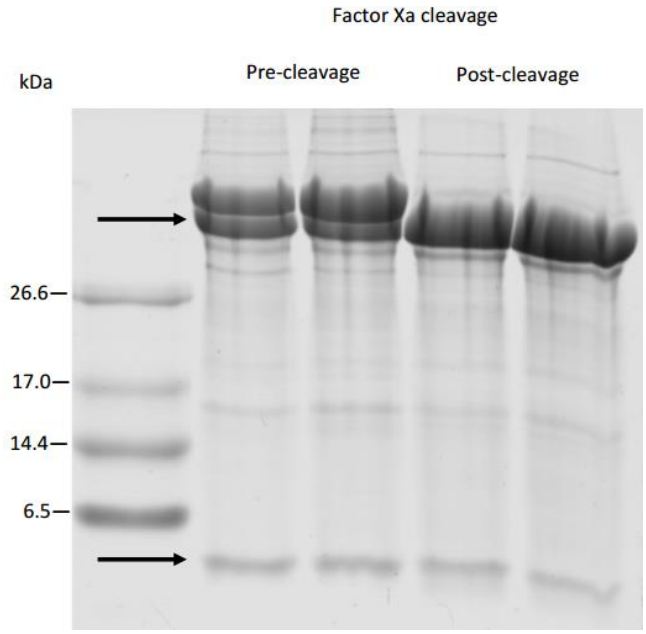

Figure 5: Analysis of Factor Xa cleavage by Coomassie-stained 16% (w/v) Kolbe gel. Desalted samples of isolated MBP-Aβ_{1-42} were analysed before and after incubation with Factor Xa protease to cleave Aβ_{1-42} from MBP. Bands representing MBP and Aβ_{1-42} are indicated by the top and bottom arrows respectively. The two lanes represent duplicates of the same pre- and post- samples.

3.1.4 Reverse-Phase Chromatography

Following confirmation of successful cleavage of MBP from Aβ, the two proteins were separated by reverse-phase chromatography. An amount corresponding to 6 mg of protein was loaded onto the column per run, and the absorbance at 215 nm carefully monitored throughout. Previous work in the lab had found that the Aβ and MBP tend to elute relatively close to each other, around 30-50ml after the beginning of the salt gradient. However, all protein-containing fractions, including the initial flow-through, were examined by 16% (w/v) Kolbe SDS-PAGE. A representative FPLC trace is shown in Figure 6a, the region of interest – the "shoulder" of the large peak – is denoted by the black arrow. A Coomassie-stained SDS-PAGE gel of the initial flow-through fractions (Figure 6b) showed the presence of only MBP at ~40 kDa and no Aβ at ~4.5 kDa. Gel analysis of the region of interest (Figure 6c) revealed the presence of a clear protein band at ~4.5 kDa, consistent with Aβ. There were a number of pure fractions containing only Aβ, but several fractions contained both Aβ and MBP. These fractions were further purified to optimise the yield of Aβ obtained from the preparation. To this end, size-exclusion

chromatography was performed since there was a significant difference in size between the two proteins. However, perhaps because of the dilution, this technique was unable to isolate additional Aβ (Appendix B).

3.1.5 Quantification of Aβ concentration

All fractions containing pure Aβ were pooled and their concentration determined by a BCA assay. The standard curve for this assay is shown in Appendix C. The coefficient of determination (R^2) calculated from the standard curve was 0.9978, indicating a high assay accuracy, and suggesting an accurate determination of the concentration of Aβ could be made. Using the equation derived from the relationship between absorbance at 562 nm and protein amount (y=0.0566x+0.0026), the concentration of Aβ was calculated. An absorbance of 0.1325 corresponds to 2.29 µg protein in 12.5 µl or 41 µM, correcting for dilution. The yield of this protocol was ~500 µg/L initial culture. This represents a reasonably high purification level, consistent with previous preparations in the group, though the overall yield was relatively low.

Conclusion

The results presented here suggest successful production of $A\beta_{1-42}$. Protein synthesis in the bacterial cultures was successfully induced, and Aβ was cleaved from MBP successfully. Reverse-phase chromatography was largely successful in separating the two proteins, with a degree of overlap of the elution peaks. The size-exclusion chromatography did not recover more Aβ peptide. Despite obtaining a relatively good purification level, the demands of the subsequent assays meant the yield of ~500 µg/L was nonetheless insufficient and so commercially-produced Aβ was purchased to supplement the stocks.

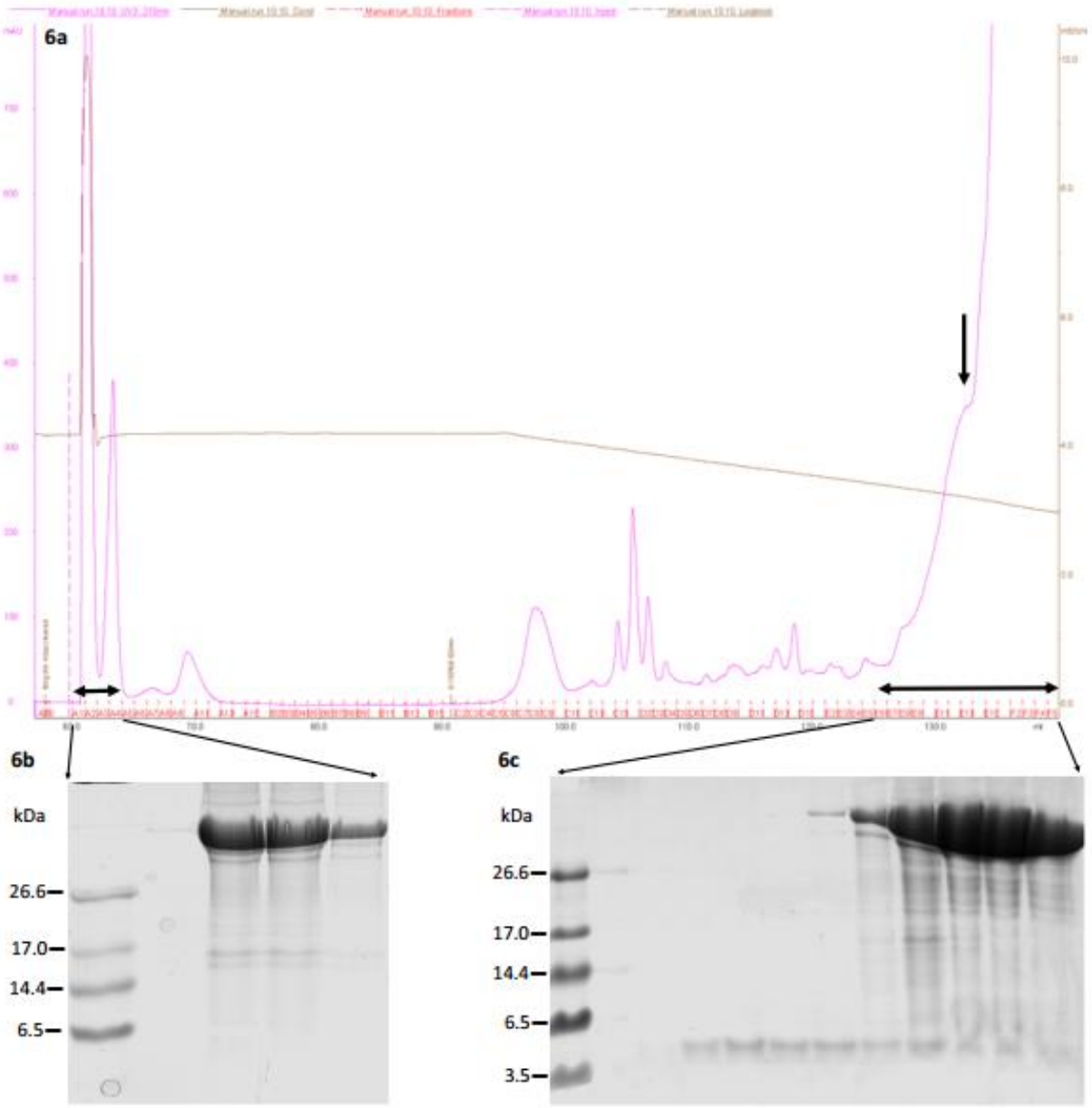

Figure 6: Results of reverse-phase chromatography to separate Aβ and MBP. a) Representative FPLC trace showing absorbance at 215 nm (pink) and salt concentration (brown). The region of interest, as suggested by previous work in the lab, is indicated by the black arrow. Fractions analysed by Coomassie-stained SDS-PAGE gels are denoted by the double-sided arrows. b) Coomassie-stained SDS-PAGE gel of flow-through fractions shows the presence of a strong high molecular weight band above 26 kDa. c) This Coomassie-stained SDS-PAGE gel of fractions of interest shows the presence of a protein band between 3.5 and 6.5 kDa, consistent with the size of Aβ. A number of the earlier fractions show pure Aβ eluent, while later fractions show Aβ contaminated with MBP. Only pure Aβ fractions were pooled for quantification.

3.2 Amyloid-Beta toxicity in SH-SY5Y neuroblastoma cell cultures

In order to investigate the relationship between zinc and $A\beta_{1-42}$, it was first necessary to establish a consistent paradigm for $A\beta_{1-42}$-induced toxicity in cell cultures. An initial probe of effective $A\beta_{1-42}$ concentration was performed. During this, it was concluded that the commonly-used MTT cell viability assay may not be the best to use in this case because of its reported interaction with Aβ – as such it was replaced by the resazurin assay. This was followed by an investigation into how "ageing" protocols affect $A\beta_{1-42}$ aggregation. Using information obtained from this work, $A\beta_{1-42}$ treatments were performed in SH-SY5Y neuroblastoma cells and primary rat cortical and hippocampal cell cultures. Finally, following establishment of optimum Zn^{2+} concentration, the effect of co-treatment of cell cultures with $A\beta_{1-42}$ and Zn^{2+} was investigated to explore their biological relationship.

3.2.1 Initial probe of effective $A\beta_{1-42}$ concentration

In order to determine an optimum $A\beta_{1-42}$ concentration that causes cell death, an investigation of effective concentrations of the peptide was performed. Previous work in the group had suggested a possible optimal concentration of $A\beta_{1-42}$ that induced cell death. While this work had been completed in hippocampal slice cultures (Elder, 2013), it was important to validate these findings in the SH-SY5Y neuroblastoma cell cultures. In the earlier study, it was found that application of 2.5µM $A\beta_{1-42}$ aged at 37°C for 3 days was sufficient to induce upwards of 50% cell death in hippocampal slice cultures. Since these experiments aimed to investigate a potential bidirectional effect of Zn^{2+} on cell viability, it was decided that beginning with a slightly lower concentration of the peptide might produce a percentage cell death effect that allowed for both an increase and decrease to be effectively measured with Zn^{2+} treatment. As such, an initial pilot experiment was performed using 1 µM $A\beta_{1-42}$, both from the current production batch, and a batch previously produced in the lab. Previous work had also suggested that a 24 h incubation period was sufficient to induce cell death, so this was the time point chosen.

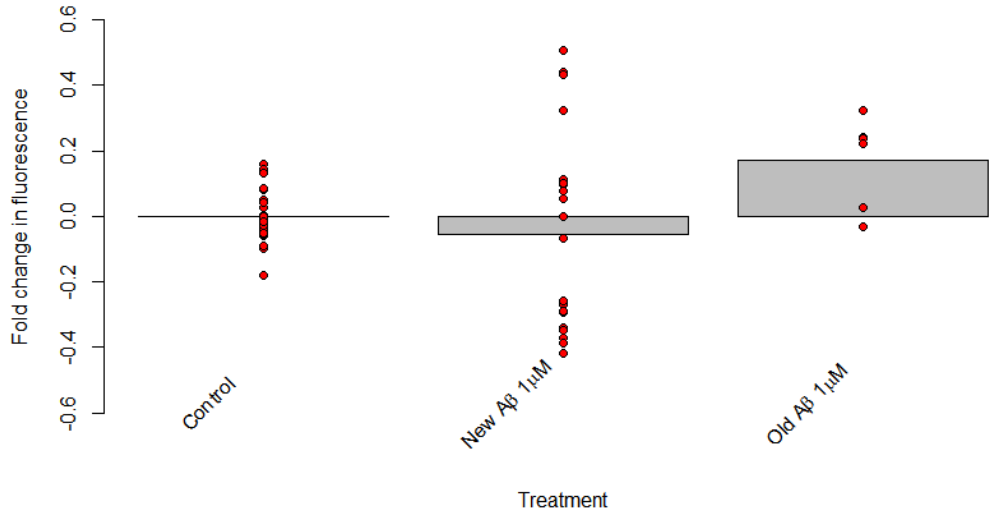

Figure 7: Dot and Bar plot showing changes in cell viability in SH-SY5Y cultures treated with 1 µM $A\beta_{1-42}$ for 24 h, as measured by the MTT assay. Data are shown as a fold-change from the mean of the control (PBS) New Aβ denotes that produced as part of this project, while old Aβ is that previously produced in the lab using the same methods. The data are highly variable and no significant effects were observed with either batch of peptide ($p>0.05$; Kruskal-Wallis test with Dunn's post-hoc test, n=3).

No effect was found on cell viability using either preparation of 1 µM $A\beta_{1-42}$ across 3 experiments with 5 replicates each (Figure 7). There was considerable variability in the data; some of the data looked to be trending downwards, but a considerable amount of data showed the opposite – an increase in cell viability. This suggests a deep underlying problem with this combination of insult and assay. Overall, this 24 h treatment with 1 µM $A\beta_{1-42}$ failed to induce significant cell death, contrary to what had been observed in previous work.

3.2.2 Comparing the MTT cell viability assay to the resazurin assay

Although the MTT assay is one of the most commonly used cell viability assays (Howlett et al., 1995; Eisenhauer et al., 2000; Dahlgren et al., 2002; Chafekar et al., 2008; Ahmed et al., 2010), this does not necessarily mean that it is suitable for all situations. As noted in section 1.4.5, a confounding interaction exists specifically between MTT and Aβ. As such, it was considered that the resazurin cell viability assay may be a more accurate measure of cell death. To test this, a pilot experiment was

performed assessing cell death induced by the glucose-deprivation (GD) assay, a very well-characterised and consistent cellular insult, which avoids the use of $A\beta_{1-42}$, by way of either the MTT or resazurin assays (Figure 8).

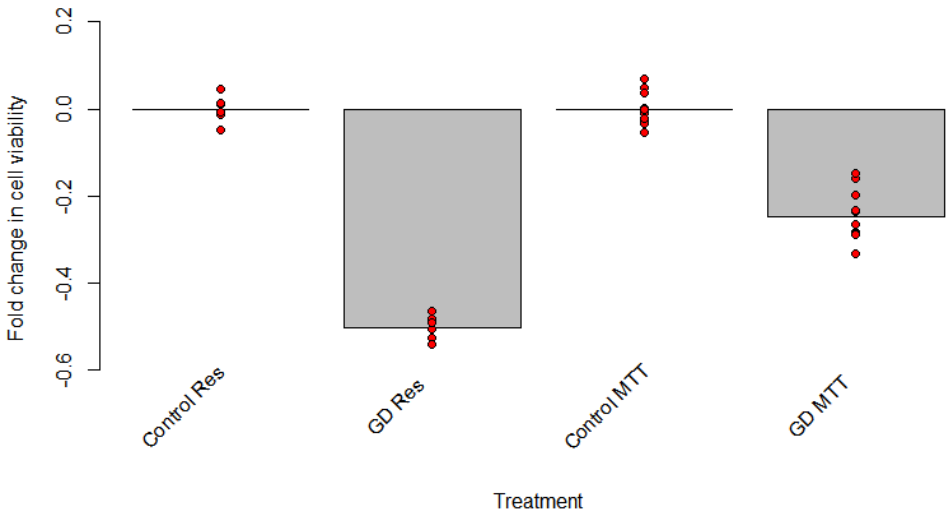

Figure 8: Comparison of Resazurin and MTT assays using 4 h glucose-deprivation as an insult. With the same insult, Resazurin read as lower cell viability than MTT, and the spread of datapoints looks considerably less with the former than the latter. Indeed, the variance of the resazurin data are less than those of the MTT data (n=2).

Using either assay, it was shown that 4 h glucose deprivation was sufficient to induce cell death – up to 50% as seen by the resazurin assay. However, most crucially in Figure 8 is the spread of data points around the mean, and therefore the variance of the dataset. Even visually, the resazurin assay appears far less variable (more precise) than the MTT assay. Calculating the variance of the datasets reveals the same story. The resazurin assay for control and GD revealed variances of 9.68 and 7.86 respectively, while the equivalent for the MTT assay were 12.98 and 38.06. This gives strong evidence that changing the cell viability assay may lessen some of the issues with high variance encountered in Figure 7, not to mention mitigating the confounding effects of using the MTT assay with Aβ.

Using a concentration curve of 1, 5 and 10 µM, which lie well within the range of toxicity observed in the literature (Garai et al., 2007; Ahmed et al., 2010), the comparison between "New" and "Old" Aβ was repeated (Figure 9). At the 24 h time point, 1, 5 and 10 µM Aβ insults were ineffective at inducing cell death, while in the case of the previously produced Aβ, treatment with 10 µM caused an upward

trend in cell viability (New Aβ μ=-0.04, 0.04, 0.03; Old Aβ μ=-0.05, 0.04, 0.19) (Figure 9a). This positive effect disappeared at the 48 h time point (New Aβ μ=-0.02, 0.01, 0.01; Old Aβ μ=-0.02, 0.02, 0.06) (Figure 9b). However, due to the low number of replicates, it was not possible to assess any differences statistically. Nevertheless, the results clearly show no decrease in cell viability and the data have low variance and therefore likely high precision.

Conclusion

These data begin to highlight some of the inconsistencies encountered with $A\beta_{1-42}$ insults to neuroblastoma cells, ranging from dosage required for toxicity to the variability in cell viability assays. From this point it was decided that the resazurin assay would be used over the MTT assay. Not least, these results led to a discussion about the efficacy and relevance of the previously-used ageing protocol. The results described here strongly suggest that simply ageing $A\beta_{1-42}$ at 37°C for three days does not always produce toxic species of the peptide, and this may underlie the incongruity with the established literature. It was therefore necessary to examine the aggregation of the peptide, in order to ascertain a protocol able to consistently produce aggregated species of Aβ.

3.3 Amyloid-Beta aggregation and toxicity

As discussed in section 1.4.5, the aggregation of Aβ peptides *in vitro* is a complex phenomenon, and the relationship between aggregation state and toxicity is fraught with a lack of clear interpretation. These experiments aimed to first determine what species of Aβ aggregates are formed by the standard ageing procedure, second, what species are formed by other ageing protocols using a number of

different solvents and buffers and third, to investigate the effects on toxicity, if any, of the most effective ageing techniques.

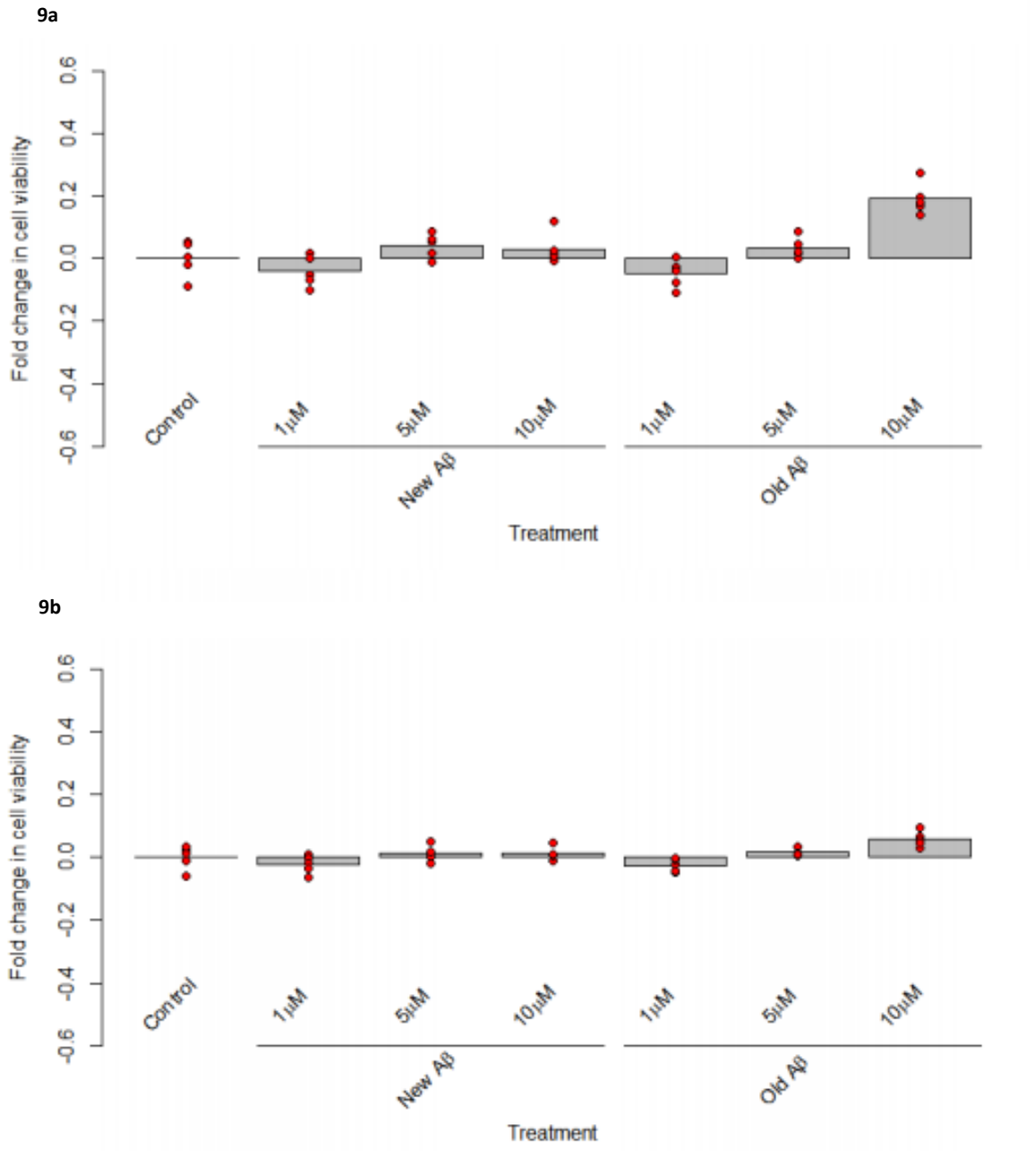

Figure 9: Bar and dot plot showing changes in cell viability as measured by the resazurin assay as a result of treatment with Aβ. Data are shown as a fold change from the mean of the Control (PBS). a) Change in cell viability in response to 24 h treatment. At this timepoint, no differences can be observed, though 10 µM old Aβ appears to be trending upwards. b) Change in cell viability in response to 48 h treatment. Again, no differences can be observed in response to up to 10 µM Aβ (n=1).

3.3.1 Effects of different buffers on Aβ aggregation

Ageing experiments were undertaken to determine the effects of several buffers on the aggregation of $A\beta_{1-42}$ peptides *in vitro*. These buffers included those commonly used in the literature – PBS (Nimmrich et al., 2008), DMSO (Dahlgren et al., 2002), MOPS (Solomonov et al., 2012) – as well as those not commonly used, but that hold some experimental (DMEM) or physiological (aCSF) relevance. All further experiments were performed with commercial Aβ peptide (Chempeptide).

The peptide (Chempeptide), was aged for up to seven days, with samples taken at 0, 2, 3, 4 and 7 days. Figure 10 shows the Coomassie-stained gels obtained from these samples. In the case of MilliQ H_2O, PBS, MOPS, and DMSO, ageing of the peptide essentially shows no change in the aggregation state over the seven-day period. In each case, day 0 samples show clear bands of monomer at 4.5 kDa, as well as bands of what appear to be trimers (MW ~ 14-15 kDa). With H_2O, PBS, MOPS, and DMSO, this same pattern of monomers and small oligomers continues throughout the ageing process, with a distinct lack of any bands at higher molecular weights indicating higher-order oligomers, protofibrils, or fibrils (Figure 10a, b, c, d). However, as seen in Figure 10e and f, incubating $A\beta_{1-42}$ with aCSF leads to the formation of higher-order aggregates, consistent with the pattern of aggregate formation previously described (Ahmed et al., 2010). Interestingly, despite identical aggregation conditions in Figures 10e and 10f, higher-order aggregates formed earlier in one experiment (Figure 10f; day 3) than the other (Figure 10e; day 7). Incubation with DMEM (Figure 10g) showed a loss of signal associated with the monomer, but no additional bands to indicate the presence of larger aggregates.

It is also important to note that scrambled $A\beta_{42}$ is also capable of forming aggregates when incubated with aCSF (Figure 10h), which form very early (day 2), but these aggregates show a different pattern of protein bands than those seen with $A\beta_{1-42}$ in aCSF (Figure 10e and f). This phenomenon is currently undescribed in the literature.

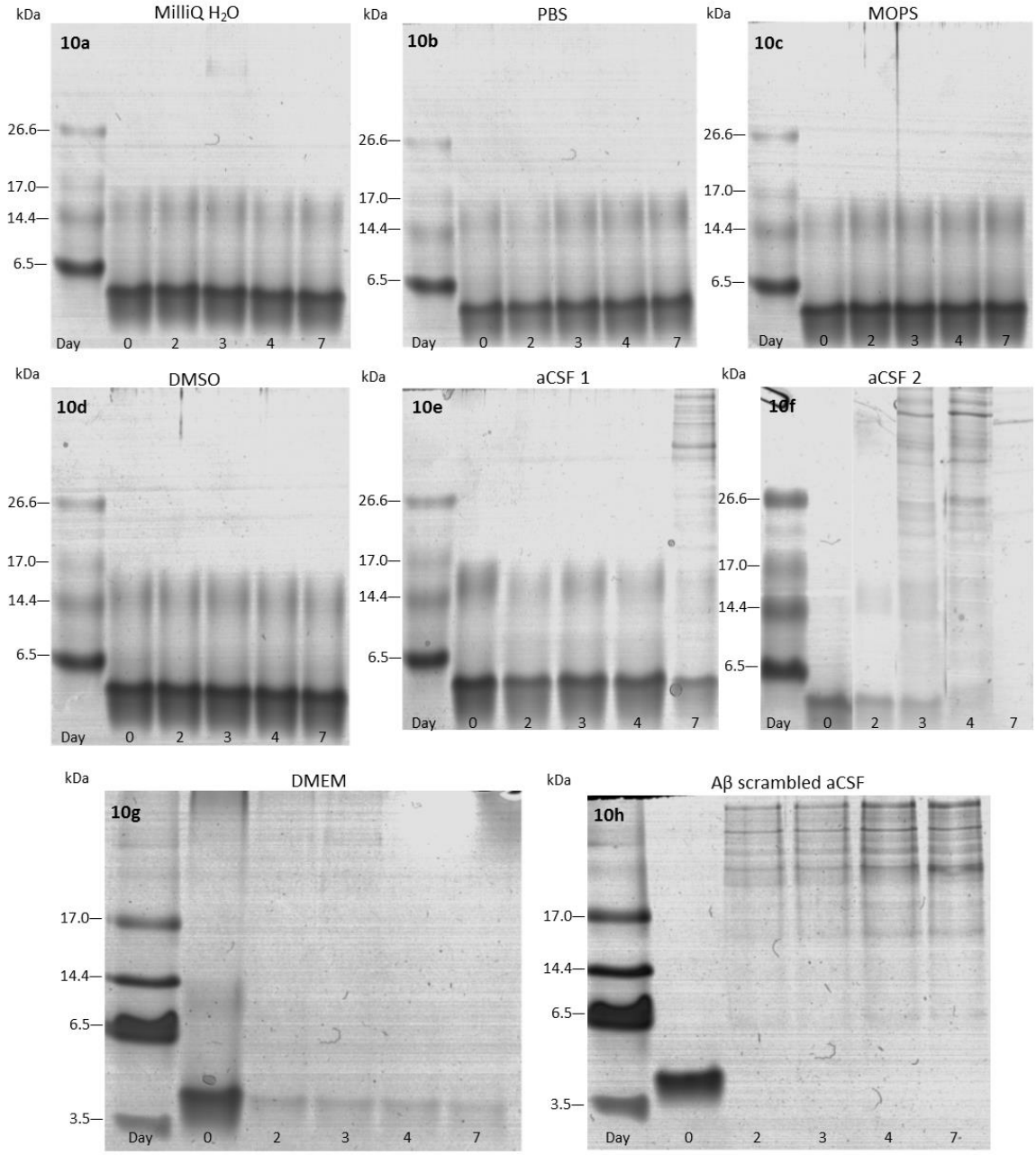

Figure 10: Effect of solvent on aggregation of $A\beta_{1-42}$ and scrambled $A\beta_{42}$ peptides incubated at 37°C. Coomassie-stained 16% (w/v) Kolbe SDS-PAGE of samples of aged Aβ peptides. Aliquots of pure $A\beta_{1-42}$ were diluted 1:1 with the following buffers and aged for up to 7 days: H_2O (a), PBS (b), MOPS (c), DMSO (d), aCSF (e and f) and DMEM (g). Scrambled $A\beta_{42}$ was also incubated in aCSF (h).

3.3.2 Structural analysis and aggregation prediction of Aβ peptides

In order to understand the aggregation dynamics of both the $A\beta_{1-42}$ and the scrambled $A\beta_{42}$, in particular with regard to the unexpected finding that the scrambled peptide was highly prone to aggregation, the peptide sequences were entered into the Aggrescan3D server, an aggregation prediction server using intrinsic aggregation propensity values for amino acids. This server is able to differentiate and largely ignore hydrophobic core residues and instead focuses on surface amino acids (Zambrano et al., 2015).

As expected, $A\beta_{1-42}$ was predicted to show a considerable propensity to aggregate, with a number of regions being marked as aggregation-prone "hot spots", notably from residues 17 to 21 and 31 to 42 (Figure 11b). These data are consistent with much of the Aβ aggregation literature, which highlight these regions as contributing to the formation of aggregates (e.g. Ahmed et al., 2010).

While generally not as aggregation-prone as $A\beta_{1-42}$, the scrambled peptide regardless was predicted to also include a number of regions scoring highly on propensity to aggregate (Figure 11d). Indeed, its secondary structure is quite globular (Figure 11c), and the regions from residues 15 to 21 and 30 to 34 scored most highly in this regard. Whether this is a property of all scrambled amyloid peptides, or whether it is a result of this particular amino acid sequence (shown in Figure 11c), is unclear. Nevertheless, structural analysis and aggregation prediction fits with the data observed in Figure 10.

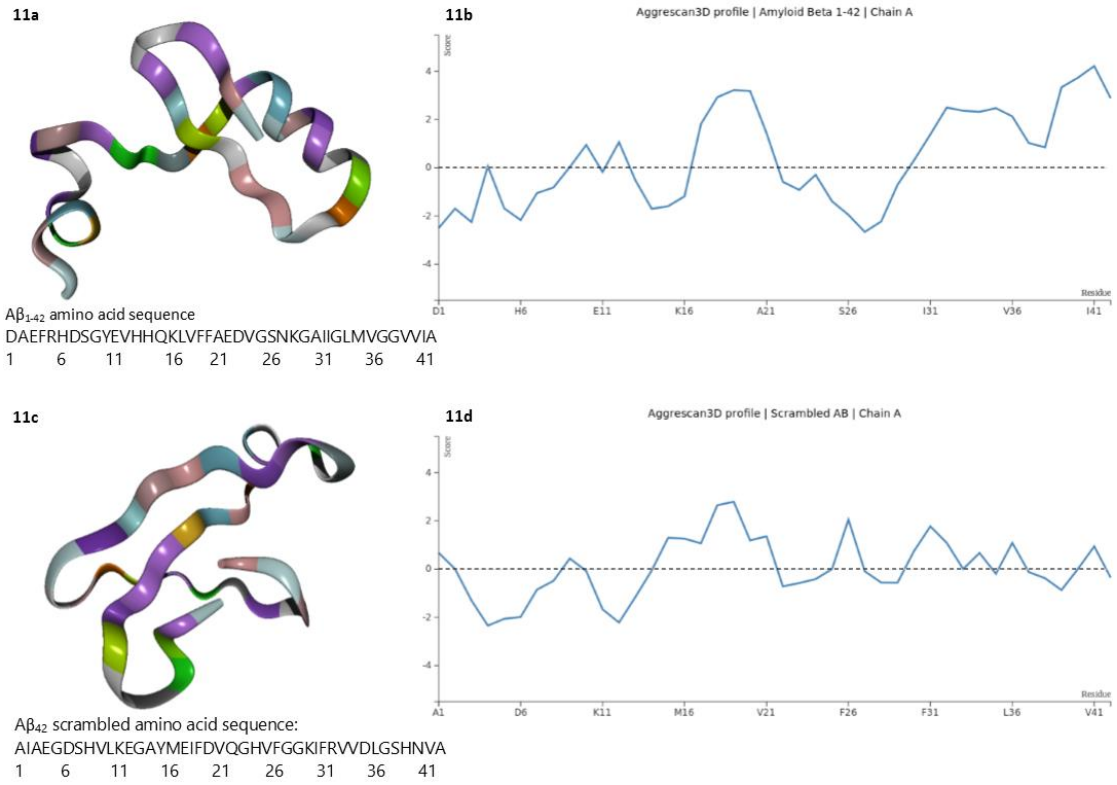

Figure 11: Data obtained from the Aggrescan3D server showing secondary structure and aggregation propensity of the amyloid peptides. a) shows a predicted secondary structure for $A\beta_{1-42}$ and its amino acid sequence, consistent with other models derived from NMR. b) Aggregation propensity of the $A\beta_{1-42}$ peptide. Residues above the dotted line indicate those prone to aggregation. c) Predicted secondary structure of the scrambled $A\beta_{42}$ peptide and its amino acid sequence below. d) Aggregation propensity of the scrambled $A\beta_{42}$ peptide, showing a surprising number of aggregation-prone regions, comparable to that of the wild-type peptide.

3.3.3 Effect of ageing Aβ on cell viability

Having established that ageing $A\beta_{1-42}$ in MilliQ H_2O, PBS, MOPS, DMSO and DMEM does not seem to affect the aggregation state of the peptide, while ageing in aCSF does, it was then crucial to determine whether this ageing had any effect on the toxicity of the peptide. To this end, SH-SY5Y cells were treated for 24 h with $A\beta_{1-42}$ and scrambled $A\beta_{42}$, diluted in either MilliQ H_2O or aCSF, either aged for 3 days or not aged. Cell viability was measured using the resazurin assay and the results displayed in Figure 12.

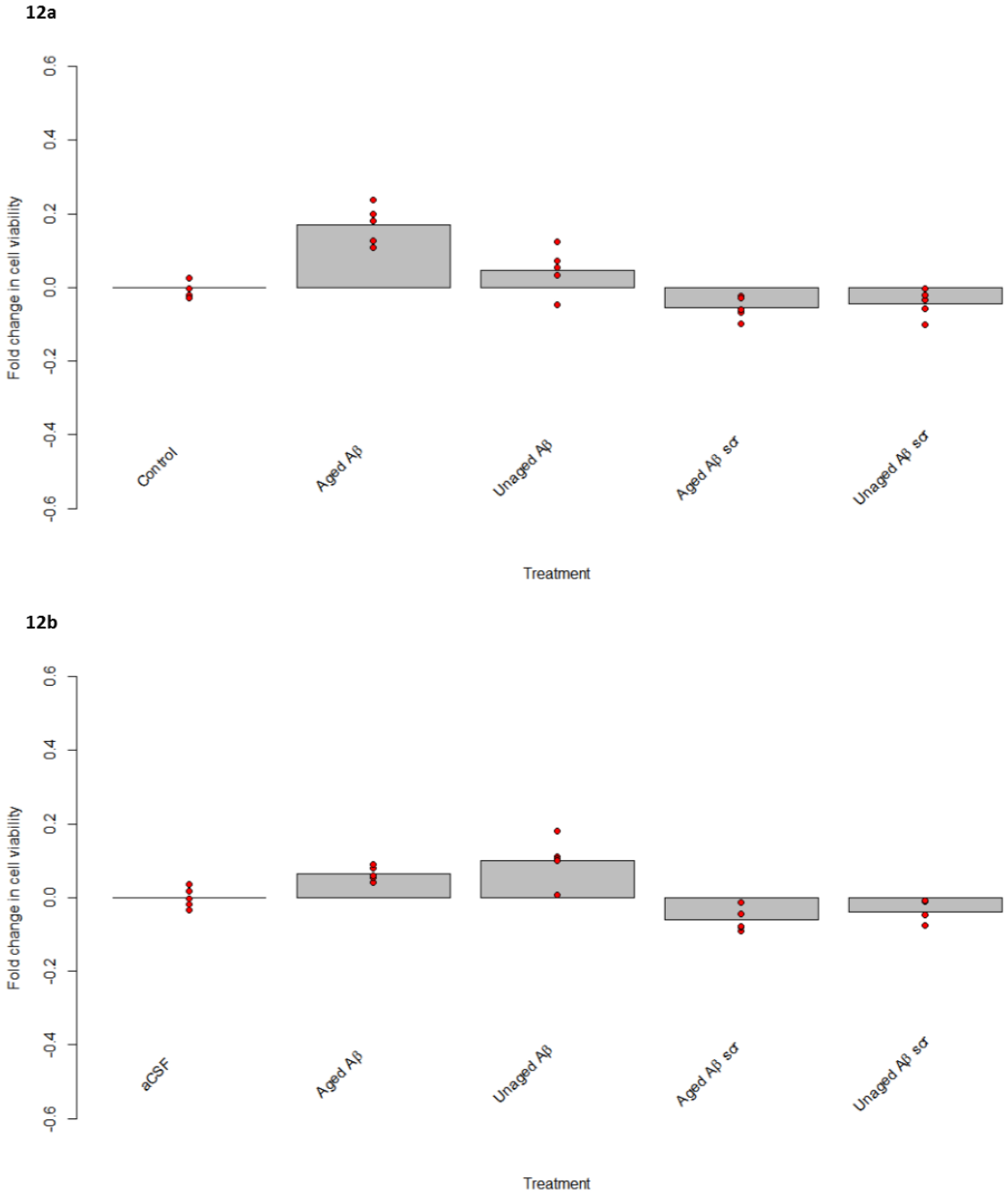

Figure 12: Bar and dot plots showing changes in SH-SY5Y cell viability in response to Aβ insult. a) The effect of ageing $A\beta_{1\text{-}42}$ on cell viability in neuroblastoma cell culture, compared to unaged $A\beta_{1\text{-}42}$ and scrambled $A\beta_{42}$. b) The effect of Aβ peptides aged in aCSF on cell viability in neuroblastoma cell culture. Cell viability measured by the resazurin assay (n=1).

No significant cell death was caused in any condition. In fact, similar to 10 µM $A\beta_{1\text{-}42}$ in Figure 9a, 20 µM aged $A\beta_{1\text{-}42}$ also showed a trend of increasing cell viability (Figure 12a; Aged Aβ µ=0.17). This modest positive effect seemed to reverse when the $A\beta_{1\text{-}42}$ was aged with aCSF, with the unaged

trending higher than the aged (Figure 12b), suggesting that aCSF may be modulating cell viability. The presence of the high molecular weight aggregates observed in aCSF-aged Aβ (Figure 10e and f) may be changing the effect of $A\beta_{1-42}$ administration to these cell cultures. It is also possible that even 20 µM $A\beta_{1-42}$ is insufficient to induce toxicity in SH-SY5Y cell cultures, whose lineage, as a form of cancer, makes them more resilient to insult. At this stage it is not possible to say for certain whether the modest increases in cell viability indicate a trophic effect or whether they simply represent experimental fluctuation.

Conclusion

Clearly, addition of certain buffers to $A\beta_{1-42}$, especially aCSF, does alter the aggregation of the peptide, causing the formation of larger aggregates, possibly protofibrils. However, the characteristics of this aggregation propensity are not reproducible. In one experiment large aggregates were seen on day 3, while in another they did not appear until day 7. Interestingly, large aggregates were also observed with aCSF-aged scrambled $A\beta_{42}$, a phenomenon not yet reported in the literature. It was discovered that this particular scrambled sequence contained aggregation “hot spots”, which may help explain this finding. Finally, it was shown that ageing with or without aCSF does seem to modulate the effect of the peptide on cell viability in SH-SY5Y cells, though clear evidence of toxicity was not observed.

3.4 Comparing toxicity in primary cells and neuroblastoma cells

To test the hypothesis that higher concentrations of $A\beta_{1-42}$ were needed to see a toxic effect, an additional concentration curve experiment was performed in the SH-SY5Y neuroblastoma cells, as well as in rat primary cortical and hippocampal cell cultures, using higher concentrations of Aβ, still aged with aCSF to induce formation of higher-order aggregates.

3.4.1 Aβ effects on SH-SY5Y neuroblastoma cell cultures

Figure 13 shows the results of several concentration curve experiments in SH-SY5Y cell cultures. There is a clear and highly significant concentration-dependent increase in cell viability, culminating in a nearly 40% increase at 40 µM. No change in cell viability was seen with the scrambled peptide. The 20 µM and 40 µM groups differed significantly from the control ($Z=-4.29$ and -5.57 respectively; $p<0.01$). The 20 µM and 40 µM treatments also differed significantly from the scrambled treatment ($Z=-3.42$ and -6.70 respectively; $p<0.001$). While consistent with some earlier data obtained during this project (see Figures 9 and 12), this protection is contrary to much of the literature on Aβ, which suggests it to be strongly cyto- and neurotoxic (discussed in section 3.4.5). However, it was important to validate these findings in a more physiologically valid primary cell culture model, in this case cortical and hippocampal cell cultures, to determine whether this positive effect of $Aβ_{1-42}$ was reproduced in other cell culture models.

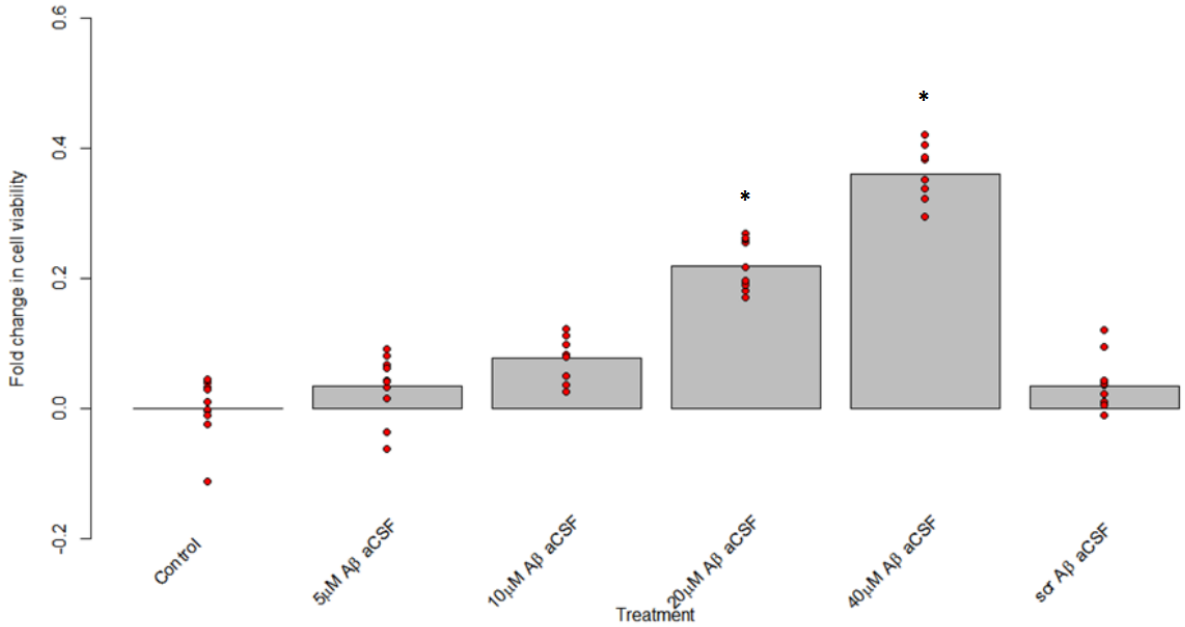

Figure 13: Bar and dot plot of changes in cell viability of SH-SY5Y cells in response to a concentration curve of Aβ for 24 h, measured using the resazurin cell viability assay. Data combined from 5 replicates over two separate experiments. Asterisks indicate groups differing significantly from the control ($p<0.001$; Kruskal-Wallis test with Dunn's post-hoc and Holm-Šidák correction, n=2).

3.4.2 Aβ effects on primary cortical and hippocampal cell cultures

Cortical and hippocampal primary cell cultures were derived from Sprague-Dawley rats, with identical experimental conditions to those used for the neuroblastoma cells. Figure 14 describes the results from the cortical cell cultures. It is immediately obvious that the trophic or protective positive effect seen in the SH-SY5Y cultures does not occur with these cultures. Furthermore, the variance of these results is much higher than that seen with the neuroblastoma cells, suggesting either inherent variability in primary cell cultures, or potentially indicative of a difference in the aggregation of the peptides used, as suggested by the aggregation SDS-PAGE gels of aCSF-aged Aβ (Figure 10e and f). This variability is especially notable when comparing individual experiments (see Appendix D) – trends observed in one experiment were not visible in another.

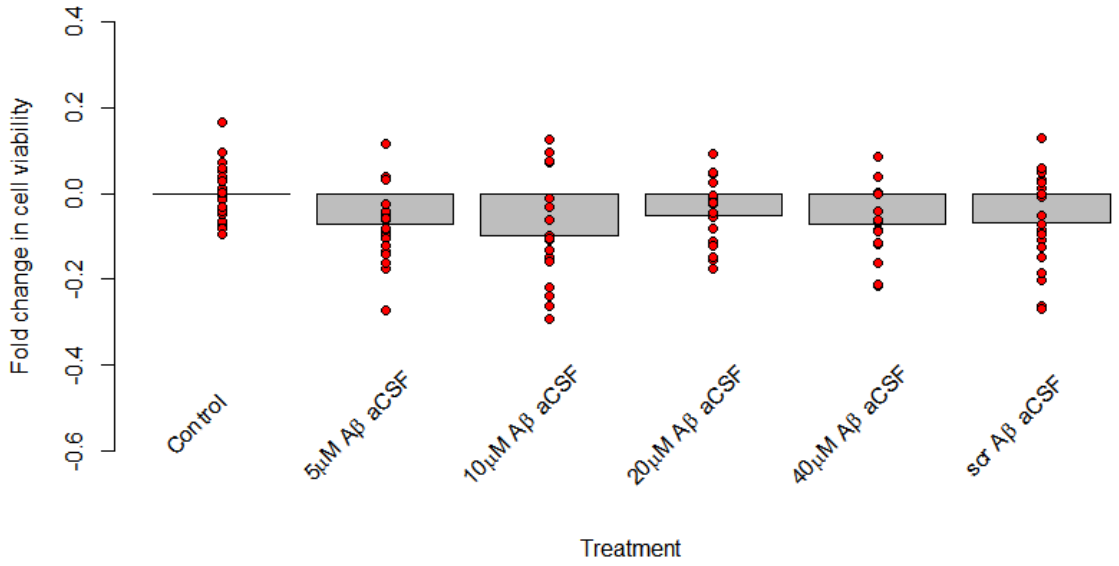

Figure 14: Bar and dot plot of cell viability changes induced by 24 h treatment with aCSF-aged $A\beta_{1-42}$ and scrambled $A\beta_{42}$ in rat cortical cell cultures. In this case, no significant differences were observed between any of the treatment groups. ($p>0.05$; Kruskal-Wallis test with Dunn's post-hoc and Holm-Šidák correction, n=4).

A similar lack of significant differences between concentrations of Aβ are seen with rat primary hippocampal cell cultures (Figure 15), and high variance within the treatment groups is seen in all groups. There are no discernible differences between cortical and hippocampal primary cultures in

regards to their reaction to Aβ. This also seems inconsistent with the literature, which suggests that hippocampal cells may be more susceptible to Aβ insult than cortical cells (Mark et al., 1997).

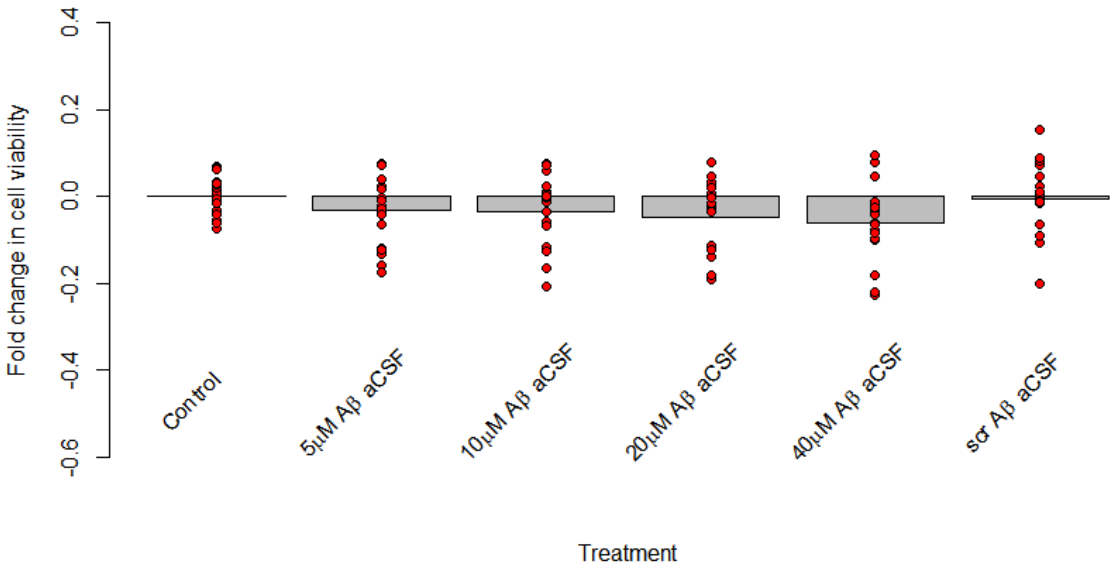

Figure 15: Bar and dot plot of cell viability changes induced by 24 h treatment with aCSF-aged $A\beta_{1-42}$ and scrambled $A\beta_{42}$ in rat hippocampal cell cultures. No significant differences were observed between any of the groups ($p>0.1$; Kruskal-Wallis test with Dunn's post-hoc and Holm-Šidák correction, n=4).

Conclusion

In SH-SY5Y neuroblastoma cell cultures, aCSF-aged $A\beta_{1-42}$ caused a dose-dependent increase in cell viability. However, the same treatment in primary rat cortical and hippocampal cells had no effect on overall cell viability. Firstly, these results raise the question of why Aβ-induced toxicity is reported so frequently and so consistently in the literature, yet these experiments fail to show any evidence of a cytotoxic effect. Second, it is unclear why there is such a considerable difference between the effect of Aβ on primary cell cultures – where it has no overt effect on cell viability – and its effect on SH-SY5Y human neuroblastoma cell cultures – where it exhibits potent trophic effects.

3.5 Zinc and Amyloid-Beta toxicity

In Section 3.4 it has been found that $A\beta_{1-42}$ consistently induces an increase in SH-SY5Y neuroblastoma cell viability. Since $A\beta_{1-42}$ contains five Zn^{2+}-binding sites in its first sixteen amino acid residues (Gaggelli et al., 2008), this next stage was to determine whether addition of exogenous zinc to the cell cultures would modulate the observed effects on cell viability. The directionality of this effect is not immediately obvious, as the literature is divided on this matter. While some research has demonstrated that exogenous zinc exacerbates Aβ-induced cytotoxicity (Solomonov et al., 2012), others have proposed that it instead protects against Aβ insult (Garai et al., 2007)

3.5.1 Concentration-dependent effect of Zinc on neuroblastoma cell culture viability

It was first necessary to examine the effects of zinc alone on cell viability of SH-SY5Y cultures. A concentration curve of $ZnCl_2$ was added to neuroblastoma cell cultures for 24 h and the cell viability determined by the resazurin assay. Figure 16 shows the results of this concentration curve, demonstrating a strong dose-dependent effect on cell survival. At concentration of 100 µM or less, $ZnCl_2$ has no effect or a positive effect on cell viability, with 25 µM $ZnCl_2$ causing around a 20% increase in resorufin fluorescence. Conversely, at concentrations of 200 µM or higher, zinc causes a considerable reduction in fluorescence, indicating significant cell death, and there is almost total death at 1 mM. This pattern is consistent with other literature describing this phenomenon (Choi et al., 1988; Bozym et al., 2010), however the slight increase in cell viability at 25 µM is not commonly described in other work. One possibility is that because DMEM does not contain any zinc, and the cell culture medium in supplemented with zinc from FBS, the control condition may actually represent a sub-optimal cellular environment. Supplementation with exogenous zinc may, in this case, cause an increase in cell survival. Alternatively, it has been demonstrated that Zn^{2+} is a potent inhibitor of

caspase-3, an enzyme heavily involved in apoptotic pathways (Perry et al., 1997). Addition of zinc to the cell culture medium may be causing inhibition of normal cell apoptosis and may account for the observed increase in cell viability. Regardless, further experiments were performed with either 5 or 25 µM $ZnCl_2$, with the former representative of no effect, and the latter, a positive one.

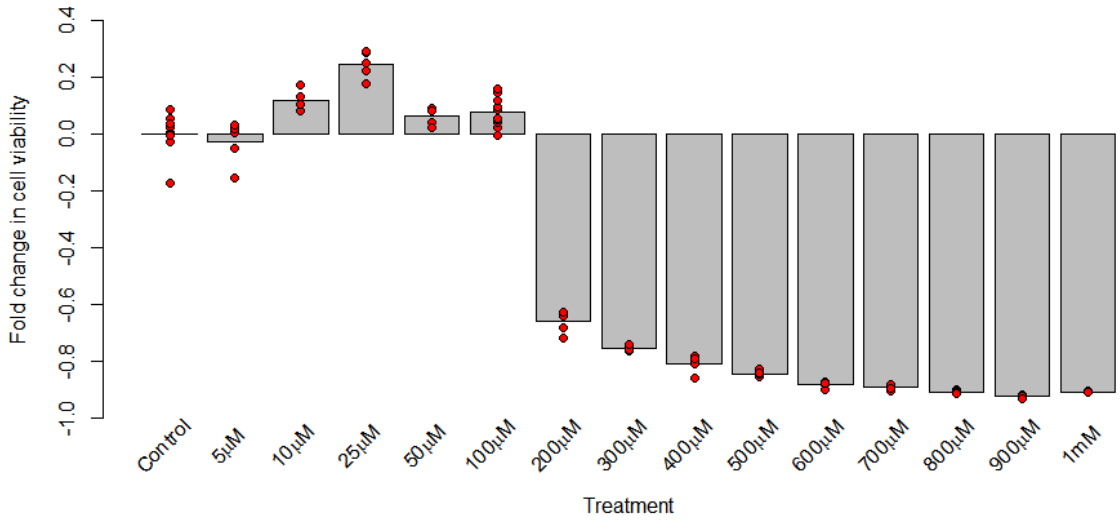

Figure 16: Bar and dot plot showing the effect on cell viability of varying concentrations of $ZnCl_2$ in the medium of cultured SH-SY5Y neuroblastoma cells. Up to 1 mM $ZnCl_2$ was added to the medium for 24 h and cell viability measured using the resazurin assay (n=2).

3.5.2 Effect of combined zinc and Aβ on neuroblastoma cell culture viability

In order to examine how the presence of Zn^{2+} in the cell culture mediummodulates Aβ-induced changes in cell viability, SH-SY5Y cell cultures were exposed to 20 µM Aβ for 24 h, with either 5 or 25 µM $ZnCl_2$. The results are displayed in Figure 17. In this experiment, the $Aβ_{1-42}$ and scrambled $Aβ_{42}$ were aged in MilliQ H_2O for 3 days. Firstly, consistent with data previously described, neither $Aβ_{1-42}$ on its own, nor the scrambled $Aβ_{42}$ had any effect on cell viability. The effects of the two concentrations of $ZnCl_2$ were also similar to those seen in Figure 16, although somewhat lower, showing a very small increase in cell viability at 25 µM and almost no change at 5 µM. However, $Aβ_{1-42}$ in combination with $ZnCl_2$ showed a considerable increase in cell viability, up to 60-70% above the control in the case of 25

µM zinc and around 40% for 5 µM. Comparing these data to the scrambled $A\beta_{42}$ strongly suggests that this significant increase is likely a result of an interaction between $A\beta_{1-42}$ and Zn^{2+}, since the scrambled groups were essentially identical to their respective controls – scrambled Aβ and zinc showed the same effect as zinc on its own. These data strongly suggest that Zn^{2+} and Aβ interact.

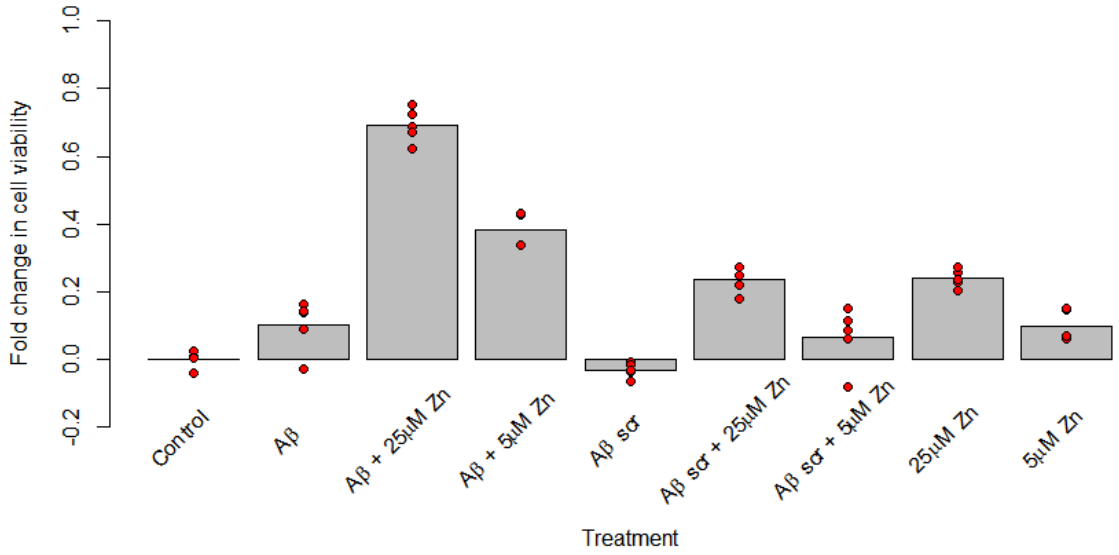

Figure 17: Bar and dot plot showing effects of $A\beta_{1-42}$ combined with $ZnCl_2$ on cell viability in SH-SY5Y cell cultures. $A\beta_{1-42}$ and scrambled $A\beta_{42}$ were applied at a concentration of 20 µM for 24 h and the $ZnCl_2$ added concurrently to the medium when used (n=1).

However, when the Aβ was aged in aCSF, this strong positive effect was no longer evident (Figure 18). Firstly, the considerable increase in cell viability observed with 20 µM $A\beta_{1-42}$ and 25 µM $ZnCl_2$ in Figure 17 is no longer present, with this condition showing no difference to $A\beta_{1-42}$ on its own. Furthermore, the positive effect seen with 20 µM Aβ-aCSF seen in Figure 13 is also conspicuously absent. Even the slight positive effect of 25 µM $ZnCl_2$ is not seen. While it is possible that this variation in the effects of the Aβ peptide may be due to variability in its agregation during the ageing process, this is unlikely to be the case for $A\beta_{1-42}$ aged in MilliQ H_2O, as its aggregation states were constant across several experiments. For $A\beta_{1-42}$ aged in aCSF, this is certainly a possibility, as the aggregation experiments (Figure 10e and f) highlighted that despite identical ageing conditions, the aggregation state of the peptide can vary significantly, with the formation of high molecular weight aggregates forming on

different days. It is possible that the Aβ-aCSF samples used for the experiments in Figure 13 had undergone a different aggregation pattern than those used for the experiment in Figure 18.

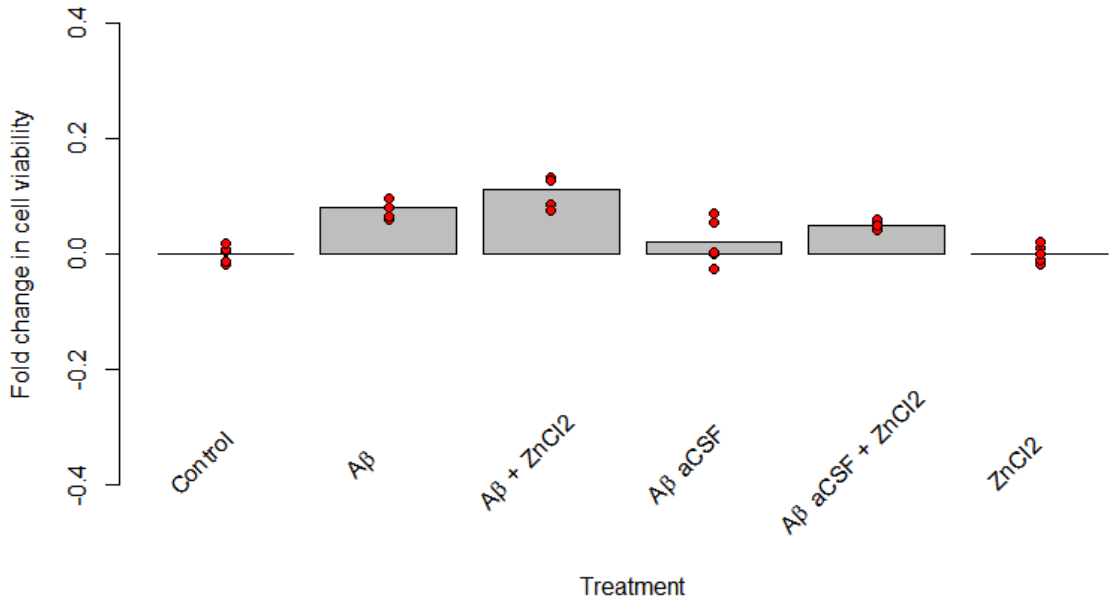

Figure 18: Bar and dot plot showing changes in SH-SY5Y cell viability after treatment with $A\beta_{1-42}$, $A\beta_{1-42}$ aged with aCSF and $ZnCl_2$. $A\beta_{1-42}$ was applied at 20 µM, and $ZnCl_2$ at 25 µM for 24 h. Cell viability was measured using the resazurin assay (n=1).

Conclusion

A concentration curve of Zn^{2+} effects on cell viability was used to establish an optimum protocol for the metal ion. While one experiment demonstrated that co-administration of aged Aβ and zinc to neuroblastoma cell cultures led to a dramatic increase in cell viability, further experiments were unable to validate these results. The data described here raise interesting questions regarding Aβ and its relationship with zinc, as well as highlighting some inherent variability in the effects of the peptide on cell viability and the difficulties in using Aβ in experimental paradigms.

Chapter 4

Discussion

The work described here was successful in producing and purifying $A\beta_{1-42}$ from bacteria transfected with human $A\beta_{1-42}$. However, establishment of a consistent protocol for $A\beta_{1-42}$-induced toxicity was unsuccessful in either SH-SY5Y neuroblastoma cells or primary rat cortical or hippocampal cell cultures. Examining the relationship between aggregation conditions and effects on cell viability revealed an interesting effect of aCSF-aged $A\beta_{1-42}$ in neuroblastoma cells – this treatment showed evidence of high molecular-weight aggregates, whilst also causing an increase in cell viability above the control. Co-treatment with Zn^{2+}, however, abolished this increase, but also showed an increase in cell viability after treatment with H_2O-aged $A\beta_{1-42}$. This research suggests that the relationship between aggregation of $A\beta_{1-42}$ and its effects on cell culture viability are complex, but that these can be regulated by exposure of the cells in culture to Zn^{2+} in the culture medium. This relationship undoubtedly requires further investigation.

4.1 Amyloid-Beta production

The protocol described and followed in this study demonstrates that amyloid-beta can be produced in-house with relatively high purity and with full knowledge of its history – an important parameter when studying the effects of aggregation. This protocol used bacteria transfected with human $A\beta_{1-42}$ cloned into the pMal-c2 vector, as when the peptide is produced alone a very low yield is obtained (Wilson, 2007). These bacterial stocks were successfully induced to express the peptide fused to maltose-binding protein, and, after initial purification of the fusion protein by affinity

chromatography, this complex was cleaved and the Aβ purified to create stocks at a concentration of 41 µM, with a yield of ~500 µg/L bacterial culture.

However, this protocol appears to have several drawbacks. Firstly, following reverse-phase chromatography to separate cleaved Aβ from MBP, it was found that, while some fractions of Aβ were well separated from MBP, there still existed a considerable (~20-30%) overlap in the elution regions of the two proteins. This meant that some of the Aβ-containing fractions were contaminated with MBP and were therefore needed to be further purified. It is not entirely clear why this would be the case, except that the solubility and hydrophobicity of the two proteins must be similar enough that their elution from the hydrophobic RPC column occurs at similar concentrations of acetonitrile. This may suggest that other systems or fusion partners might be used for production, such as glutathione S-transferase (GST), and purification on a glutathione column used in other projects in the laboratory. Nevertheless, *E. coli* MBP remains a very useful and effective fusion protein, as it greatly improves the solubility of bound proteins and prevents their aggregation (Kapust and Waugh, 1999).

Attempts to further purify MBP-contaminated fractions of Aβ by SEC proved entirely ineffective. In fact, SDS-PAGE analysis of protein-containing SEC fractions revealed that the peptide could not be detected in any of the fractions analysed. It could have been that the total amount of Aβ in the loaded samples with the well-recognised dilution of samples during gel exclusion chromatography was great enough to prevent Aβ being visible by Coomassie staining, or that the peptide ended up spread over several fractions in small amounts. Unfortunately, this meant that the overall yield was not as high as it could have been. Further optimization of this Aβ purification could be valuable to determine a more effective and efficient method of separating cleaved Aβ and MBP. Several groups have developed different protocols for Aβ purification using intestinal fatty acid binding protein (IFABP) (Garai et al., 2009), or immobilized metal affinity chromatography (IMAC) and a glutathione S-transferase (GST)-tag (Chhetri et al., 2015). The latter especially reported a yield of 15mg/L of culture, compared the 3-4mg/L in the previous study and ~500µg/L for the protocol in this study.

Third, while this protocol is an effective method of expressing and purifying Aβ, it is important to note that it cannot compete in yield to what is now available with commercial production of the peptide. High yields of the protein, greater amounts and guarantees of higher purity can be obtained, although the cost is significant. In the past batches of commercial Aβ were found to be inconsistent in their activity and that stimulated production within the Tate research laboratory (Tate personal communication). Despite obtaining a relatively high protein concentration of Aβ, it was nevertheless necessary to subsequently purchase commercial batches of the peptide, as the amount produced was insufficient for all the experiments in this study.

4.2 Cellular insult paradigm

4.2.1 The MTT assay is inappropriate for examining Amyloid-Beta toxicity.

The discovery, as early as 1995, that the reagents in the MTT cell viability assay interact with Aβ in such a way as to confound the results has startlingly not been accepted by many current researchers in the Alzheimer's field, with many groups continuing to use the assay to study the effects of Aβ. As well as its component interaction with Aβ, the MTT assay suffers from several drawbacks. Firstly, the MTT assay is very much an end-point assay, as the production of formazan crystals is toxic to cell cultures. This limits its effectiveness for assessing changes in cell viability over time. Second, as previously reported, MTT, of all cell viability assays dependent on cellular metabolism, is the least consistent, showing the highest comparative variability for the same insult (van Tonder et al., 2015). The results described in this study seem to support that conclusion and found that the alternative resazurin cell viability assay may be more suited to examining toxicity in cell culture. Not only does this assay not suffer from any known interactions with experimental compounds (as the MTT assay does with Aβ), but also shows less variability and more consistency. In addition, the compound is minimally toxic to living cells, allowing for multiple assays across time points in the same cultures.

4.2.2 Amyloid-beta effects on cell viability are dependent on its aggregation.

As previously described, it has been suggested that the effect of Aβ on cell viability is strongly dependent on its aggregation state, and that its aggregation state varies depending on the conditions in which it was aged. Here, we confirmed that specific ageing conditions do strongly impact the aggregation state of the peptide. The majority of buffers tested – MilliQ H_2O, PBS, DMSO, DMEM and MOPS – revealed no change in aggregation state over 7 days as tested by SDS-PAGE. While SDS-PAGE analysis of DMEM-aged Aβ showed a reduction in the monomer band intensity, the absence of bands indicating other aggregates suggests that no further aggregation took place. Throughout this period, gel analysis revealed the presence of monomers of Aβ, as well as a dispersed band consistent with soluble oligomers – dimers, trimers and small-order aggregates.

One chemical mixture was able to induce production of higher molecular weight aggregates – those within aCSF. This condition produced very high molecular weight aggregates, consistent with previous reports of the appearance of protofibrils and fibrillar $Aβ_{1-42}$ (Ahmed et al., 2010). However, it appears that this aggregation is not entirely consistent – while one gel showed these aggregates forming on day 7, another gel showed their formation on day 3. It may be that a nucleation state has to be formed for the higher aggregates to be produced and that may be the variable parameter. Therefore, without confirming aggregation states after each individual ageing event of $Aβ_{1-42}$, it is difficult to determine what specific aggregates are present in samples of Aβ aged with aCSF. This may be reflected in the variability of cell viability experiments performed with these samples (Section 3.3.3 onwards).

The SDS-PAGE results shown in Figure 10h describe aggregation in the scrambled Aβ peptide, with high molecular weight aggregates, comparable in size to protofibrils and fibrils of $Aβ_{1-42}$, appearing as early as day 2. This phenomenon has not been reported in the literature previously (and to the author's knowledge, an examination of the aggregation of the scrambled peptide has not been attempted), probably because each form of scrambled peptide is different to others used, depending

on the exact amino acid sequence. Examining the primary and secondary structure of the scrambled peptide using the Aggrescan 3D server predicted significant aggregation propensity (Figure 11), to the extent of being comparable to the $A\beta_{1-42}$ peptide itself. This finding has implications for the interpretation of data obtained from the cell viability experiments, and brings into question what is an appropriate control.

4.2.3 Amyloid-Beta is inconsistent as a cellular insult

Despite the frequent use of Aβ as a cellular insult in research into Alzheimer's disease, this study highlighted some of the difficulties in using this paradigm. This research was unable to develop a paradigm that consistently caused significant cell death in either SH-SY5Y neuroblastoma cell cultures or primary rat cortical or hippocampal cell cultures. Up to 20 μM Aβ aged with MilliQ H_2O did not lead to any significant changes in cell viability. Despite the commonly-held understanding that small oligomers are the most toxic species of Aβ, and the finding here that 3-day ageing of the peptide in water produced a considerable amount of aggregates consistent with soluble small aggregates alongside monomers, there was no toxicity observed in any cases. In fact, treatment of neuroblastoma cells with 10 μM Aβ for 24 hours gave the first indication that the peptide may indeed be neuroprotective and not exclusively toxic.

Under certain conditions, Aβ may show trophic effects. In SH-SY5Y neuroblastoma cells, treatment with aCSF-aged Aβ showed a dose-dependent increase in cell viability over the control (Figure 13). While trophic and neuroprotective effects of Aβ have been observed previously (Kimura et al., 2006; Giuffrida et al., 2009), the concentration of the peptide required for a positive effect tends to be significantly lower – in the pico- to nano-molar range – contrary to the 20-40 μM range used here. It was initially thought that perhaps the neuroblastoma cell cultures may be under oxidative stress, particularly as many of the experiments were performed in cell cultures approaching passage numbers of 10-15, and the addition of Aβ may have been ameliorating oxidative damage, potentially by

precipitating redox-active metal ions such as Zn^{2+} and Cu^{2+}. However, when the experiment was repeated in passage 5 cells that would not show the same level of oxidative stress as the "older" cell cultures, the obtained results were identical (data not shown).

Alternatively, the lack of Aβ-induced toxicity observed may be characteristic of the immortal neuroblastoma cell line. Both differentiated and undifferentiated SH-SY5Y neuroblastoma cells have been demonstrated to show a dopaminergic nature – they express tyrosine hydroxylase, dopamine-beta-hydroxylase and the dopamine transporter (Xie et al., 2010) – though differentiated cells show more of this character. The toxicity of Aβ, on the other hand, is reportedly NMDA-dependent (Birnbaum et al., 2015), but some evidence suggests that neuroblastomas may not express ionotropic glutamate receptors (Weber et al., 2010), or that their NMDARs may be non-functional (Sun et al., 2010). However, the fact that toxicity was not observed in primary rat cortical or hippocampal cell cultures suggests that this factor may not necessarily account for the results observed, in particular the Aβ-induced increases in cell viability seen in SH-SY5Y cells. On the other hand, the presence of glial cells in the primary rat neuronal cultures may be vital to understanding the lack of any effect of Aβ on their viability. It is now recognised that glial cells play an important role in homeostasis of the neuronal environment and this has been shown to include control over the clearance and breakdown of Aβ (reviewed by Ries & Sastre, 2016). Glial cells secrete neprilysin, insulin-degrading enzyme, endothelin-converting enzyme and a variety of matrix metalloproteinases, cathepsins and chaperones demonstrated to be involved in the degradation and clearance of Aβ from the extracellular space. The activity of these enzymes and proteases may account for the absence of a consistent toxic effect of Aβ on primary rat neuronal cultures, another factor that must be taken into account when developing cellular models to study AD.

One factor to consider may be the difference between intracellular and extracellular Aβ. While some evidence shows that the toxic effects of Aβ may be as a result of an interaction with NMDA receptors (Birnbaum et al., 2015), others have reported that chronologically, accumulation of the peptide

intraneuronally occurs first, and this may lead to p53-related apoptosis (Ohyagi, 2008). However, it has also been demonstrated that neurons can take up Aβ from the extracellular environment – possibly an important part of normal clearance of the peptide – suggesting that addition of exogenous Aβ may also increase its intraneuronal concentration (Kanekiyo et al., 2013). An important future step may be to determine firstly whether exogenous Aβ can be taken up by neurons in culture, and second, whether intracellular or extracellular Aβ has a greater effect on cell viability.

The discovery that scrambled $A\beta_{42}$ also formed aggregates suggests that peptide aggregation alone is not sufficient to produce cellular toxicity. Scrambled $A\beta_{42}$ consistently had no effect on cell viability in either SH-SY5Y neuroblastoma cell cultures or cultured primary rat cortical and hippocampal cells. In addition, it is suggestive that the positive, trophic effects of oligomeric and fibrillar $A\beta_{1\text{-}42}$ must be a result of a specific interaction of the peptide, rather than a general effect of either peptide supplementation or aggregation.

4.3 Zinc and Amyloid-Beta interactions

4.3.1 Zinc has a dose-dependent effect on SH-SY5Y cell viability

In order to determine optimum concentrations of $ZnCl_2$ for cell culture experiments, a concentration curve of the zinc salt was tested in SH-SY5Y neuroblastoma cell cultures, ranging from 5 µM to 1 mM. A clear dose-dependent effect was observed, with concentrations less than 100 µM showing a positive or no effect on cell viability, while higher concentrations lead to markedly decreased cell viability to less than 10% of control. Although physiological concentrations of zinc are overall in the pico- to nanomolar range, when Zn^{2+} is released synaptically, concentrations in the synaptic cleft can reach as high as 30 µM (Frederickson and Bush, 2001). Due to the tight regulation of intracellular Zn^{2+} ions by zinc transporters, it is difficult to alter intracellular zinc by addition of exogenous zinc, though evidence suggests that intracellular concentrations of around 100 nM is fatal. It is possible that application

of >100 µM zinc to cell culture media may overload zinc transporters and drive the intracellular concentration into this toxic range. However, it is equally likely that such a high concentration of zinc simply causes the pH of the media to drop to a toxic level, leading to the high levels of cell death seen in this study.

Similarly, the finding that 5-100 µM $ZnCl_2$ has a neutral or positive effect on cell culture viability is likely closely modulated by the zinc transporters. Nevertheless, as serum-free DMEM contains no free zinc, it is equally likely that the positive effect of Zn^{2+} is simply due to this supplementation of the culture media with a biologically-relevant and essential metal ion.

4.3.2 Zinc modulates Amyloid-Beta induced changes in cell viability

The range of zinc concentrations used in Section 3.5.2 (5-25 µM) was used firstly because it was a non-toxic amount and secondly because it is consistent with previous findings that 8 µM Zn^{2+} is protective against Aβ toxicity (Garai et al., 2007). Similar to the results obtained in Section 3.5.1, 5 and 25µM $ZnCl_2$ resulted in an increase in cell viability compared to the control. This seems likely a result of supplementation of DMEM- with essential zinc. However, the combination of Zn^{2+} and $Aβ_{1-42}$ aged in water was observed to increase cell viability beyond the increase observed with Zn^{2+} on its own. By contrast, the scrambled $Aβ_{42}$ with zinc did not raise cell viability above zinc alone. This evidence suggested that the increase was a result of a specific interaction between $Aβ_{1-42}$ (in this case specifically monomers and small oligomers) and Zn^{2+}. The reason for the positive effects of this proposed interaction is unclear. Firstly, the possible trophic or neuroprotective effect of $Aβ_{1-42}$ require further exploration, as this extent of increased cell viability at concentrations of Aβ as high as 40 µM has not been reported previously. Second, previous reports of Aβ-Zn^{2+} interactions have been contradictory – while some reports suggest a positive interaction (Garai et al., 2007), others report an increase in toxicity (Solomonov et al., 2012). Both agree, however, that Zn^{2+} has profound effects on the structure of Aβ aggregates. This relationship undoubtedly requires further investigation, not only

in regards to why Aβ-zinc treatment shows trophic effects in SH-SY5Y cells, but also clarification of the effect of Zn^{2+} on the structure of Aβ aggregates, which appears to play an important role in the physiological effects of the peptide.

4.4 Conclusions

This research has described a successful protocol for the production and purification of $A\beta_{1-42}$, although due to the amount of the peptide unusable due to MBP contamination, it clearly requires further optimization and minor adjustments to the experimental strategy. This study initially aimed to determine a consistent protocol for Aβ-induced cell death – a well-described paradigm of cell toxicity. However, far from observing cell death, Aβ-treatment of SH-SY5Y neuroblastoma cells as high as 40µM actually increased cell viability by up to 40%, while no significant changes were observed in primary rat neuronal cultures. This effect was shown to be dependent on the aggregation state of the peptide, which in turn is heavily dependent on the "ageing" environment, with aCSF causing formation of high molecular weight aggregates, and all other tested buffers only showing formation of monomers and small oligomers. Finally, it was demonstrated that addition of exogenous Zn^{2+} positively modulated this already positive effect on cell viability of Aβ, beyond the trophic effect of Zn^{2+} alone.

4.5 Future Directions

Given the conflicting results obtained in this study, future research must work to elucidate the true relationship between Aβ aggregation and its effects on cell viability. While many studies regularly report Aβ-induced toxicity in a variety of cellular and animal models, this research failed to replicate any of those results. It may be necessary to produce and isolate individual species of Aβ aggregates – monomers, small oligomers, larger soluble aggregates, protofibrils and fibrils – in order to determine the true relationship between aggregation and toxicity.

It will also be necessary to repeat the experiments reported here to replicate the findings that aCSF-aged $A\beta_{1-42}$ showed trophic or neuroprotective effects. As previously mentioned, such effects have been observed, but with significantly lower concentrations of the peptide. It will also be important to determine whether these effects can be demonstrated in primary cell cultures (which did not show increased cell viability in this study), as well as repeating the experiment in differentiated neuroblastoma cell cultures, which exhibit more neuronal characteristics (Shipley et al., 2016). Other neuronal cell models may be more suited to examining Aβ-induced toxicity than neuroblastoma cells, for example Neuro2a cells, which show cholinergic characteristics and are often used in the study of AD, or the NTera-2 cell line, which can be differentiated to express NMDA receptors (Younkin et al., 1993).

If a consistent cellular insult paradigm can be established, potentially with specific Aβ aggregate species and different cell culture models, the next stage would be to further examine the relationship between Aβ and Zn^{2+}. This study has demonstrated that the combination of $A\beta_{1-42}$ and Zn^{2+} can have profound effects on cell viability beyond that of each individually. However, the directionality of this relationship is conflicted in the literature, and may differ between different allomers and aggregation states of Aβ. A concentration curve of Zn^{2+} with specific species of Aβ may help elucidate this relationship, though as previous research has suggested, AD pathophysiology may develop as a result of aberrant compartmentalization of metal ions (Ayton et al., 2015). Using metal protein targeting compounds such as clioquinol or PBT2 may allow control of Zn^{2+} compartmentalization and examination of how metal ion localization affects cell activity and survival.

It may also be interesting to investigate how Zn^{2+} may influence neuroprotection by APP-derived processed proteins or peptides such as sAPPα and 16-mer. The sAPPα protein shows significant neuroprotective effects (Goodman and Mattson, 1994; Furukawa et al., 1996) and there have been suggestions that the 16-mer peptide may also have mild neuroprotective properties (Potemkin, 2014; Morissey, 2016). The 16-mer, as discussed previously, has a number of possible Zn^{2+}-binding sites, and

this sequence also constitutes an apparently unstructured C-terminal region of sAPPα. It is possible that, in addition to trophic gene regulation effects of sAPPα (Ryan et al., 2013), its neuroprotective effects may be mediated by its zinc-binding potential, perhaps directly by co-binding with Aβ around the Zn^{2+} ion. It has been suggested that amyloid plaques are a protective mechanism (Cohen et al., 2006; Nilsson et al., 2013), preferentially precipitating Aβ aggregates to clear toxic species such as protofibrils or soluble oligomers. sAPPα may act to sequester toxic Aβ aggregates into benign plaques, that can potentially be cleared by the phagocytic properties of microglia. If this could be demonstrated, it may significantly alter the direction of research into treatments for AD, many of which target Aβ plaques by immunotherapy or altering Aβ production. Indeed the recent immunotherapy strategy targeting the toxic soluble aggregates is appearing to be much more effective than previous plaque focussed attempts (Sevigny et al., 2016).

References

ADI (2009) World Alzheimer's Report 2009.

Adlard PA et al. (2008) Rapid restoration of cognition in Alzheimer's transgenic mice with 8-hydroxy quinoline analogs is associated with decreased interstitial Abeta. Neuron 59:43–55.

Adlard PA, Bica L, White AR, Nurjono M, Filiz G, Crouch PJ, Donnelly PS, Cappai R, Finkelstein DI, Bush AI (2011) Metal ionophore treatment restores dendritic spine density and synaptic protein levels in a mouse model of Alzheimer's disease. PLoS One 6:e17669.

Adlard PA, Parncutt JM, Finkelstein DI, Bush AI (2010) Cognitive loss in zinc transporter-3 knock-out mice: a phenocopy for the synaptic and memory deficits of Alzheimer's disease? J Neurosci 30:1631–1636.

Ahmed M, Davis J, Aucoin D, Sato T, Ahuja S, Aimoto S, Elliott JI, Van Nostrand WE, Smith SO (2010) Structural conversion of neurotoxic amyloid-beta(1-42) oligomers to fibrils. Nat Struct Mol Biol 17:561–567.

Aisen PS, Gauthier S, Vellas B, Briand R, Saumier D, Laurin J, Garceau D (2007) Alzhemed: a potential treatment for Alzheimer's disease. Curr Alzheimer Res 4:473–478.

Alzheimers New Zealand (2012) Updated Dementia Economic Impact New Zealand Alzheimers New Zealand.

Alzheon (2016) Alzheon Announces Efficacy Analyses of Prior Tramiprosate Phase 3 Studies Showing Clinically Meaningful Benefits on Key Clinical Endpoints in Alzheimer's Disease Patients with APOE4 Genotype. Available at: http://alzheon.com/alzheon-announces-efficacy-analyses-prior-tramiprosate-phase-3-studies-showing-clinically-meaningful-benefits-key-clinical-endpoints-alzheimers-disease-patients-apoe/ [Accessed November 5, 2016].

Anoopkumar-Dukie S, Carey JB, Conere T, O'Sullivan E, van Pelt FN & Allshire A (2005) Resazurin assay of radiation response in cultured cells. The British Journal of Radiology, 78:934, 945-947.

Arevalo M-A, Roldan PM, Chacon PJ, Rodriguez-Tebar A (2009) Amyloid beta serves as an NGF-like neurotrophic factor or acts as a NGF antagonist depending on its concentration. J Neurochem

111:1425–1433.

Arimon M, Diez-Perez I, Kogan MJ, Durany N, Giralt E, Sanz F, Fernandez-Busquets X (2005) Fine structure study of Abeta1-42 fibrillogenesis with atomic force microscopy. FASEB J Off Publ Fed Am Soc Exp Biol 19:1344–1346.

Ayton S, Lei P, Bush AI (2015) Biometals and their therapeutic implications in Alzheimer's disease. Neurotherapeutics 12:109–120.

Bard F et al. (2000) Peripherally administered antibodies against amyloid beta-peptide enter the central nervous system and reduce pathology in a mouse model of Alzheimer disease. Nat Med 6:916–919.

Barnham KJ, Bush AI (2014) Biological metals and metal-targeting compounds in major neurodegenerative diseases. Chem Soc Rev 43:6727–6749.

Barnham KJ, McKinstry WJ, Multhaup G, Galatis D, Morton CJ, Curtain CC, Williamson NA, White AR, Hinds MG, Norton RS, Beyreuther K, Masters CL, Parker MW, Cappai R (2003) Structure of the Alzheimer's Disease Amyloid Precursor Protein Copper Binding Domain: A REGULATOR OF NEURONAL COPPER HOMEOSTASIS . J Biol Chem 278:17401–17407.

Barrow CJ, Zagorski MG (1991) Solution structures of beta peptide and its constituent fragments: relation to amyloid deposition. Science 253:179–182.

Bayer TA, Schäfer S, Simons A, Kemmling A, Kamer T, Tepests R, Eckert A, Schüssel K, Eikenberg O, Sturchler-Pierrat C, Abramowski D, Staufenbiel M, Multhaup G (2003) Dietary Cu stabilizes brain superoxide dismutase 1 activity and reduces amyloid Aβ production in APP23 transgenic mice. Proc Natl Acad Sci U S A 100:14187–14192.

Becerril-Ortega J, Bordji K, Freret T, Rush T, Buisson A (2014) Iron overload accelerates neuronal amyloid-beta production and cognitive impairment in transgenic mice model of Alzheimer's disease. Neurobiol Aging 35:2288–2301.

Bennett DA, Schneider JA, Arvanitakis Z, Kelly JF, Aggarwal NT, Shah RC, Wilson RS (2006) Neuropathology of older persons without cognitive impairment from two community-based

studies. Neurology 66:1837–1844.

Benoit M, Berrut G, Doussaint J, Bakchine S, Bonin-guillaume S, David R, Robert P (2012) Apathy and Depression in Mild Alzheimer's Disease : A Cross-Sectional Study Using Diagnostic Criteria. 31:325–334.

Birnbaum JH, Bali J, Rajendran L, Nitsch RM, Tackenberg C (2015) Calcium flux-independent NMDA receptor activity is required for A[beta] oligomer-induced synaptic loss. Cell Death Dis 6:e1791.

Bitan G, Tarus B, Vollers SS, Lashuel HA, Condron MM, Straub JE, Teplow DB (2003) A molecular switch in amyloid assembly: Met35 and amyloid beta-protein oligomerization. J Am Chem Soc 125:15359–15365.

Bjorklund NL, Reese LC, Sadagoparamanujam V-M, Ghirardi V, Woltjer RL, Taglialatela G (2012) Absence of amyloid beta oligomers at the postsynapse and regulated synaptic Zn2+ in cognitively intact aged individuals with Alzheimer's disease neuropathology. Mol Neurodegener 7:23.

Black SAG, Stys PK, Zamponi GW, Tsutsui S (2014) Cellular prion protein and NMDA receptor modulation: protecting against excitotoxicity. Front cell Dev Biol 2:45.

Bloudek LM, Spackman DE, Blankenburg M, Sullivan SD (2011) Review and meta-analysis of biomarkers and diagnostic imaging in Alzheimer's disease. J Alzheimers Dis 26:627–645.

Borchardt T, Camakaris J, Cappai R, Masters CL, Beyreuther K, Multhaup G (1999) Copper inhibits beta-amyloid production and stimulates the non-amyloidogenic pathway of amyloid-precursor-protein secretion. Biochem J 344 Pt 2:461–467.

Bowler J V, Eliasziw M, Steenhuis R, Munoz DG, Fry R, Merskey H, Hachinski VC (1997) Comparative evolution of Alzheimer disease, vascular dementia, and mixed dementia. Arch Neurol 54:697–703.

Bozym RA, Chimienti F, Giblin LJ, Gross GW, Korichneva I, Li Y, Libert S, Maret W, Parviz M, Frederickson CJ, Thompson RB (2010) Free zinc ions outside a narrow concentration range are toxic to a variety of cells in vitro. Exp Biol Med (Maywood) 235:741–750.

Braak H, Braak E (1991) Neuropathological stageing of Alzheimer-related changes. Acta Neuropathol 82:239–259.

Breteler MM (2000) Vascular risk factors for Alzheimer's disease: an epidemiologic perspective. Neurobiol Aging 21:153–160.

Brodaty H, Hadzi-Pavlovic D (1990) Psychosocial Effects on Carers of Living with Persons with Dementia. Aust N Z J Psychiatry 24:351–361.

Brody DL, Magnoni S, Schwetye KE, Spinner ML, Esparza TJ, Stocchetti N, Zipfel GJ, Holtzman DM (2008) Amyloid-beta dynamics correlate with neurological status in the injured human brain. Science 321:1221–1224.

Brookmeyer R, Corrada MM, Curriero FC, Kawas C (2002) Survival Following a Diagnosis of Alzheimer Disease. Arch Neurol 59:1764–1767.

Brunnstrom H, Englund E (2009) Cause of death in patients with dementia disorders. Eur J Neurol 16:488–492.

Burmester T, Weich B, Reinhardt S, Hankeln T (2000) A vertebrate globin expressed in the brain. Nature 407:520–523.

Bush AI, Pettingell WHJ, Paradis MD, Tanzi RE (1994) Modulation of A beta adhesiveness and secretase site cleavage by zinc. J Biol Chem 269:12152–12158.

Caragounis A, Du T, Filiz G, Laughton KM, Volitakis I, Sharples RA, Cherny RA, Masters CL, Drew SC, Hill AF, Li Q-X, Crouch PJ, Barnham KJ, White AR (2007) Differential modulation of Alzheimer's disease amyloid beta-peptide accumulation by diverse classes of metal ligands. Biochem J 407:435–450.

Cater MA, McInnes KT, Li Q-X, Volitakis I, La Fontaine S, Mercer JFB, Bush AI (2008) Intracellular copper deficiency increases amyloid-beta secretion by diverse mechanisms. Biochem J 412:141–152.

Chafekar SM, Baas F, Scheper W (2008) Oligomer-specific Aβ toxicity in cell models is mediated by selective uptake. Biochim Biophys Acta - Mol Basis Dis 1782:523–531.

Chartier-Harlin MC, Crawford F, Houlden H, Warren A, Hughes D, Fidani L, Goate A, Rossor M, Roques P, Hardy J (1991) Early-onset Alzheimer's disease caused by mutations at codon 717 of the beta-amyloid precursor protein gene. Nature 353:844–846.

Chen J, Wang M, Turko I V (2013) Quantification of Amyloid Precursor Protein Isoforms Using Quantification Concatamer Internal Standard. Anal Chem 85:303–307.

Cherny RA, Atwood CS, Xilinas ME, Gray DN, Jones WD, McLean CA, Barnham KJ, Volitakis I, Fraser FW, Kim Y, Huang X, Goldstein LE, Moir RD, Lim JT, Beyreuther K, Zheng H, Tanzi RE, Masters CL, Bush AI (2001) Treatment with a copper-zinc chelator markedly and rapidly inhibits beta-amyloid accumulation in Alzheimer's disease transgenic mice. Neuron 30:665–676.

Chhetri G, Pandey T, Chinta R, Kumar A, Tripathi T (2015) An improved method for high-level soluble expression and purification of recombinant amyloid-beta peptide for in vitro studies. Protein Expr Purif 114:71–76.

Chiu M-J, Chen Y-F, Chen T-F, Yang S-Y, Yang F-PG, Tseng T-W, Chieh J-J, Chen J-CR, Tzen K-Y, Hua M-S, Horng H-E (2014) Plasma tau as a window to the brain-negative associations with brain volume and memory function in mild cognitive impairment and early Alzheimer's disease. Hum Brain Mapp 35:3132–3142.

Choi DW, Yokoyama M, Koh J (1988) Zinc neurotoxicity in cortical cell culture. Neuroscience 24:67–79.

Cleary JP, Walsh DM, Hofmeister JJ, Shankar GM, Kuskowski MA, Selkoe DJ, Ashe KH (2005) Natural oligomers of the amyloid-[beta] protein specifically disrupt cognitive function. Nat Neurosci 8:79–84.

Cohen E, Bieschke J, Perciavalle RM, Kelly JW, Dillin A (2006) Opposing activities protect against age-onset proteotoxicity. Science 313:1604–1610.

Crouch PJ, Savva MS, Hung LW, Donnelly PS, Mot AI, Parker SJ, Greenough MA, Volitakis I, Adlard PA, Cherny RA, Masters CL, Bush AI, Barnham KJ, White AR (2011) The Alzheimer's therapeutic PBT2 promotes amyloid-beta degradation and GSK3 phosphorylation via a metal chaperone activity. J Neurochem 119:220–230.

Cuajungco MP, Goldstein LE, Nunomura A, Smith MA, Lim JT, Atwood CS, Huang X, Farrag YW, Perry G, Bush AI (2000) Evidence that the beta-amyloid plaques of Alzheimer's disease represent the redox-silencing and entombment of abeta by zinc. J Biol Chem 275:19439–19442.

Cunningham C, Wilcockson DC, Campion S, Lunnon K, Perry VH (2005) Central and systemic endotoxin challenges exacerbate the local inflammatory response and increase neuronal death during chronic neurodegeneration. J Neurosci 25:9275–9284.

Dahlgren KN, Manelli AM, Stine WBJ, Baker LK, Krafft GA, LaDu MJ (2002) Oligomeric and fibrillar species of amyloid-beta peptides differentially affect neuronal viability. J Biol Chem 277:32046–32053.

Davies CA, Mann DM, Sumpter PQ, Yates PO (1987) A quantitative morphometric analysis of the neuronal and synaptic content of the frontal and temporal cortex in patients with Alzheimer's disease. J Neurol Sci 78:151–164.

Dawson GR, Seabrook GR, Zheng H, Smith DW, Graham S, O'Dowd G, Bowery BJ, Boyce S, Trumbauer ME, Chen HY, Van der Ploeg LH, Sirinathsinghji DJ (1999) Age-related cognitive deficits, impaired long-term potentiation and reduction in synaptic marker density in mice lacking the beta-amyloid precursor protein. Neuroscience 90:1–13.

de la Torre JC, Mussivand T (1993) Can disturbed brain microcirculation cause Alzheimer's disease? Neurol Res 15:146–153.

Deibel MA, Ehmann WD, Markesbery WR (1996) Copper, iron, and zinc imbalances in severely degenerated brain regions in Alzheimer's disease: possible relation to oxidative stress. J Neurol Sci 143:137–142.

Doody RS, Thomas RG, Farlow M, Iwatsubo T, Vellas B, Joffe S, Kieburtz K, Raman R, Sun X, Aisen PS, Siemers E, Liu-Seifert H, Mohs R (2014) Phase 3 trials of solanezumab for mild-to-moderate Alzheimer's disease. N Engl J Med 370:311–321.

Drew SC, Barnham KJ (2011) The heterogeneous nature of Cu2+ interactions with Alzheimer's amyloid-beta peptide. Acc Chem Res 44:1146–1155.

Eisenhauer PB, Johnson RJ, Wells JM, Davies TA, Fine RE (2000) Toxicity of various amyloid beta peptide species in cultured human blood-brain barrier endothelial cells: increased toxicity of dutch-type mutant. J Neurosci Res 60:804–810.

Elder M (2013) Secreted amyloid precursor protein alpha attenuates apoptosis in organotypiic hippocampal slices. Bachelor of Science (Honours) thesis. University of Otago.

Esch FS, Keim PS, Beattie EC, Blacher RW, Culwell AR, Oltersdorf T, McClure D, Ward PJ (1990) Cleavage of amyloid beta peptide during constitutive processing of its precursor. Science (80-) 248:1122 LP-1124.

Falangola MF, Lee S-P, Nixon RA, Duff K, Helpern JA (2005) Histological co-localization of iron in Abeta plaques of PS/APP transgenic mice. Neurochem Res 30:201–205.

Faller P, Hureau C, La Penna G (2014) Metal ions and intrinsically disordered proteins and peptides: from Cu/Zn amyloid-beta to general principles. Acc Chem Res 47:2252–2259.

Famulari AL, Marschoff ER, Llesuy SF, Kohan S, Serra JA, Dominguez RO, Repetto M, Reides C, Sacerdote de Lustig E (1996) The antioxidant enzymatic blood profile in Alzheimer's and vascular diseases. Their association and a possible assay to differentiate demented subjects and controls. J Neurol Sci 141:69–78.

Farrer LA, Cupples LA, Haines JL, Hyman B, Kukull WA, Mayeux R, Myers RH, Pericak-Vance MA, Risch N, van Duijn CM (1997) Effects of age, sex, and ethnicity on the association between apolipoprotein E genotype and Alzheimer disease. A meta-analysis. APOE and Alzheimer Disease Meta Analysis Consortium. JAMA 278:1349–1356.

Faux NG, Ritchie CW, Gunn A, Rembach A, Tsatsanis A, Bedo J, Harrison J, Lannfelt L, Blennow K, Zetterberg H, Ingelsson M, Masters CL, Tanzi RE, Cummings JL, Herd CM, Bush AI (2010) PBT2 rapidly improves cognition in Alzheimer's Disease: additional phase II analyses. J Alzheimers Dis 20:509–516.

Fein JA, Sokolow S, Miller CA, Vinters H V, Yang F, Cole GM, Gylys KH (2008) Co-Localization of Amyloid Beta and Tau Pathology in Alzheimer's Disease Synaptosomes. Am J Pathol 172:1683–1692.

Femminella GD, Ferrara N, Rengo G (2015) The emerging role of microRNAs in Alzheimer's disease. Front Physiol 6:40.

Ferrada E, Arancibia V, Loeb B, Norambuena E, Olea-Azar C, Huidobro-Toro JP (2007) Stoichiometry and conditional stability constants of Cu(II) or Zn(II) clioquinol complexes; implications for Alzheimer's and Huntington's disease therapy. Neurotoxicology 28:445–449.

Finder VH, Glockshuber R (2007) Amyloid-beta aggregation. Neurodegener Dis 4:13–27.

Förstl A, Kurz H (1999) Clinical features of Alzheimer's disease. Eur Arch Psychiatry Clin Neurosci 249(6):288–290.

Fraser PE, Nguyen JT, Inouye H, Surewicz WK, Selkoe DJ, Podlisny MB, Kirschner DA (1992) Fibril formation by primate, rodent, and Dutch-hemorrhagic analogues of Alzheimer amyloid beta-protein. Biochemistry 31:10716–10723.

Fraser PE, Nguyen JT, Surewicz WK, Kirschner DA (1991) pH-dependent structural transitions of Alzheimer amyloid peptides. Biophys J 60:1190–1201.

Frederickson CJ, Bush AI (2001) Synaptically released zinc: Physiological functions and pathological effects. BioMetals 14:353–366.

Furukawa K, Sopher BL, Rydel RE, Begley JG, Pham DG, Martin GM, Fox M, Mattson MP (1996) Increased activity-regulating and neuroprotective efficacy of alpha-secretase-derived secreted amyloid precursor protein conferred by a C-terminal heparin-binding domain. J Neurochem 67:1882–1896.

Gaggelli E, Janicka-Klos A, Jankowska E, Kozlowski H, Migliorini C, Molteni E, Valensin D, Valensin G, Wieczerzak E (2008) NMR studies of the Zn2+ interactions with rat and human beta-amyloid (1-28) peptides in water-micelle environment. J Phys Chem B 112:100–109.

Garai K, Crick SL, Mustafi SM, Frieden C (2009) Expression and purification of amyloid-β peptides from Escherichia coli. Protein Expr Purif 66:107–112.

Garai K, Sahoo B, Kaushalya SK, Desai R, Maiti S (2007) Zinc lowers amyloid-beta toxicity by selectively precipitating aggregation intermediates. Biochemistry 46:10655–10663.

Garai K, Sengupta P, Sahoo B, Maiti S (2006) Selective destabilization of soluble amyloid beta oligomers by divalent metal ions. Biochem Biophys Res Commun 345:210–215.

Garcia-Osta A, Alberini CM (2009) Amyloid beta mediates memory formation. Learn Mem 16:267–272.

Geekiyanage H, Chan C (2011) MicroRNA-137/181c regulates serine palmitoyltransferase and in turn amyloid beta, novel targets in sporadic Alzheimer's disease. J Neurosci 31:14820–14830.

Geekiyanage H, Jicha GA, Nelson PT, Chan C (2012) Blood serum miRNA: Non-invasive biomarkers for Alzheimer's disease. Exp Neurol 235:491–496.

Gervais F, Paquette J, Morissette C, Krzywkowski P, Yu M, Azzi M, Lacombe D, Kong X, Aman A, Laurin J, Szarek WA, Tremblay P (2007) Targeting soluble Abeta peptide with Tramiprosate for the treatment of brain amyloidosis. Neurobiol Aging 28:537–547.

Gibson GE, Zhang H, Sheu KR, Park LC (2000) Differential alterations in antioxidant capacity in cells from Alzheimer patients. Biochim Biophys Acta 1502:319–329.

Giuffrida ML, Caraci F, Pignataro B, Cataldo S, De Bona P, Bruno V, Molinaro G, Pappalardo G, Messina A, Palmigiano A, Garozzo D, Nicoletti F, Rizzarelli E, Copani A (2009) Beta-amyloid monomers are neuroprotective. J Neurosci 29:10582–10587.

Glenner GG, Wong CW (1984a) Alzheimer's disease: Initial report of the purification and characterization of a novel cerebrovascular amyloid protein. Biochem Biophys Res Commun 120:885–890.

Glenner GG, Wong CW (1984b) Alzheimer's disease and Down's syndrome: sharing of a unique cerebrovascular amyloid fibril protein. Biochem Biophys Res Commun 122:1131–1135.

Goate A, Chartier-Harlin MC, Mullan M, Brown J, Crawford F, Fidani L, Giuffra L, Haynes A, Irving N, James L (1991) Segregation of a missense mutation in the amyloid precursor protein gene with familial Alzheimer's disease. Nature 349:704–706.

Gold M, Alderton C, Zvartau-Hind M, Egginton S, Saunders AM, Irizarry M, Craft S, Landreth G, Linnamagi U, Sawchak S (2010) Rosiglitazone monotherapy in mild-to-moderate Alzheimer's

disease: results from a randomized, double-blind, placebo-controlled phase III study. Dement Geriatr Cogn Disord 30:131–146.

Goodman L (1953) Alzheimer's disease; a clinico-pathologic analysis of twenty-three cases with a theory on pathogenesis. J Nerv Ment Dis 118:97–130.

Goodman Y, Mattson MP (1994) Secreted forms of beta-amyloid precursor protein protect hippocampal neurons against amyloid beta-peptide-induced oxidative injury. Exp Neurol 128:1–12.

Gottwald M, Rozanski R (1999) Rivastigmine, a brain-region selective acetylcholinesterase inhibitor for treating Alzheimer's disease: review and current status. Expert Opin Investig Drugs 8:1673–1682.

Grossberg GT, Lake JT (1998) The Role of the Psychiatrist in Alzheimer's Disease. J Clin Psychiatry 59:3–6.

Grundke-Iqbal I, Iqbal K, Quinlan M, Tung YC, Zaidi MS, Wisniewski HM (1986) Microtubule-associated protein tau. A component of Alzheimer paired helical filaments. J Biol Chem 261:6084–6089.

Guo Q, Fu W, Holtsberg FW, Steiner SM, Mattson MP (1999a) Superoxide mediates the cell-death-enhancing action of presenilin-1 mutations. J Neurosci Res 56:457–470.

Guo Q, Sebastian L, Sopher BL, Miller MW, Ware CB, Martin GM, Mattson MP (1999b) Increased vulnerability of hippocampal neurons from presenilin-1 mutant knock-in mice to amyloid beta-peptide toxicity: central roles of superoxide production and caspase activation. J Neurochem 72:1019–1029.

Hanyu H, Sato T, Kiuchi A, Sakurai H, Iwamoto T (2009) Pioglitazone improved cognition in a pilot study on patients with Alzheimer's disease and mild cognitive impairment with diabetes mellitus. J Am Geriatr Soc 57:177–179.

Hartley DM, Walsh DM, Ye CP, Diehl T, Vasquez S, Vassilev PM, Teplow DB, Selkoe DJ (1999) Protofibrillar intermediates of amyloid beta-protein induce acute electrophysiological changes and progressive neurotoxicity in cortical neurons. J Neurosci 19:8876–8884.

Hartmann T, Bieger SC, Bruhl B, Tienari PJ, Ida N, Allsop D, Roberts GW, Masters CL, Dotti CG, Unsicker K, Beyreuther K (1997) Distinct sites of intracellular production for Alzheimer's disease A beta40/42 amyloid peptides. Nat Med 3:1016–1020.

Hatanpaa K, Brady DR, Stoll J, Rapoport SI, Chandrasekaran K (1996) Neuronal activity and early neurofibrillary tangles in Alzheimer's disease. Ann Neurol 40:411–420.

He Y, Zheng M-M, Ma Y, Han X-J, Ma X-Q, Qu C-Q, Du Y-F (2012) Soluble oligomers and fibrillar species of amyloid beta-peptide differentially affect cognitive functions and hippocampal inflammatory response. Biochem Biophys Res Commun 429:125–130.

Hebert SS, Horre K, Nicolai L, Papadopoulou AS, Mandemakers W, Silahtaroglu AN, Kauppinen S, Delacourte A, De Strooper B (2008) Loss of microRNA cluster miR-29a/b-1 in sporadic Alzheimer's disease correlates with increased BACE1/beta-secretase expression. Proc Natl Acad Sci U S A 105:6415–6420.

Hertel C, Hauser N, Schubenel R, Seilheimer B, Kemp JA (1996) Beta-amyloid-induced cell toxicity: enhancement of 3-(4,5-dimethylthiazol-2-yl)-2,5-diphenyltetrazolium bromide-dependent cell death. J Neurochem 67:272–276.

Hickman SE, El Khoury J (2014) TREM2 and the neuroimmunology of Alzheimer's disease. Biochem Pharmacol 88:495–498.

Howlett DR, Jennings KH, Lee DC, Clark MS, Brown F, Wetzel R, Wood SJ, Camilleri P, Roberts GW (1995) Aggregation state and neurotoxic properties of Alzheimer beta-amyloid peptide. Neurodegeneration 4:23–32.

Huang X et al. (1999) Cu(II) potentiation of alzheimer abeta neurotoxicity. Correlation with cell-free hydrogen peroxide production and metal reduction. J Biol Chem 274:37111–37116.

Huang X, Atwood CS, Moir RD, Hartshorn MA, Tanzi RE, Bush AI (2004) Trace metal contamination initiates the apparent auto-aggregation, amyloidosis, and oligomerization of Alzheimer's Abeta peptides. J Biol Inorg Chem 9:954–960.

Hung YH, Robb EL, Volitakis I, Ho M, Evin G, Li Q-X, Culvenor JG, Masters CL, Cherny RA, Bush AI (2009)

Paradoxical condensation of copper with elevated beta-amyloid in lipid rafts under cellular copper deficiency conditions: implications for Alzheimer disease. J Biol Chem 284:21899–21907.

Hyman B, Van Hoesen G, Damasio A, Barnes C (1984) Alzheimer's Disease: Cell-Specific Pathology Isolates the Hippocampal Formation. Science 225:1168–1170.

Jack CR, Wengenack TM, Reyes DA, Garwood M, Curran GL, Borowski BJ, Lin J, Preboske GM, Holasek SS, Adriany G, Poduslo JF (2005) In Vivo Magnetic Resonance Microimaging of Individual Amyloid Plaques in Alzheimer's Transgenic Mice. J Neurosci 25:10041–10048.

James SA, Volitakis I, Adlard PA, Duce JA, Masters CL, Cherny RA, Bush AI (2012) Elevated labile Cu is associated with oxidative pathology in Alzheimer disease. Free Radic Biol Med 52:298–302.

Janus C, Pearson J, McLaurin J, Mathews PM, Jiang Y, Schmidt SD, Chishti MA, Horne P, Heslin D, French J, Mount HT, Nixon RA, Mercken M, Bergeron C, Fraser PE, St George-Hyslop P, Westaway D (2000) A beta peptide immunization reduces behavioural impairment and plaques in a model of Alzheimer's disease. Nature 408:979–982.

Jiang Q, Lee CYD, Mandrekar S, Wilkinson B, Cramer P, Zelcer N, Mann K, Lamb B, Willson TM, Collins JL, Richardson JC, Smith JD, Comery TA, Riddell D, Holtzman DM, Tontonoz P, Landreth GE (2008) ApoE promotes the proteolytic degradation of Aβ. Neuron 58:681–693.

Johnson GVW, Stoothoff WH (2004) Tau phosphorylation in neuronal cell function and dysfunction. J Cell Sci 117:5721–5729.

Johnson KA, Jones K, Holman BL, Becker JA, Spiers PA, Satlin A, Albert MS (1998) Preclinical prediction of Alzheimer's disease using SPECT. Neurology 50:1563–1571.

Jost BC, Grossberg GT (1995) The natural history of Alzheimer's disease: a brain bank study. J Am Geriatr Soc 43:1248–1255.

Jun S, Gillespie JR, Shin B, Saxena S (2009) The second Cu(II)-binding site in a proton-rich environment interferes with the aggregation of amyloid-beta(1-40) into amyloid fibrils. Biochemistry 48:10724–10732.

Kaether C, Haass C, Steiner H (2006) Assembly, trafficking and function of gamma-secretase.

Neurodegener Dis 3:275–283.

Kanekiyo T, Cirrito JR, Liu C-C, Shinohara M, Li J, Schuler DR, Shinohara M, Li J, Holtzman DM & Bu, G. (2013). Neuronal Clearance of Amyloid-β by Endocytic Receptor LRP1. The Journal of Neuroscience, 33(49), 19276–19283.

Kapust RB, Waugh DS (1999) Escherichia coli maltose-binding protein is uncommonly effective at promoting the solubility of polypeptides to which it is fused. Protein Sci 8:1668–1674.

Kimura N, Takahashi M, Tashiro T, Terao K (2006) Amyloid beta up-regulates brain-derived neurotrophic factor production from astrocytes: rescue from amyloid beta-related neuritic degeneration. J Neurosci Res 84:782–789.

Kirschner DA, Inouye H, Duffy LK, Sinclair A, Lind M, Selkoe DJ (1987) Synthetic peptide homologous to beta protein from Alzheimer disease forms amyloid-like fibrils in vitro. Proc Natl Acad Sci U S A 84:6953–6957.

Knopman D, Schneider L, Davis K, Talwalker S, Smith F, Hoover T, Gracon S (1996) Long-term tacrine (Cognex) treatment: effects on nursing home placement and mortality, Tacrine Study Group. Neurology 47:166–177.

Kosaka N, Iguchi H, Yoshioka Y, Takeshita F, Matsuki Y, Ochiya T (2010) Secretory Mechanisms and Intercellular Transfer of MicroRNAs in Living Cells. J Biol Chem 285:17442–17452.

Kumar DKV, Choi SH, Washicosky KJ, Eimer WA, Tucker S, Ghofrani J, Lefkowitz A, McColl G, Goldstein LE, Tanzi RE, Moir RD (2016) Amyloid-beta peptide protects against microbial infection in mouse and worm models of Alzheimer's disease. Sci Transl Med 8:340ra72.

Kuo YM, Emmerling MR, Vigo-Pelfrey C, Kasunic TC, Kirkpatrick JB, Murdoch GH, Ball MJ, Roher AE (1996) Water-soluble Abeta (N-40, N-42) oligomers in normal and Alzheimer disease brains. J Biol Chem 271:4077–4081.

Lammich S, Kojro E, Postina R, Gilbert S, Pfeiffer R, Jasionowski M, Haass C, Fahrenholz F (1999) Constitutive and regulated alpha-secretase cleavage of Alzheimer's amyloid precursor protein by a disintegrin metalloprotease. Proc Natl Acad Sci U S A 96:3922–3927.

Langa K, Larson E, Crimmins E, Faul J, Levine D, Kabeto M, Weir D (2017) A comparison of the prevalence of dementia in the united states in 2000 and 2012. JAMA Intern Med 177:51–58.

Lannfelt L, Blennow K, Zetterberg H, Batsman S, Ames D, Harrison J, Masters CL, Targum S, Bush AI, Murdoch R, Wilson J, Ritchie CW (2008) Safety, efficacy, and biomarker findings of PBT2 in targeting Abeta as a modifying therapy for Alzheimer's disease: a phase IIa, double-blind, randomised, placebo-controlled trial. Lancet Neurol 7:779–786.

Ledesma MD, Avila J, Correas I (1995) Isolation of a phosphorylated soluble tau fraction from Alzheimer's disease brain. Neurobiol Aging 16:515–522.

Lei P, Ayton S, Finkelstein DI, Spoerri L, Ciccotosto GD, Wright DK, Wong BXW, Adlard PA, Cherny RA, Lam LQ, Roberts BR, Volitakis I, Egan GF, McLean CA, Cappai R, Duce JA, Bush AI (2012) Tau deficiency induces parkinsonism with dementia by impairing APP-mediated iron export. Nat Med 18:291–295.

Lesne S, Koh MT, Kotilinek L, Kayed R, Glabe CG, Yang A, Gallagher M, Ashe KH (2006) A specific amyloid-beta protein assembly in the brain impairs memory. Nature 440:352–357.

Leutner S, Czech C, Schindowski K, Touchet N, Eckert A, Muller WE (2000) Reduced antioxidant enzyme activity in brains of mice transgenic for human presenilin-1 with single or multiple mutations. Neurosci Lett 292:87–90.

Liu B, Moloney A, Meehan S, Morris K, Thomas SE, Serpell LC, Hider R, Marciniak SJ, Lomas DA, Crowther DC (2011) Iron promotes the toxicity of amyloid beta peptide by impeding its ordered aggregation. J Biol Chem 286:4248–4256.

Lopez-Toledo G, Cardenas-Aguayo M del C, Gomez-Virgilio L, Luna-Muñoz J, Meraz-Rios MA (2016) Evaluation of the effect of amyloid beta oligomers on neurotrophins and GSK-3/creb signal transduction pathways. Alzheimer's Dement J Alzheimer's Assoc 11:P364.

Lovell MA, Robertson JD, Teesdale WJ, Campbell JL, Markesbery WR (1998) Copper, iron and zinc in Alzheimer's disease senile plaques. J Neurol Sci 158:47–52.

Lovell MA, Smith JL, Xiong S, Markesbery WR (2005) Alterations in zinc transporter protein-1 (ZnT-1)

in the brain of subjects with mild cognitive impairment, early, and late-stage Alzheimer's disease. Neurotox Res 7:265–271.

Lue LF, Rydel R, Brigham EF, Yang LB, Hampel H, Murphy GMJ, Brachova L, Yan SD, Walker DG, Shen Y, Rogers J (2001a) Inflammatory repertoire of Alzheimer's disease and nondemented elderly microglia in vitro. Glia 35:72–79.

Lue LF, Walker DG, Rogers J (2001b) Modeling microglial activation in Alzheimer's disease with human postmortem microglial cultures. Neurobiol Aging 22:945–956.

Lyubartseva G, Smith JL, Markesbery WR, Lovell MA (2010) Alterations of zinc transporter proteins ZnT-1, ZnT-4 and ZnT-6 in preclinical Alzheimer's disease brain. Brain Pathol 20:343–350.

Maccioni RB, Farias G, Morales I, Navarrete L (2010) The revitalized tau hypothesis on Alzheimer's disease. Arch Med Res 41:226–231.

Maeda S, Sahara N, Saito Y, Murayama S, Ikai A, Takashima A (2006) Increased levels of granular tau oligomers: an early sign of brain aging and Alzheimer's disease. Neurosci Res 54:197–201.

Mandrekar-Colucci S, Karlo JC, Landreth GE (2012) Mechanisms underlying the rapid peroxisome proliferator-activated receptor-gamma-mediated amyloid clearance and reversal of cognitive deficits in a murine model of Alzheimer's disease. J Neurosci 32:10117–10128.

Mann DM, Iwatsubo T, Ihara Y, Cairns NJ, Lantos PL, Bogdanovic N, Lannfelt L, Winblad B, Maat-Schieman ML, Rossor MN (1996) Predominant deposition of amyloid-beta 42(43) in plaques in cases of Alzheimer's disease and hereditary cerebral hemorrhage associated with mutations in the amyloid precursor protein gene. Am J Pathol 148:1257–1266.

Mark RJ, Pang Z, Geddes JW, Uchida K, Mattson MP (1997) Amyloid β-Peptide Impairs Glucose Transport in Hippocampal and Cortical Neurons: Involvement of Membrane Lipid Peroxidation. J Neurosci 17:1046 LP-1054.

Mattson MP (2004) Metal-catalyzed disruption of membrane protein and lipid signaling in the pathogenesis of neurodegenerative disorders. Ann N Y Acad Sci 1012:37–50.

Maurer I, Zierz S, Moller HJ (2000) A selective defect of cytochrome c oxidase is present in brain of

Alzheimer disease patients. Neurobiol Aging 21:455–462.

May PC et al. (2011) Robust central reduction of amyloid-beta in humans with an orally available, non-peptidic beta-secretase inhibitor. J Neurosci 31:16507–16516.

McLean CA, Cherny RA, Fraser FW, Fuller SJ, Smith MJ, Vbeyreuther K, Bush AI, Masters CL (1999) Soluble pool of Aβ amyloid as a determinant of severity of neurodegeneration in Alzheimer's disease. Ann Neurol 46:860–866.

Mikulca JA, Nguyen V, Gajdosik DA, Teklu SG, Giunta EA, Lessa EA, Tran CH, Terak EC, Raffa RB (2014) Potential novel targets for Alzheimer pharmacotherapy: II. Update on secretase inhibitors and related approaches. J Clin Pharm Ther 39:25–37.

Miller BW, Willett KC, Desilets AR (2011) Rosiglitazone and pioglitazone for the treatment of Alzheimer's disease. Ann Pharmacother 45:1416–1424.

Mold M, Ouro-Gnao L, Wieckowski BM, Exley C (2013) Copper prevents amyloid-β(1–42) from forming amyloid fibrils under near-physiological conditions in vitro. Sci Rep 3.

Morgan D, Diamond DM, Gottschall PE, Ugen KE, Dickey C, Hardy J, Duff K, Jantzen P, DiCarlo G, Wilcock D, Connor K, Hatcher J, Hope C, Gordon M, Arendash GW (2000) A beta peptide vaccination prevents memory loss in an animal model of Alzheimer's disease. Nature 408:982–985.

Morissey J (2016) Neuroprotection by APP-derived peptides. Unpublished raw data.

Morley JE, Farr SA, Banks WA, Johnson SN, Yamada KA, Xu L (2010) A physiological role for amyloid-beta protein: enhancement of learning and memory. J Alzheimers Dis 19:441–449.

Mosmann T (1983) Rapid colorimetric assay for cellular growth and survival: Application to proliferation and cytotoxicity assays. Journal of Immunological Methods, 65(1):55-63.

Nelson TJ, Alkon DL (2005) Oxidation of cholesterol by amyloid precursor protein and beta-amyloid peptide. J Biol Chem 280:7377–7387.

Nguyen LT, Haney EF, Vogel HJ (2011) The expanding scope of antimicrobial peptide structures and

their modes of action. Trends Biotechnol 29:464–472.

Nilsson P, Loganathan K, Sekiguchi M, Matsuba Y, Hui K, Tsubuki S, Tanaka M, Iwata N, Saito T, Saido TC (2013) Aβ Secretion and Plaque Formation Depend on Autophagy. Cell Rep 5:61–69.

Nimmrich V, Grimm C, Draguhn A, Barghorn S, Lehmann A, Schoemaker H, Hillen H, Gross G, Ebert U, Bruehl C (2008) Amyloid beta oligomers (A beta(1-42) globulomer) suppress spontaneous synaptic activity by inhibition of P/Q-type calcium currents. J Neurosci 28:788–797.

Ohyagi Y (2008) Intracellular amyloid beta-protein as a therapeutic target for treating Alzheimer's disease. Curr Alzheimer Res 5(6): 555-561.

Olsson B, Lautner R, Andreasson U, Öhrfelt A, Portelius E, Bjerke M, Hölttä M, Rosén C, Olsson C, Strobel G, Wu E, Dakin K, Petzold M, Blennow K, Zetterberg H (2016) CSF and blood biomarkers for the diagnosis of Alzheimer's disease: a systematic review and meta-analysis. Lancet Neurol 15:673–684.

Opazo C, Huang X, Cherny RA, Moir RD, Roher AE, White AR, Cappai R, Masters CL, Tanzi RE, Inestrosa NC, Bush AI (2002) Metalloenzyme-like activity of Alzheimer's disease beta-amyloid. Cu-dependent catalytic conversion of dopamine, cholesterol, and biological reducing agents to neurotoxic H(2)O(2). J Biol Chem 277:40302–40308.

Oren Z, Lerman JC, Gudmundsson GH, Agerberth B, Shai Y (1999) Structure and organization of the human antimicrobial peptide LL-37 in phospholipid membranes: relevance to the molecular basis for its non-cell-selective activity. Biochem J 341 (Pt 3:501–513.

Orgogozo J-M, Gilman S, Dartigues J-F, Laurent B, Puel M, Kirby LC, Jouanny P, Dubois B, Eisner L, Flitman S, Michel BF, Boada M, Frank A, Hock C (2003) Subacute meningoencephalitis in a subset of patients with AD after Abeta42 immunization. Neurology 61:46–54.

Pedersen JT, Ostergaard J, Rozlosnik N, Gammelgaard B, Heegaard NHH (2011) Cu(II) mediates kinetically distinct, non-amyloidogenic aggregation of amyloid-beta peptides. J Biol Chem 286:26952–26963.

Perry DK, Smyth MJ, Stennicke HR, Salvesen GS, Duriez P, Poirier GG, Hannun YA (1997) Zinc is a potent

inhibitor of the apoptotic protease, caspase-3. A novel target for zinc in the inhibition of apoptosis. J Biol Chem 272:18530–18533.

Petkova AT, Leapman RD, Guo Z, Yau W-M, Mattson MP, Tycko R (2005) Self-propagating, molecular-level polymorphism in Alzheimer's beta-amyloid fibrils. Science 307:262–265.

Podlisny MB, Ostaszewski BL, Squazzo SL, Koo EH, Rydell RE, Teplow DB, Selkoe DJ (1995) Aggregation of secreted amyloid beta-protein into sodium dodecyl sulfate-stable oligomers in cell culture. J Biol Chem 270:9564–9570.

Potemkin N (2014) Neuroprotection by sAPPα and its 16 amino acid C-terminal peptide in response to Oxygen Glucose Deprivation and Amyloid Beta Insults. Bachelor of Science (Honours) thesis. University of Otago.

Priller C, Bauer T, Mitteregger G, Krebs B, Kretzschmar HA, Herms J (2006) Synapse Formation and Function Is Modulated by the Amyloid Precursor Protein. J Neurosci 26:7212 LP-7221.

Prince M, Wimo A, Guerchet M, Gemma-Claire A, Wu Y-T, Prina M (2015) World Alzheimer Report 2015: The Global Impact of Dementia - An analysis of prevalence, incidence, cost and trends. Alzheimer's Dis Int: 84.

Puglielli L, Friedlich AL, Setchell KDR, Nagano S, Opazo C, Cherny RA, Barnham KJ, Wade JD, Melov S, Kovacs DM, Bush AI (2005) Alzheimer disease β-amyloid activity mimics cholesterol oxidase. J Clin Invest 115:2556–2563.

Ransmayr G (1998) Difficulties in the clinical diagnosis of vascular dementia and dementia of the Alzheimer type--comparison of clinical classifications. J Neural Transm Suppl 53:79–90.

Rapoport M, Dawson HN, Binder LI, Vitek MP, Ferreira A (2002) Tau is essential to beta -amyloid-induced neurotoxicity. Proc Natl Acad Sci U S A 99:6364–6369.

Reisberg B, Auer SR, Monteiro I, Boksay I, Sclan SG (1996) Behavioral Disturbances of Dementia : An Overview of Phenomenology and Methodologic Concerns. Int Psychogeriatr. 8 Suppl 2:169-80.

Reisberg B, Doody R, Stoffler A, Schmitt F, Ferris S, Mobius HJ (2003) Memantine in moderate-to-severe Alzheimer's disease. N Engl J Med 348:1333–1341.

Religa D, Strozyk D, Cherny RA, Volitakis I, Haroutunian V, Winblad B, Naslund J, Bush AI (2006) Elevated cortical zinc in Alzheimer disease. Neurology 67:69–75.

Ries M, & Sastre M (2016) Mechanisms of Aβ Clearance and Degradation by Glial Cells. Frontiers in Aging Neuroscience, 8:160.

Risner ME, Saunders AM, Altman JFB, Ormandy GC, Craft S, Foley IM, Zvartau-Hind ME, Hosford DA, Roses AD (2006) Efficacy of rosiglitazone in a genetically defined population with mild-to-moderate Alzheimer's disease. Pharmacogenomics J 6:246–254.

Ritchie CW, Bush AI, Mackinnon A, Macfarlane S, Mastwyk M, MacGregor L, Kiers L, Cherny R, Li Q-X, Tammer A, Carrington D, Mavros C, Volitakis I, Xilinas M, Ames D, Davis S, Beyreuther K, Tanzi RE, Masters CL (2003) Metal-protein attenuation with iodochlorhydroxyquin (clioquinol) targeting Abeta amyloid deposition and toxicity in Alzheimer disease: a pilot phase 2 clinical trial. Arch Neurol 60:1685–1691.

Roberson ED, Scearce-Levie K, Palop JJ, Yan F, Cheng IH, Wu T, Gerstein H, Yu G-Q, Mucke L (2007) Reducing endogenous tau ameliorates amyloid beta-induced deficits in an Alzheimer's disease mouse model. Science 316:750–754.

Rodriguez-Martin T, Cuchillo-Ibanez I, Noble W, Nyenya F, Anderton BH, Hanger DP (2013) Tau phosphorylation affects its axonal transport and degradation. Neurobiol Aging 34:2146–2157.

Rogers J, Mastroeni D, Leonard B, Joyce J, Grover A (2007) Neuroinflammation in Alzheimer's disease and Parkinson's disease: are microglia pathogenic in either disorder? Int Rev Neurobiol 82:235–246.

Rogers SL (1998) Perspectives in the management of Alzheimer's disease: clinical profile of donepezil. Dement Geriatr Cogn Disord 9 Suppl 3:29–42.

Rogers SL, Farlow MR, Doody RS, Mohs R, Friedhoff LT (1998) A 24-week, double-blind, placebo-controlled trial of donepezil in patients with Alzheimer's disease. Donepezil Study Group. Neurology 50:136–145.

Roher AE, Chaney MO, Kuo YM, Webster SD, Stine WB, Haverkamp LJ, Woods AS, Cotter RJ, Tuohy JM,

Krafft GA, Bonnell BS, Emmerling MR (1996) Morphology and toxicity of Abeta-(1-42) dimer derived from neuritic and vascular amyloid deposits of Alzheimer's disease. J Biol Chem 271:20631–20635.

Rosen C, Mattsson N, Johansson PM, Andreasson U, Wallin A, Hansson O, Johansson J-O, Lamont J, Svensson J, Blennow K, Zetterberg H (2011) Discriminatory Analysis of Biochip-Derived Protein Patterns in CSF and Plasma in Neurodegenerative Diseases. Front Aging Neurosci 3:1.

Rowe CC et al. (2007) Imaging beta-amyloid burden in aging and dementia. Neurology 68:1718–1725.

Ryan MM, Morris GP, Mockett BG, Bourne K, Abraham WC, Tate WP, Williams JM (2013) Time-dependent changes in gene expression induced by secreted amyloid precursor protein-alpha in the rat hippocampus. BMC Genomics 14:376.

Salloway S et al. (2014) Two phase 3 trials of bapineuzumab in mild-to-moderate Alzheimer's disease. N Engl J Med 370:322–333.

Salvador GA, Uranga RM, Giusto NM (2010) Iron and mechanisms of neurotoxicity. Int J Alzheimers Dis 2011:720658.

Samochocki M, Hoffle A, Fehrenbacher A, Jostock R, Ludwig J, Christner C, Radina M, Zerlin M, Ullmer C, Pereira EFR, Lubbert H, Albuquerque EX, Maelicke A (2003) Galantamine is an allosterically potentiating ligand of neuronal nicotinic but not of muscarinic acetylcholine receptors. J Pharmacol Exp Ther 305:1024–1036.

Sarell CJ, Wilkinson SR, Viles JH (2010) Substoichiometric levels of Cu2+ ions accelerate the kinetics of fiber formation and promote cell toxicity of amyloid-{beta} from Alzheimer disease. J Biol Chem 285:41533–41540.

Sato T, Hanyu H, Hirao K, Kanetaka H, Sakurai H, Iwamoto T (2011) Efficacy of PPAR-gamma agonist pioglitazone in mild Alzheimer disease. Neurobiol Aging 32:1626–1633.

Schägger H & von Jagow G (1987) Tricine-sodium dodecyl sulfate-polyacrylamide gel electrophoresis for the separation of proteins in the range from 1 to 100 kDa. Analytical Biochemistry 166(2):368-379.

Scheltens P, Blennow K, Breteler MMB, Strooper B De, Frisoni GB, Salloway S, Flier WM Van Der (2016) Alzheimer's disease. Lancet 6736:1–13.

Scheltens P, Launer LJ, Barkhof F, Weinstein HC, van Gool WA (1995) Visual assessment of medial temporal lobe atrophy on magnetic resonance imaging : interobserver reliability. J Neurol 242:557–560.

Schenk D et al. (1999) Immunization with amyloid-beta attenuates Alzheimer-disease-like pathology in the PDAPP mouse. Nature 400:173–177.

Selkoe DJ, Hardy J (2016) The amyloid hypothesis of Alzheimer's disease at 25 years. EMBO Mol Med 8:595–608.

Serpell LC (2000) Alzheimer's amyloid fibrils: structure and assembly. Biochim Biophys Acta 1502:16–30.

Sevigny J et al. (2016) The antibody aducanumab reduces Abeta plaques in Alzheimer's disease. Nature 537:50–56.

Shankar GM, Bloodgood BL, Townsend M, Walsh DM, Selkoe DJ, Sabatini BL (2007) Natural oligomers of the Alzheimer amyloid-beta protein induce reversible synapse loss by modulating an NMDA-type glutamate receptor-dependent signaling pathway. J Neurosci 27:2866–2875.

Shankar GM, Li S, Mehta TH, Garcia-Munoz A, Shepardson NE, Smith I, Brett FM, Farrell MA, Rowan MJ, Lemere CA, Regan CM, Walsh DM, Sabatini BL, Selkoe DJ (2008) Amyloid-beta protein dimers isolated directly from Alzheimer's brains impair synaptic plasticity and memory. Nat Med 14:837–842.

Shearman MS, Hawtin SR, Tailor VJ (1995) The intracellular component of cellular 3-(4,5-dimethylthiazol-2-yl)-2, 5-diphenyltetrazolium bromide (MTT) reduction is specifically inhibited by beta-amyloid peptides. J Neurochem 65:218–227.

Shipley MM, Mangold CA, Szpara ML (2016) Differentiation of the SH-SY5Y Human Neuroblastoma Cell Line. J Vis Exp:53193.

Sims NR, Bowen DM, Smith CC, Flack RH, Davison AN, Snowden JS, Neary D (1980) Glucose metabolism

and acetylcholine synthesis in relation to neuronal activity in Alzheimer's disease. Lancet 1:333–336.

Singh M (2010) The C-terminal domain of secreted amyloid precursor protein alpha (sAPPα): a key region for protection against Alzheimer's disease? Bachelor Biomed Sci (Honours) thesis. University of Otago.

Smith PK, Krohn RI, Hermanson GT, Mallia AK, Gartner FH, Provenzano MD, Fujimoto EK, Goeke NM, Olson BJ, Klenk DC (1985) Measurement of protein using bicinchoninic acid. Analytical Biochemistry 150(1):76-85.

Solomonov I, Korkotian E, Born B, Feldman Y, Bitler A, Rahimi F, Li H, Bitan G, Sagi I (2012) Zn2+-Abeta40 complexes form metastable quasi-spherical oligomers that are cytotoxic to cultured hippocampal neurons. J Biol Chem 287:20555–20564.

Sood R, Domanov Y, Pietiainen M, Kontinen VP, Kinnunen PKJ (2008) Binding of LL-37 to model biomembranes: insight into target vs host cell recognition. Biochim Biophys Acta 1778:983–996.

Soscia SJ, Kirby JE, Washicosky KJ, Tucker SM, Ingelsson M, Hyman B, Burton MA, Goldstein LE, Duong S, Tanzi RE, Moir RD (2010) The Alzheimer's Disease-Associated Amyloid β-Protein Is an Antimicrobial Peptide. PLoS One 5(3):e9505.

Soucek T, Cumming R, Dargusch R, Maher P, Schubert D (2003) The regulation of glucose metabolism by HIF-1 mediates a neuroprotective response to amyloid beta peptide. Neuron 39:43–56.

Springate BA, Tremont G (2014) Dimensions of Caregiver Burden in Dementia: Impact of Demographic, Mood, and Care Recipient Variables. Am J Geriatr Psychiatry 22:294–300.

Stein TD, Anders NJ, DeCarli C, Chan SL, Mattson MP, Johnson JA (2004) Neutralization of transthyretin reverses the neuroprotective effects of secreted amyloid precursor protein (APP) in APPSW mice resulting in tau phosphorylation and loss of hippocampal neurons: support for the amyloid hypothesis. J Neurosci 24:7707–7717.

Stelzmann RA, Schnitzlein HN, Murtagh FR (1995) An english translation of Alzheimer's 1907 paper, "über eine eigenartige erkankung der hirnrinde." Clin Anat 8:429–431.

Stephan A, Laroche S, Davis S (2001) Generation of aggregated beta-amyloid in the rat hippocampus impairs synaptic transmission and plasticity and causes memory deficits. J Neurosci 21:5703–5714.

Stoltenberg M, Bush AI, Bach G, Smidt K, Larsen A, Rungby J, Lund S, Doering P, Danscher G (2007) Amyloid plaques arise from zinc-enriched cortical layers in APP/PS1 transgenic mice and are paradoxically enlarged with dietary zinc deficiency. Neuroscience 150:357–369.

Sun X, He G, Song W (2006) BACE2, as a novel APP theta-secretase, is not responsible for the pathogenesis of Alzheimer's disease in Down syndrome. FASEB J Off Publ Fed Am Soc Exp Biol 20:1369–1376.

Sun Z-W, Zhang L, Zhu S-J, Chen W-C, Mei B (2010) Excitotoxicity effects of glutamate on human neuroblastoma SH-SY5Y cells via oxidative damage. Neurosci Bull 26:8–16.

Tapiola T, Alafuzoff I, Herukka S-K, Parkkinen L, Hartikainen P, Soininen H, Pirttila T (2009) Cerebrospinal fluid {beta}-amyloid 42 and tau proteins as biomarkers of Alzheimer-type pathologic changes in the brain. Arch Neurol 66:382–389.

Tariot PN, Solomon PR, Morris JC, Kershaw P, Lilienfeld S, Ding C (2000) A 5-month, randomized, placebo-controlled trial of galantamine in AD. The Galantamine USA-10 Study Group. Neurology 54:2269–2276.

Tominaga-Yoshino K, Uetsuki T, Yoshikawa K, Ogura A (2001) Neurotoxic and neuroprotective effects of glutamate are enhanced by introduction of amyloid precursor protein cDNA. Brain Res 918:121–130.

Tomita S, Kirino Y, Suzuki T (1998) Cleavage of Alzheimer's Amyloid Precursor Protein (APP) by Secretases Occurs after O-Glycosylation of APP in the Protein Secretory Pathway: Identification of intracellular compartments in which APP cleavage occurs without using toxic agents that interfere. J Biol Chem 273:6277–6284.

Townsend M, Shankar GM, Mehta T, Walsh DM, Selkoe DJ (2006) Effects of secreted oligomers of amyloid beta-protein on hippocampal synaptic plasticity: a potent role for trimers. J Physiol 572:477–492.

Tsai J, Grutzendler J, Duff K, Gan W-B (2004) Fibrillar amyloid deposition leads to local synaptic abnormalities and breakage of neuronal branches. Nat Neurosci 7:1181–1183.

Tyrrell J, Cosgrave M, McCarron M, McPherson J, Calvert J, Kelly A, McLaughlin M, Gill M, Lawlor BA (2001) Dementia in people with Down's syndrome. Int J Geriatr Psychiatry 16:1168–1174.

van Tonder A, Joubert AM, Cromarty AD (2015) Limitations of the 3-(4,5-dimethylthiazol-2-yl)-2,5-diphenyl-2H-tetrazolium bromide (MTT) assay when compared to three commonly used cell enumeration assays. BMC Res Notes 8:47.

Vassar R et al. (1999) Beta-secretase cleavage of Alzheimer's amyloid precursor protein by the transmembrane aspartic protease BACE. Science 286:735–741.

Vellas B, Sol O, Snyder PJ, Ousset P-J, Haddad R, Maurin M, Lemarie J-C, Desire L, Pando MP (2011) EHT0202 in Alzheimer's disease: a 3-month, randomized, placebo-controlled, double-blind study. Curr Alzheimer Res 8:203–212.

Vickers KC, Palmisano BT, Shoucri BM, Shamburek RD, Remaley AT (2011) MicroRNAs are Transported in Plasma and Delivered to Recipient Cells by High-Density Lipoproteins. Nat Cell Biol 13:423–433.

Villemagne VL, Rowe CC, Barnham KJ, Cherny R, Woodward M, Pejoska S, Salvado O, Bourgeat P, Perez K, Fowler C, Rembach A, Maruff P, Tanzi R, Ritchie CW, Masters CL (2016) An exploratory molecular imaging study targeting Abeta with a novel 8-OH Quinoline in Alzheimer's disease (The PBT-204 Imagine Study). Alzheimer's Dement J Alzheimer's Assoc 12:P417.

Walker DG, Lue LF, Beach TG (2001) Gene expression profiling of amyloid beta peptide-stimulated human post-mortem brain microglia. Neurobiol Aging 22:957–966.

Walsh DM, Lomakin A, Benedek GB, Condron MM, Teplow DB (1997) Amyloid beta-protein fibrillogenesis. Detection of a protofibrillar intermediate. J Biol Chem 272:22364–22372.

Walsh DM, Hartley DM, Kusumoto Y, Fezoui Y, Condron MM, Lomakin A, Benedek GB, Selkoe DJ, Teplow DB (1999) Amyloid beta-protein fibrillogenesis. Structure and biological activity of protofibrillar intermediates. J Biol Chem 274:25945–25952.

Walsh DM, Klyubin I, Fadeeva J V, Cullen WK, Anwyl R, Wolfe MS, Rowan MJ, Selkoe DJ (2002a) Naturally secreted oligomers of amyloid beta protein potently inhibit hippocampal long-term potentiation in vivo. Nature 416:535–539.

Walsh DM, Klyubin I, Fadeeva J V, Rowan MJ, Selkoe DJ (2002b) Amyloid-beta oligomers: their production, toxicity and therapeutic inhibition. Biochem Soc Trans 30:552–557.

Wang HY, Lee DH, D'Andrea MR, Peterson PA, Shank RP, Reitz AB (2000) beta-Amyloid(1-42) binds to alpha7 nicotinic acetylcholine receptor with high affinity. Implications for Alzheimer's disease pathology. J Biol Chem 275:5626–5632.

Wang J, Dickson DW, Trojanowski JQ, Lee VM (1999) The levels of soluble versus insoluble brain Abeta distinguish Alzheimer's disease from normal and pathologic aging. Exp Neurol 158:328–337.

Wang Q, Walsh DM, Rowan MJ, Selkoe DJ, Anwyl R (2004) Block of long-term potentiation by naturally secreted and synthetic amyloid beta-peptide in hippocampal slices is mediated via activation of the kinases c-Jun N-terminal kinase, cyclin-dependent kinase 5, and p38 mitogen-activated protein kinase as well a. J Neurosci 24:3370–3378.

Wang Y, Cella M, Mallinson K, Ulrich JD, Young KL, Robinette ML, Gilfillan S, Krishnan GM, Sudhakar S, Zinselmeyer BH, Holtzman DM, Cirrito JR, Colonna M (2015) TREM2 lipid sensing sustains the microglial response in an Alzheimer's disease model. Cell 160:1061–1071.

Weber M, Liebert U, Muller K (2010) The human SH-SY5Y cell line does not express functional ionotropic glutamate receptors - a patch clamp study. Available at: https://www.researchgate.net/publication/260893189 [Accessed December 7, 2016].

Weidemann A, Eggert S, Reinhard FBM, Vogel M, Paliga K, Baier G, Masters CL, Beyreuther K, Evin G (2002) A novel epsilon-cleavage within the transmembrane domain of the Alzheimer amyloid precursor protein demonstrates homology with Notch processing. Biochemistry 41:2825–2835.

West MJ, Coleman PD, Flood DG, Troncoso JC (1994) Differences in the pattern of hippocampal neuronal loss in normal ageing and Alzheimer's disease. Lancet 344:769–772.

White AR, Du T, Laughton KM, Volitakis I, Sharples RA, Xilinas ME, Hoke DE, Holsinger RMD, Evin G,

Cherny RA, Hill AF, Barnham KJ, Li Q-X, Bush AI, Masters CL (2006) Degradation of the Alzheimer disease amyloid beta-peptide by metal-dependent up-regulation of metalloprotease activity. J Biol Chem 281:17670–17680.

Willem M et al. (2015) eta-Secretase processing of APP inhibits neuronal activity in the hippocampus. Nature 526:443–447.

Wilson C (2007) The expression, purification and functional assessment of recombinant beta-amyloid peptides. Master of Science thesis, University of Otago.

Wogulis M, Wright S, Cunningham D, Chilcote T, Powell K, Rydel RE (2005) Nucleation-dependent polymerization is an essential component of amyloid-mediated neuronal cell death. J Neurosci 25:1071–1080.

Wong BX, Tsatsanis A, Lim LQ, Adlard PA, Bush AI, Duce JA (2014) beta-Amyloid precursor protein does not possess ferroxidase activity but does stabilize the cell surface ferrous iron exporter ferroportin. PLoS One 9:e114174.

Wood JG, Mirra SS, Pollock NJ, Binder LI (1986) Neurofibrillary tangles of Alzheimer disease share antigenic determinants with the axonal microtubule-associated protein tau (tau). Proc Natl Acad Sci U S A 83:4040–4043.

World Health Organisation (2008) World Health Statistics. Geneva.

Xie H, Hu L, Li G (2010) SH-SY5Y human neuroblastoma cell line: in vitro cell model of dopaminergic neurons in Parkinson's disease. Chin Med J (Engl) 123:1086–1092.

Xu Y, Shen J, Luo X, Zhu W, Chen K, Ma J, Jiang H (2005) Conformational transition of amyloid beta-peptide. Proc Natl Acad Sci U S A 102:5403–5407.

Younkin DP, Tang CM, Hardy M, Reddy UR, Shi QY, Pleasure SJ, Lee VM, Pleasure D (1993) Inducible expression of neuronal glutamate receptor channels in the NT2 human cell line. Proc Natl Acad Sci U S A 90:2174–2178.

Zambrano R, Jamroz M, Szczasiuk A, Pujols J, Kmiecik S, Ventura S (2015) AGGRESCAN3D (A3D): server for prediction of aggregation properties of protein structures. Nucleic Acids Res .

Zhang R, Miller RG, Madison C, Jin X, Honrada R, Harris W, Katz J, Forshew DA, McGrath MS (2013) Systemic immune system alterations in early stages of Alzheimer's disease. J Neuroimmunol 256:38–42.

Zhang Y, McLaughlin R, Goodyer C, LeBlanc A (2002) Selective cytotoxicity of intracellular amyloid beta peptide1-42 through p53 and Bax in cultured primary human neurons. J Cell Biol 156:519–529.

Zhang Z, Song M, Liu X, Su Kang S, Duong DM, Seyfried NT, Cao X, Cheng L, Sun YE, Ping Yu S, Jia J, Levey AI, Ye K (2015) Delta-secretase cleaves amyloid precursor protein and regulates the pathogenesis in Alzheimer's disease. Nat Commun 6:8762.

Zhao G, Mao G, Tan J, Dong Y, Cui M-Z, Kim S-H, Xu X (2004) Identification of a new presenilin-dependent zeta-cleavage site within the transmembrane domain of amyloid precursor protein. J Biol Chem 279:50647–50650.

Zou K, Gong J-S, Yanagisawa K, Michikawa M (2002) A novel function of monomeric amyloid beta-protein serving as an antioxidant molecule against metal-induced oxidative damage. J Neurosci 22:4833–4841.

Appendices

Appendix A: R statistical analysis scripts

Calculating means and fold change of cell viability data

```
## Open raw data file
filename<-file.choose()
data2=read.csv(filename,header=TRUE,sep=",");
name<-basename(filename)

## Calculate means
means<-array(0,dim=c(ncol(data2),1))
for (i in seq(ncol(data2)))
                means[i]=mean(data2[,i],na.rm=TRUE);
end

## Reformat means with data labels
data1means<-data.frame(colnames(data2),means)

data1means

## Calculate fold change compared to means of the control
FoldChange<-array(0,dim=c(nrow(data2),ncol(data2)))

for (i in seq(ncol(data2)))
        for (j in seq(nrow(data2)))
                FoldChange[j,i]=((data2[j,i])/(means[1])*100);
end

## Reformat Fold change data with data labels
colnames(FoldChange)=colnames(data2)

## Save file
write.csv(FoldChange, file=paste("Foldchange",name), row.names=F) # automatic field separator is ","
getwd() # shows you filepath where file is saved.
```

Draw bar and dot plot of fold change cell viability data

```
## Open file
filename<-file.choose()
data4=read.csv(filename,header=TRUE,sep=",");
name<-basename(filename)
na.pass(data4)
data4<-(data4/100)-1
```

```
## Reformat data
meltdata<-melt(data4,na.rm=TRUE)
colnames(meltdata)<-c("Treatment","Value")
formatdata<-meltdata[order(meltdata$Treatment),]
#fix(formatdata)

## Assign the barplot to x so that x will contain the bar positions.
x = barplot(tapply(formatdata$Value, formatdata$Treatment, FUN=mean), ylim=c(-0.25,1), xlab="Treatment", ylab="Fold change in cell viability" ,xaxt="n")
points(rep(x, table(formatdata$Treatment)), formatdata$Value[order(formatdata$Treatment)], pch=21, bg="red")
## assign x and y axis limits
## assign x and y axis legends

## Add X-axis labels
label<-c("Control",expression(paste("New A",beta," 1",mu,"M")), expression(paste("Old A",beta," 1",mu,"M"))) # change depending on experimental variables
text(cex=1, x=x-0.25, y=min(data4, na.rm=TRUE)-0.1, label, xpd=TRUE, srt=45, pos=1)
```

Perform Kruskal-Wallis test with Dunn's *post-hoc* test

```
## Open file for Kruskal-Wallis test
filename<-file.choose()
data3=read.csv(filename,header=TRUE,sep=",");
name<-basename(filename)
na.pass(data3)
data3

## Reformat data for Kruskal-Wallis test
meltdata<-melt(data3,na.rm=TRUE)
colnames(meltdata)<-c("Treatment","Value")
formatdata<-meltdata[order(meltdata$Treatment),]
fix(formatdata)

## Define test parameters
statsdata=as.data.frame(formatdata)
colnames(statsdata)<-c("Treatment","Value")
Treatment = statsdata$Treatment
Value = statsdata$Value

KW.DT<-dunn.test(Value, Treatment, method="hs", kw=TRUE, list=TRUE, alpha=0.01)
```

Appendix B: Size-exclusion chromatography to separate $A\beta_{1-42}$ from MBP

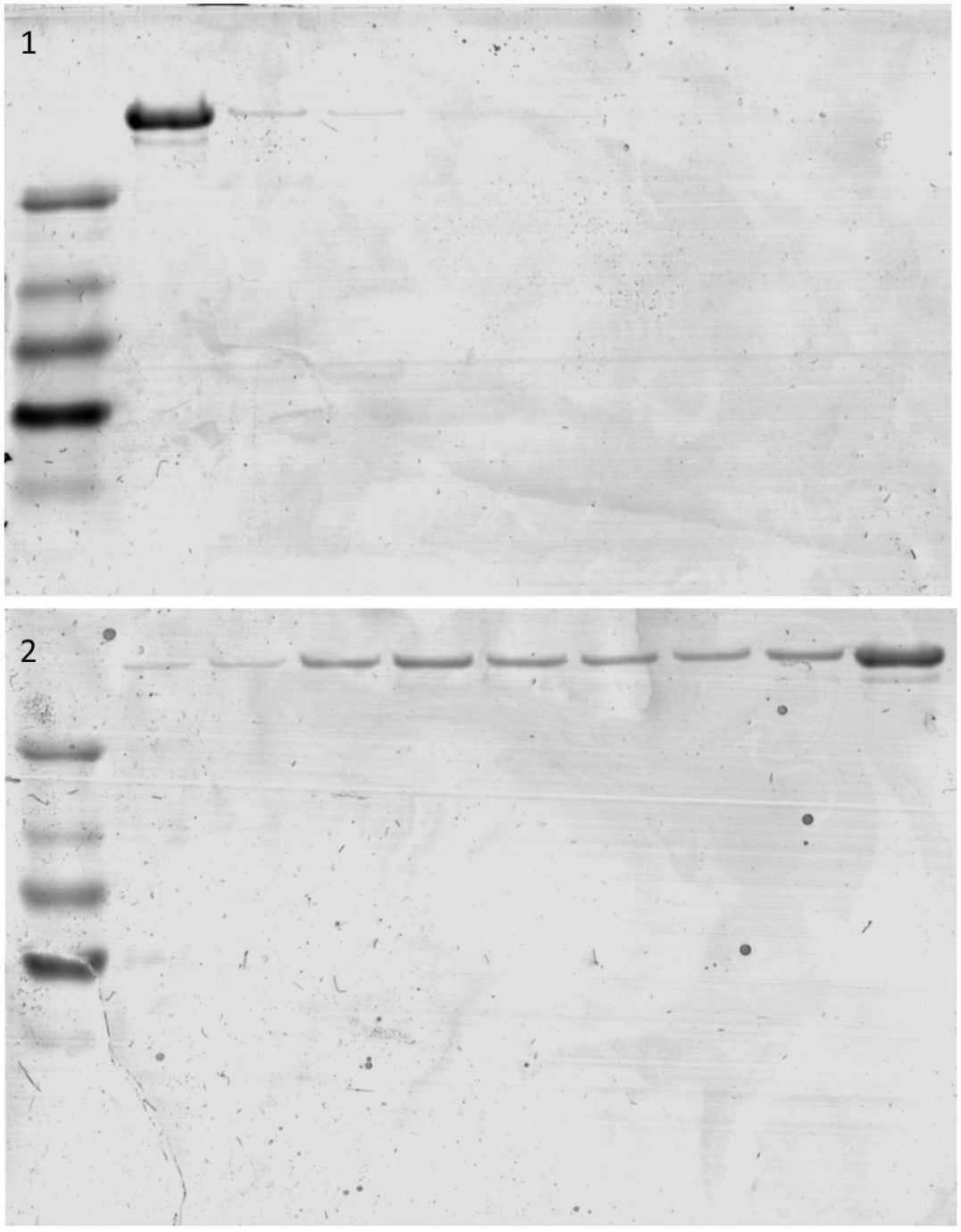

Figure S1: Analysis of protein-containing fractions obtained from size-exclusion chromatography. Coomassie-stained 16% (w/v) Kolbe gels of all protein-containing fractions eluted from the Superdex 75 agarose-dextrose column loaded with pooled samples from reverse-phase chromatography containing both $A\beta_{1-42}$ and MBP. The high molecular weight band is consistent with MBP.

Appendix C: Standard curve of BSA concentrations used to determine Aβ concentration.

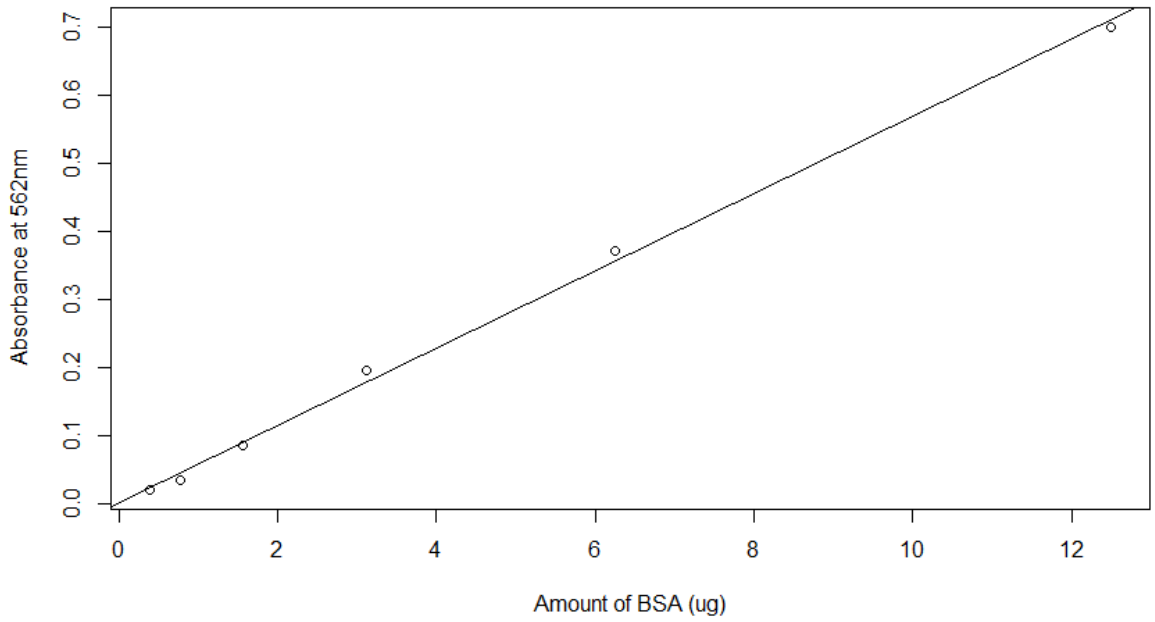

Figure S2: Standard curve of BSA amounts used to determine concentration of Aβ. Known amounts of BSA are plotted against their corresponding 562 nm absorbance values. Coefficient of determination for this standard curve was 0.9978. The equation describing the relationship between the two variables was as follows: y=0.0566x+0.0026. This formula was used to determine Aβ concentration, correcting for the 1:1 dilution factor of the peptide sample in the assay.

Appendix D: Individual primary cell culture data

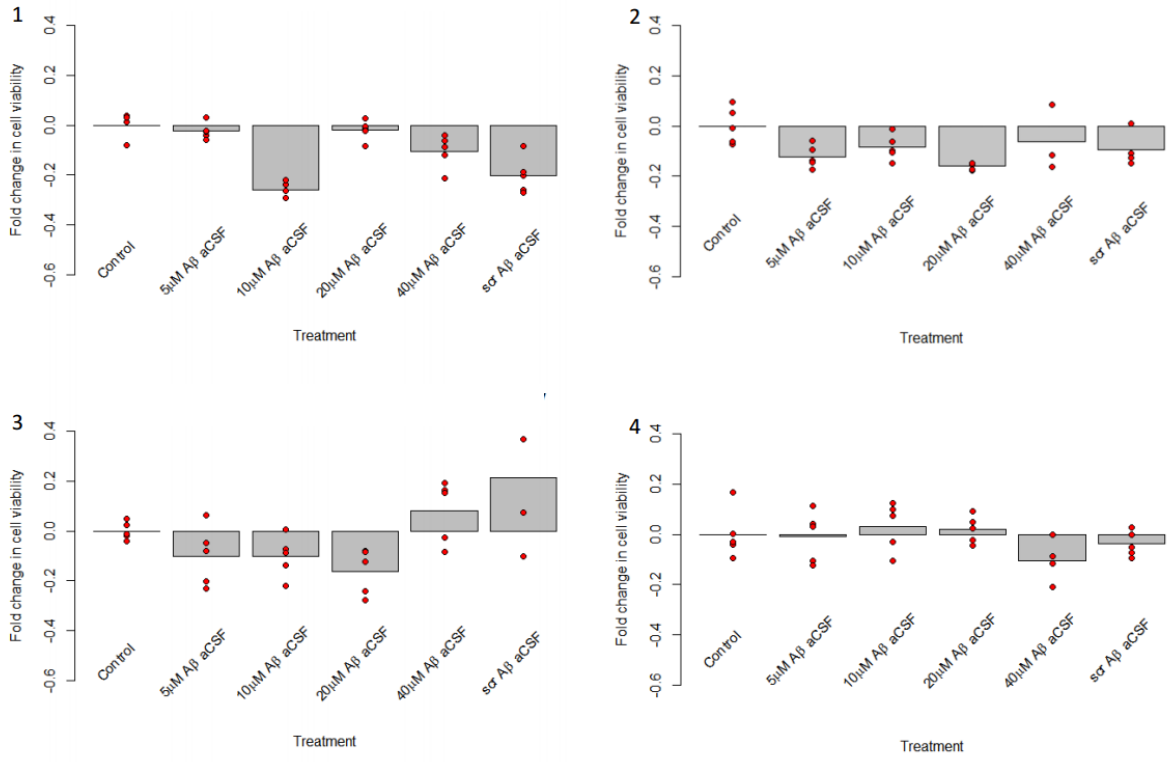

Figure S3: Bar and dot plots showing cell viability changes in primary rat cortical cell cultures after treatment with $A\beta_{1\text{-}42}$ and scrambled $A\beta_{42}$. Each plot represents an individual experiment, whose data points were combined to give Figure 14. These data well illustrate the variability of $A\beta_{1\text{-}42}$ as a cellular insult encountered in this model.

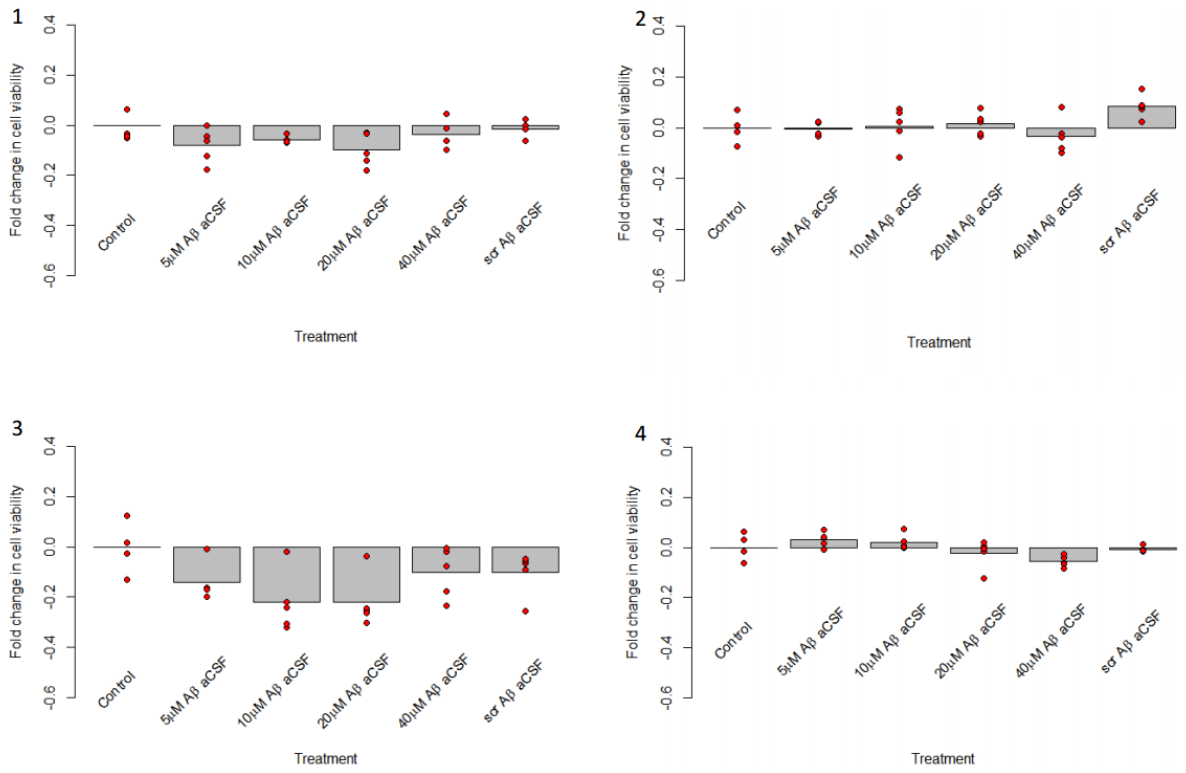

Figure S4. Bar and dot plots showing cell viability changes in primary rat hippocampal cell cultures after treatment with $A\beta_{1\text{-}42}$ and scrambled $A\beta_{42}$. Each plot represents an individual experiment, whose data points were combined to give Figure 15. As above, the variability of these data precluded an accurate estimation of the effect of $A\beta_{1\text{-}42}$ treatment in primary rat hippocampal cell cultures.